RADIATION DISTRIBUTION IN A MATURE CORN CANOPY

DEDICATION

This thesis is respectfully dedicated to the memory of CAMERON DOUGLAS ALLEN, B.A., M.Sc. (1947-1973) a good friend and a valued colleague who died in a car accident on 9 July, 1973 near Elora, en route to his research site.

SPATIAL AND TEMPORAL VARIATION IN THE DISTRIBUTION OF RADIATION IN A MATURE CORN CANOPY

by

William John Kyle, M.Sc.

A Thesis

Submitted to the School of Graduate Studies

in Partial Fulfillment of the

Requirements for the Degree

Doctor of Philosophy

McMaster University

June, 1974

1975

William John Kyle

DOCTOR OF PHILOSOPHY (1974)
(Geography)

McMASTER UNIVERSITY
Hamilton, Ontario

TITLE: Spatial and Temporal Variation in the Distribution of Radiation in a Mature Corn Canopy.

AUTHOR: William John Kyle, B.Sc. (University of Nottingham)
M.Sc. (McMaster University)

SUPERVISOR: Dr. J. A. Davies

NUMBER OF PAGES: x, 139

SCOPE AND CONTENTS:

A study of the spatial and temporal variability of global solar, net solar and net radiation in two plots of corn, seeded differently, was undertaken using a moving tramway sampling system. Horizontal frequency distributions of radiant flux density revealed a systematic variation dependent on canopy structure.

A modified exponential model was developed as an empirical solution to the problem of estimating radiation fluxes in plant canopies. Since the extinction coefficients are dependent on present data its validity must await independent evaluation by other workers.

SOLCOMP, a simple layer model for global and net solar radiation was developed from theoretical considerations. This model performed well and illustrates that it is possible to model the radiation regime in a crop with a simple, theoretically-based construct using a small number of easily obtained input parameters. A further development, NETCOMP, suitable for estimating net radiation in the canopy showed potential but could not be fully tested due to lack of information on canopy temperature regimes.

ACKNOWLEDGEMENTS

The author would like to express gratitude to the many people who gave freely of advice and assistance during the field investigation and preparation of this thesis.

Special acknowledgement is due to Dr. J.A. Davies, whose guidance and support throughout this study has been gratefully appreciated; to Dr. K.M. King of the University of Guelph, Department of Soil Science for making the field site available; to other members of my supervisory committee, Dr. W.R. Rouse, Dr. G.P. Harris and Dr. M-k Woo for helpful criticism; to fellow graduate students at McMaster for many hours of discussion.

Finally, I would like to acknowledge the support given me by my friends at McMaster and, in particular, my wife, Tina, for her encouragement and patience during my graduate studies.

This study was supported by a research grant from the National Research Council of Canada.

TABLE OF CONTENTS

LIST OF FIGURES

LIST OF TABLES

LIST OF APPENDIXES

CHAPTER 1

INTRODUCTION

A. Perspective

Microclimatology is dominated by theory of energy exchanges between the atmosphere and the underlying surface. The radiation balance (net available energy from radiation) controls surface heat exchanges, and also photosynthesis when there is vegetation present. Vertical divergence (change in flux density or energy per unit time per unit area) of radiation in the lowest 10 m of the atmosphere above a bare surface is very small. Vegetated surfaces have depth and are composed of absorbers and scatterers of radiation. Thus, within a vegetative canopy there is considerable divergence of flux density, both in the horizontal and the vertical.

A canopy receives a quantity of radiation which varies with solar position and the prevailing weather. This solar energy is modified as it interacts with the canopy. Each leaf, depending upon its position, is subject to a radiation field different from that above the canopy. These regimes are variable in space and time. Spatial variation is caused by the heterogeneous distribution of the foliage elements and temporal variation is due to changes in incident solar radiation caused by the regular periodism in the earth's rotation and revolution. Irregular variation in energy supply over periods ranging

from seconds to centuries is induced by changes in atmospheric turbidity, clouds, and short and long term climatic variations.

Natural vegetation is composed of a complex ecosystem of species, of different morphology, with different radiation absorption and scattering properties. The spatial variation in radiation under natural canopies is thus very complex. Conversely, agricultural crops consist of relatively simple systems of evenly-spaced plants of the same species. For simplicity, most radiation investigations in plant canopies have been concerned with crops.

Measurement of radiation fluxes within a crop poses many problems (Anderson, 1971). The main problem lies in adequate sampling of sunflecks superimposed on a background of diffuse radiation consisting of unimpeded diffuse radiation from the sky, passing through gaps in the canopy, and radiation scattered by the foliage. To sample the diverse radiation regime adequately, large numbers of stationary sensors (Impens, Lemeur and Moermans, 1970), linear sensors capable of integrating radiation in the horizontal plane (Szeicz, Monteith and dos Santos, 1964), and moving tramway systems (Norman, 1971) have been used. All are expensive and representative sampling is difficult.

In the past 20 years many canopy radiation models have been developed. These attempt to simulate the canopy radiation regime and thus avoid the expense and difficulty of direct field measurements. They range in complexity from semi-empirical approaches (Monsi and Saeki, 1953) to exhaustive analytical treatments (Cowan, 1968; Kuroiwa, 1968). In the case of many theoretical models most of the required

parameters are unmeasurable or are very difficult to measure and the models are difficult to evaluate.

In addition, theoretical estimates for parameters of the mean radiation field are calculated but the spatial variation is often neglected. For direct radiation, this variation is very large (Anderson, 1966). Such information is needed to account for the radiation distribution over the leaves in photosynthesis calculations and is of interest in understanding the complex of energy exchanges within the crop.

Allen and Lemon (1972) have used horizontal frequency distributions of radiant flux density to study this problem. Their data suggest that these distributions provide insight into the parameters which determine the spatial variation in radiation.

B. Aims

An experimental study of spatial and temporal variation in the radiation regimes within a corn canopy was undertaken during the summer of 1972 with the objective of understanding the complex of interactions affecting the radiation regime in a relatively simple crop system. Measurements of radiation within the crop were made with traversing systems so that the frequency distributions of radiant energy could be analysed. On different occasions during the study

global solar $K\downarrow$[1], net solar K^*[2], and net radiation Q^*[3] were measured directly above the canopy and at four levels within the crop. These measurements were augmented by measurements of the canopy structure parameters, leaf area index[4], leaf inclination and azimuth orientation.

Corn was selected for investigation since it has a relatively simple structure, unlike natural vegetation and some other crops, which enables the number of variables to be minimised. In particular, the large leaves are displayed in two ranks, chiefly in a single vertical plane. In addition, the crop is relatively rigid which results in minor wind modification; exhibits little diurnal movement, thereby eliminating problems of foliage distribution dependence on time of day; and has a moderate leaf area index so that, even in the densest region of the canopy, illumination is high. The height and geometry of the crop also make it very amenable to measurements with moving sensors.

Equidistant plant spacing was chosen to simplify canopy arrangement. This eliminates problems of leaf clustering and possible azimuth orientation preferences due to row alignment, major sources of non-uniform leaf distribution in most canopies. This canopy structure was as homogeneous as possible. A row plot, conventionally seeded and

---

[1] downward direct and diffuse solar (wavelengths 0.3–3.0 μm) radiation as received on a horizontal surface from a solid angle of 2π.

[2] net flux of downward and upward solar radiation.

[3] net flux of downward and upward solar and terrestrial (wavelengths greater than 3.0 μm) radiation.

[4] leaf area, one side only, subtended per unit area of land (Watson, 1947).

planted in north-south rows, represented a more realistic arrangement found in agronomic practice. Studies in the past have led to the general conclusion that north-south rows give better radiation interception and higher yields than other orientations. By using these two canopy arrangements the influence, if any, of row effects on canopy radiation should become apparent.

With these preliminary comments on the rationale behind the investigation, the aims of this study of the spatial and temporal variations in the radiation regimes in a corn crop may be stated. They are:

(i) to investigate the nature and magnitude of the variability in the radiation regime in the two crop arrangements;

(ii) to ascertain the parameters which have most effect on the measured horizontal frequency distributions of radiant flux density;

(iii) to investigate methods of obtaining a representative value of the radiation fluxes for microclimatological or agronomic purposes;

and (iv) to attempt to formulate a simple model of the radiation regime in a crop suitable for microclimatological or agronomic purposes.

C. Thesis format

The following chapter presents a summary of the approaches to the problem of estimating radiant energy fluxes in plant canopies, together with a brief review of pertinent literature. Chapter 3

outlines the methodology of the investigation. The results of the measurements of $K\downarrow$, $K^{\uparrow}$ and Q^{*}, their horizontal and vertical variation and their temporal distribution are presented in Chapter 4. The problem of specifying a representative profile is also addressed. Chapter 5 is reserved for the evaluation of the most commonly used model of radiation attenuation and its associated problems. In Chapter 6 the development and evaluation of a simple theoretical model of the radiation regime is presented.

CHAPTER 2

PROBLEMS OF ESTIMATING ENERGY FLUXES IN PLANT CANOPIES

A. Global and net solar radiation

Monsi and Saeki (1953) and Kasanaga and Monsi (1954) were the first to show that the attenuation of global radiation within a crop decreases exponentially with depth and is thus analagous to radiation absorption in homogeneous media. Based on their observations, they developed a simple model for the attenuation by treating the crop as a collection of infinitely thin, randomly oriented, perfectly black and opaque planes, all inclined at the same angle λ to the horizontal.

The amount of radiant energy intercepted by a thin plane of foliage area df exposed to direct radiation is the area of shadow cast by unit area of foliage A on a horizontal plane A_h, multiplied by the horizontal irradiance H.

$$dH = -(A_h / A)\, H\, df = -k\, H\, df. \qquad (1)$$

Integrating

$$H_f = H_0 \exp(-kf), \qquad (2)$$

where H_f is the radiant flux density at f, H_o is the flux density above the crop and k is an extinction coefficient.

When calculated in terms of the radiation incident on a horizontal surface, k was found to be 1 when $\Lambda = 0$ and to decrease with increasing values of Λ. That is, more radiation penetrates a canopy when the leaves are nearly vertical than when they are nearly horizontal. This model oversimplifies the real variations within a crop.

In the past 20 years considerable effort has been directed toward development of models for the attenuation of global radiation. Many of these are based on the original work of Monsi and Saeki (1953) and associated later developments (de Wit, 1965; Monteith, 1965; Chartier, 1966; Duncan, Loomis, Williams and Hanau, 1967; Cowan, 1968; Kuroiwa, 1968; Anderson and Denmead, 1969; Isobe, 1969). All of these models attempt to relate plant parameters and solar radiation.

A number of problems which have arisen are discussed by Anderson (1966, 1969, 1970). In the exponential model, values of k vary widely for direct, but little for diffuse radiation. Anderson (1966) has shown that when relative intensity of direct radiation (the ratio of flux density in the canopy to that above the crop) is considered over a range of angles of penetration P, k is not constant unless $\Lambda = 0$ when $k = 1$. She found:

$$k = \cos \Lambda, \qquad \text{when} \quad P > \Lambda; \tag{3}$$

$$k = \cos \Lambda \, [1 + 2 (\tan \Theta - \Theta) / P], \quad \text{when } P < \Lambda < \pi/2; \tag{4}$$

$$k = 2 \cot P / \pi, \qquad \text{when } \Lambda = \pi/2; \qquad (5)$$

$$k = 1 / 2 \sin P, \qquad \text{with random } \Lambda; \qquad (6)$$

where

$$\theta = \cos^{-1} (\tan P / \tan \Lambda).$$

Hence, k is a function of both Λ and P. This dependence of the extinction coefficient on P has three important consequences (Anderson, 1970). First, extinction of direct solar radiation in crops depends on solar zenith angle ζ[1], and hence on latitude, time of year and time of day. Second, the extinction of diffuse radiation is not strictly exponential except when $\Lambda = 0$. Third, the percentage of diffuse and direct radiation reaching a particular depth in a crop is not necessarily similar, but will depend upon the ratio of diffuse to direct radiation above the crop.

Study of radiation distributions in plant communities has played a very important role in the theoretical analysis of gross photosynthesis. It was under diffuse radiation that the 'light distribution' in a crop was first studied. Under these conditions there is negligible horizontal variation of radiant energy within a canopy and spatially-averaged flux densities may be used with confidence. On the contrary, when the incident radiation is composed primarily of direct solar radiation, the horizontal variation of radiant flux density is essential in calculating gross photosynthesis. This has been pointed out by Monteith (1965), who

---

[1] solar zenith angle is defined as the angle between the sun and the local vertical.

attributed the requirement to the non-linearity of photosynthesis with radiant energy received by the leaves. It is thus necessary to know how the radiant energy incident on the leaves is distributed.

Theoretical and experimental studies by Mototani (1968), Norman (1971), Norman, Miller and Tanner (1971) and Miller and Norman (1971) have investigated the horizontal variability of solar radiation in a crop. From these investigations three general conclusions may be drawn. First, variability increases with the ratio of direct to diffuse radiation. Second, near the top of a canopy the distribution of radiant energy is bi-modal, corresponding to the high frequency of patches of light and shade. Third, on descending into the canopy, the radiation is gradually diffused and the pattern becomes uni-modal near the base.

The needs of remote sensing have, in recent years, led to an interest in using theories of radiation scattered through multiple layers in plant canopies (Allen and Richardson, 1968; Allen, Gayle and Richardson, 1970; Idso and de Wit, 1970; Weinmann and Guetter, 1972). In general, these models assume that the transfer of global radiation in a crop can be described by the equation of radiative transfer through multiply scattering media. Unlike, the previous models, this approach has a further disadvantage for microscale work. Most of the models are formulated in terms of bulk absorption, scattering and reflection parameters. The model of Idso and de Wit (1970) is a notable exception which does consider the interaction between sun and leaves.

This model is potentially useful for radiation regime modelling. It provides information on important factors such as the fraction of

leaves in each layer receiving diffuse radiation only and the fractions which also receive direct radiation at various angles of incidence of the solar beam. Thus, at each layer, the proportion of sunfleck area to total area is known. This information is necessary in calculations of gross photosynthesis (Monteith, 1965). However, the model is complex and requires a large number of calculations.

A further problem associated with present models arises from the assumption that foliage is randomly distributed in space. Real foliage is not usually distributed this way and general measures of non-randomness are lacking (Anderson, 1970). Acock, Thornley and Warren Wilson (1970) considered this aspect of the radiation regime and presented an analysis of non-randomness. From this it appears likely that non-randomness is a significant factor only in canopies of low leaf area index, where a moderate proportion of the incident radiation is not intercepted.

B. Net radiation

Investigations of diurnal radiation fluxes above crops have indicated that net radiation flux is closely correlated with global radiation flux (Monteith and Szeicz, 1961). This suggests that net terrestrial radiation L^{*1} is relatively constant during the day or that it is correlated with $K\downarrow$. Investigations over a number of surfaces have shown both of these to be true (Stanhill, Hofstede and Kalma, 1966; Davies and Buttimor, 1969; Davies, Robinson and Nunez, 1970;

---

[1] net flux of downward and upward terrestrial radiation.

Proctor, Kyle and Davies, 1972).

Vertical divergence of net terrestrial radiation within a crop is often small (Kyle, 1971) and hence the distribution of net and global radiation within a crop should be similar. Based on this posit, wide use has been made of the exponential model. Uchijima (1962) used this framework;

$$Q^*_z = Q^*_0 \exp(-k f), \qquad (7)$$

where Q^*_z is net radiation on a horizontal surface at depth z, Q^*_0 is net radiation above the crop and k is an extinction coefficient.

Since global radiation is the principal component of net radiation, it is reasonable to postulate that the extinction coefficient will be dependent on solar zenith angle and leaf inclination angle as shown by Anderson (1966). However, conflicting reports appear in the literature. Impens and Lemeur (1969) and McCaughey and Davies (1974) found a diurnal variation in net radiation extinction coefficients, Brown and Covey (1966) did not.

In energy balance studies, hourly averages of net radiation are generally required. Previous studies suggest that it is unwise to assume a constant extinction coefficient. In an attempt to incorporate this variation, McCaughey (1972) expanded the exponent in equation 7:

$$Q^*_z = Q^*_0 \exp\left[-K f (\sec \zeta)^{\frac{h-z}{z}} \cos(\phi - \pi/2)\right]. \qquad (8)$$

The first term in the modification, $(\sec \zeta)^{\frac{h-z}{z}}$, defines the path

length of direct beam radiation as it passes through the foliage. The exponent $\frac{h-z}{z}$ where h is crop height and z is depth from the top of the crop, accommodates the increase in diffuse radiation with penetration into the canopy. He assumed that diffuse radiation was isotropic in the canopy space and thus the dependence of the extinction coefficient on solar zenith angle should decrease with depth. Towards the base of the canopy $\frac{h-z}{z}$ approaches zero and the dependence is removed. The term, $\cos(\phi - \pi/2)$, where ϕ is a relative azimuth angle, defined as the angle between the solar azimuth and the row orientation, was introduced to accommodate a row effect observed by McCaughey (1972). When the sun was shining down the row (a relative azimuth angle of zero), the extinction coefficient K approached zero. This he attributed to the minimum optical depth occurring at zero relative azimuth.

Investigations such as those above indicate a close parallel between the net and global radiation regimes. The same observations concerning horizontal variability of global radiation then apply to net radiation. That is, variability increases with the ratio of direct to diffuse radiation; near the top of the canopy the frequency distribution is bi-modal, corresponding to sunfleck and shade areas; and, the pattern is uni-modal near the base of the crop. The net radiation frequency distributions of Allen and Lemon (1972) are similar to those found by other workers (Mototani, 1968; Norman, 1971) for global radiation.

CHAPTER 3

SITE, INSTRUMENTATION AND FIELD METHODS

A. Measurement site

The research was conducted at the University of Guelph Research Station at Elora in southern Ontario (43° 50' N, 80° 25' W) during August and September 1972. Observations were made in two plots of field corn (*Zea mays*, var. United 109) which formed part of a relatively flat 30 hectare field. One plot, designated the row plot, contained corn seeded in north-south rows, 0.8 m apart, at a density of approximately 62,000 plants per hectare. The other, the equidistant plot, was hand-seeded with plants approximately 0.4 m apart in a square grid pattern. The density of plants was also about 62,000 per hectare. Figure 1 shows the measurement locations in the field.

B. Instrumentation and field methods

1. Radiation measurements

(a) Radiation instruments

Three types of commercially-available radiation sensors were used for the measurement of radiant flux densities. An Eppley Precision Spectral Radiometer Model 2 (Eppley Laboratory, Newport, U.S.A.) was used to measure global radiation above the crop. This sensor has a

FIGURE 1. MEASUREMENT SITE.

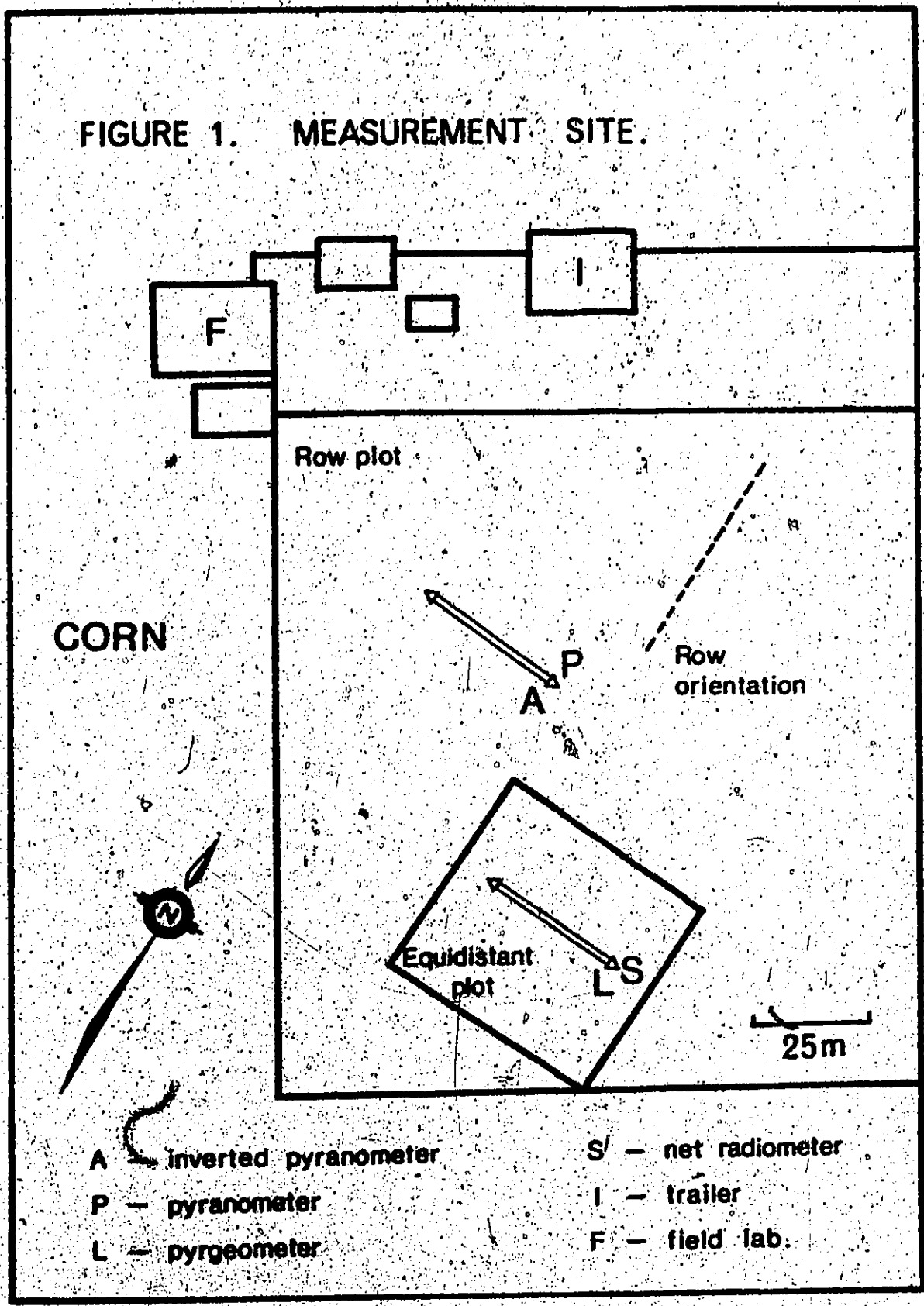

50-junction, wirewound, plated (copper-constantan) thermopile enclosed in concentric glass hemispheres. The receiver is mounted on an equatorial plane below the hemispheres and is coated with Parson's Optical Black. An internal temperature compensation circuit permits sensitivity to remain constant to within ± 0.5% over an ambient temperature range of - 20 to + 40C.

Eppley Black and White pyranometers were used to measure global radiation within the crop. The instrument is available with either a 48- or 90-junction thermopile (radial, wirewound, plated copper-constantan) enclosed in a glass hemisphere. Both types were used in this study. The thermopile is a differential type with the hot-junction receivers coated with Parson's Optical Black, and the cold-junction receivers coated with a white barium sulphate paint. An internal compensation circuit maintains the sensitivity within the range ± 1.5% from - 20 to + 40C.

Net radiometers (Type S-1, Swissteco Co., Melbourne, Australia) used in the study are a modified version of a design by Funk (1959). The sensor consists of a wirewound, plated (copper-constantan) thermopile. In this design, one set of junctions is in good thermal contact with an upward facing plate, while the other is in contact with a plate which faces the ground. Both plates are coated with Parson's Optical Black. The thermopile receivers are enclosed within a pair of polyethylene hemispheres. Ports are located within the head and handle to purge and inflate the domes with dry gas and also to provide outside air curtain ventilation of the domes to prevent condensation on the outer surfaces. The polyethylene domes are replaced by double glass domes

to transmit shortwave radiation alone when the instrument functions as a net pyranometer. The instruments were used in both configurations.

Table 1 lists some of the important characteristics of these radiometers. The information is derived primarily from Latimer (1972). The radiometer response is normally expressed in mV per W m^{-2}. Linearity of response is the integral percent error of the instrument when the response is assumed linear over a given range of energy flux. Most thermopiles exhibit a change in response due to variation in ambient temperature. This is overcome in the Eppley instruments by the use of a temperature compensation circuit which maintains a nearly constant response over a large temperature range. In the absence of such a circuit the temperature dependence is expressed in percent per C.

For an ideal sensor, the dependence of directional response of the receiver on solar azimuth[1] and zenith angles, should be proportional to the cosine of the zenith angle but constant for all azimuth angles. The World Meteorological Organisation (1969) recommends that the cosine response should be defined when the sun is at a zenith angle of 80° on a cloudless day and should not exceed ± 5 to 7 percent for pyranometers, and ± 10 percent for net radiometers. The response time of an instrument is a measure of the speed of response. The time constant is the elapsed time required for a signal to be reduced to 1/e or 36.8 percent of its initial value after a sudden step change in irradiation. The values in Table 1 conform to World Meteorological Organisation (1969) standards

---

[1] the angle of the sun from south.

TABLE 1. Characteristics of radiometers used in study

Characteristic	Eppley Precision Model 2	Eppley B & W 8 - 48	Eppley B & W 6 - 90	Swissteco Type S - 1
Response: (approx.)	0.010	0.010	0.025	0.045(20C)
Linearity of response: (0-1.4 kW m^{-2})	± 1.0	± 1.0	± 1.0	± 1.0
Temperature dependence: -20 to +40C	± 0.5	± 1.5	± 1.5	-0.05(per C)
Cosine response: at 80° zenith angle.	± 1.0	± 5.0	± 5.0	± 4.0
Impedance (nominal)	450	300	300	150 - 200
Time constant:				
63.2%	1.0	3.0	3.0	15.0
95%	3.0	10.0	10.0	45.0

Units:		
	Response	mV / W m^{-2}
	Linearity of response	per cent
	Temperature dependence	per cent
	Cosine response	per cent
	Impedance	Ohms
	Time constant	seconds

for high quality radiation instruments.

(b) Instrument calibration

All sensors were calibrated prior to the field season. The Eppley Precision Spectral Radiometer was new and the calibration provided by the Eppley Laboratory accepted. The Eppley Black and White pyranometers were calibrated by field comparison with the Eppley Precision instrument. Six of the Swissteco instruments were new and had been calibrated by C.S.I.R.O. Radiation Laboratory, Australia. The remainder were calibrated by the National Radiation Laboratory, Toronto. These calibrations were accepted.

At the end of the field season the pyranometers were calibrated against the Eppley Precision Spectral Radiometer. Re-calibration of the Swissteco net radiometers by field comparison indicated very minor changes in the calibration constants. Table 2 summarises the calibration information for all sensors and indicates their deployment in the field.

(c) Tramway system

Space-time sampling within each plot was achieved with a tramway system developed from a design by Leonard and Eschner (1968). Each tramway system was supported by two 3 m high galvanised steel T.V. towers of triangular cross-section. The towers were sited 10 m apart so that the tramways were oriented in an east-west direction.

Each system consisted of four tramways at 0.5, 1, 1.5 and 2 m above the ground surface (Figure 2). The choice of orientation and measurement heights was based on previous experience with corn (Kyle, 1971). With north-south rows it is desirable to traverse in an

FIGURE 2. AERIAL TRAMWAY SYSTEM.

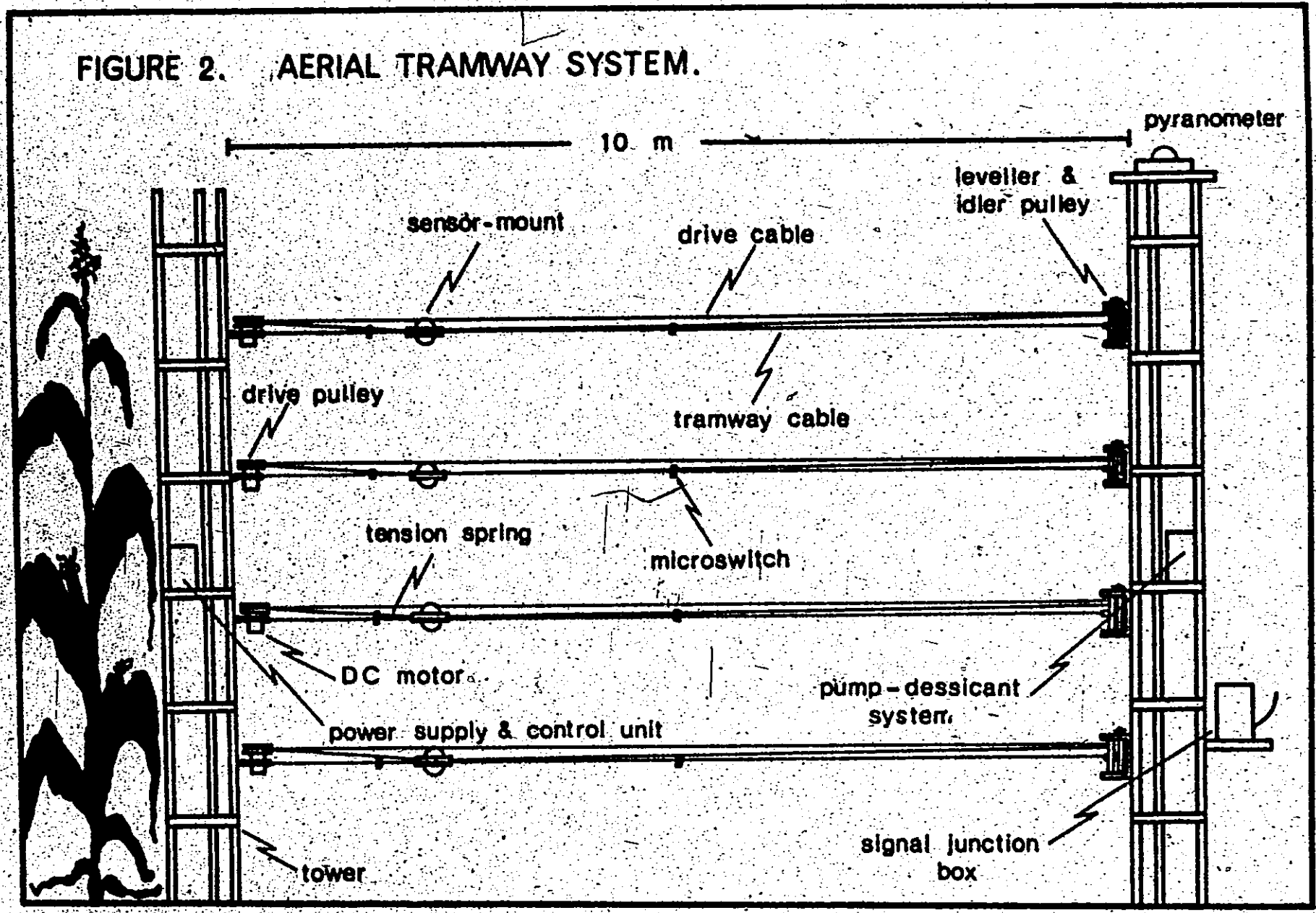

east-west direction in order to sample row and inter-row spaces adequately. The height, at maturity, of corn is about 2.2 m, with leaf overlap occurring at a height of approximately 1.5 m. The choice of sensor heights permitted sampling within the relatively homogeneous complete canopy region and also in the more discontinuous incomplete canopy region where greatest variability in flux magnitude occurs (Kyle, 1971).

To avoid shadows cast by sensors the tramways were offset from the vertical with the uppermost tramway in a more northerly position. The instruments were mounted on Plexiglas sensor mounts and were automatically traversed at known speed by gear-reduced D.C. electric motors. The motors reversed polarity, and hence traverse direction, when the sensor mounts activated microswitches at the extremes of the transect. Further details of the tramway system will be found in Appendix II.

(d) Signal recording and data retrieval

All signals from the instruments were passed through shielded cables to a junction box at the tower. From there they were led by multi-conductor shielded cable to a recording site in a mobile trailer.

Signals were measured with a data logger (Solartron, Farnborough, United Kingdom) and recorded on magnetic tape at 200 b.p.i. Data from field tapes were transferred to storage tapes. In this way data were available for inspection at the end of a sample run and at the same time were stored for easy retrieval during processing. After the field season all data were checked for spurious information, checks being based on field notes and observations. Calibrations were applied and the data finally stored in energy units.

TABLE 2. Radiation sensors, their calibration and deployment

Sensor	Function	Location[1]	Calibration constant (mV / Wm^{-2}) Initial	Final	Adopted
Eppley Precision Model 2					
E11665F3	$K\downarrow$	AC	0.0096	0.0096	0.0096
Eppley Model 8 - 48					
E 9454	$K\downarrow$	2 m	0.0108	0.0105	0.0106
E 9725	$K\downarrow$	1.5 m	0.0088	0.0087	0.0088
Eppley Model 6 - 90					
E 9695	$K\downarrow$	1 m	0.0255	0.0244	0.0250
E 9697	$K\downarrow$	0.5 m	0.0240	0.0242	0.0241
Swissteco Model S - 1					
S 6571	$K^{\uparrow}$	AC	0.1659	0.1659	0.1659
S 6698	$K^{\uparrow}$	2 m	0.0363	0.0363	0.0363
S 6716	$K^{\uparrow}$	1.5 m	0.0330	0.0330	0.0330
S 6984	$K^{\uparrow}$	1 m	0.0449	0.0450	0.0449
S 6909	$K^{\uparrow}$	0.5 m	0.0470	0.0468	0.0470
S 6571	$Q^{\uparrow}$	AC	0.1659	0.1659	0.1659
S 68899	$Q^{\uparrow}$	2 m	0.0480	0.0480	0.0480
S 6903	$Q^{\uparrow}$	1.5 m	0.0475	0.0476	0.0475
S 6906	$Q^{\uparrow}$	1 m	0.0458	0.0458	0.0458
S 6908	$Q^{\uparrow}$	0.5 m	0.0451	0.0450	0.0451

[1] AC indicates a sensor located above the crop. Heights of sensors are given as distances above the ground.

(c) Errors in radiation measurement

There are two likely sources of error in the measurement of radiation fluxes.

1. Sensor error. This is difficult to determine because it depends to a great extent on the care and maintenance of the sensor in the field. It may be estimated from a consideration of the characteristics of the radiometers (Table 1). Values quoted in Table 3 have been gleaned from several sources and are probably the maximum errors likely to be encountered with well maintained sensors.
2. Recording error. The value given in Table 3 is derived from the manufacturer's quoted accuracy for the data logger (1μV). The value presented is probably an upper limit.

The results of the calculation of the root-mean-square error of the procedure used for obtaining each measured flux (Table 3) indicate highest accuracy for the global radiation flux measurement. The maximum error likely to be encountered, associated with the net solar and net radiation fluxes, is a reasonable 8 - 9 per cent.

2. Crop parameter measurements

(a) Routine measurements

At regular intervals during the study period the height of the corn was measured using a sample size of 20 plants. This routine measurement indicated that during this time the plants were at or near maturity in each plot (Figure 3).

Similarly, leaf area index was determined at three sample areas of 1 m^2 in both plots. Details of the measurement of leaf area and the

TABLE 3. Estimate of errors encountered in radiation measurement

Flux	Instrument Error	Recording Error	R.M.S. Error
K↓ above	2%	1%	2.2%
K↓ within	5%	1%	5.1%
K*	8%	1%	8.1%
Q*	8%	1%	8.1%

FIGURE 3. CROP HEIGHT IN EACH PLOT DURING THE STUDY.

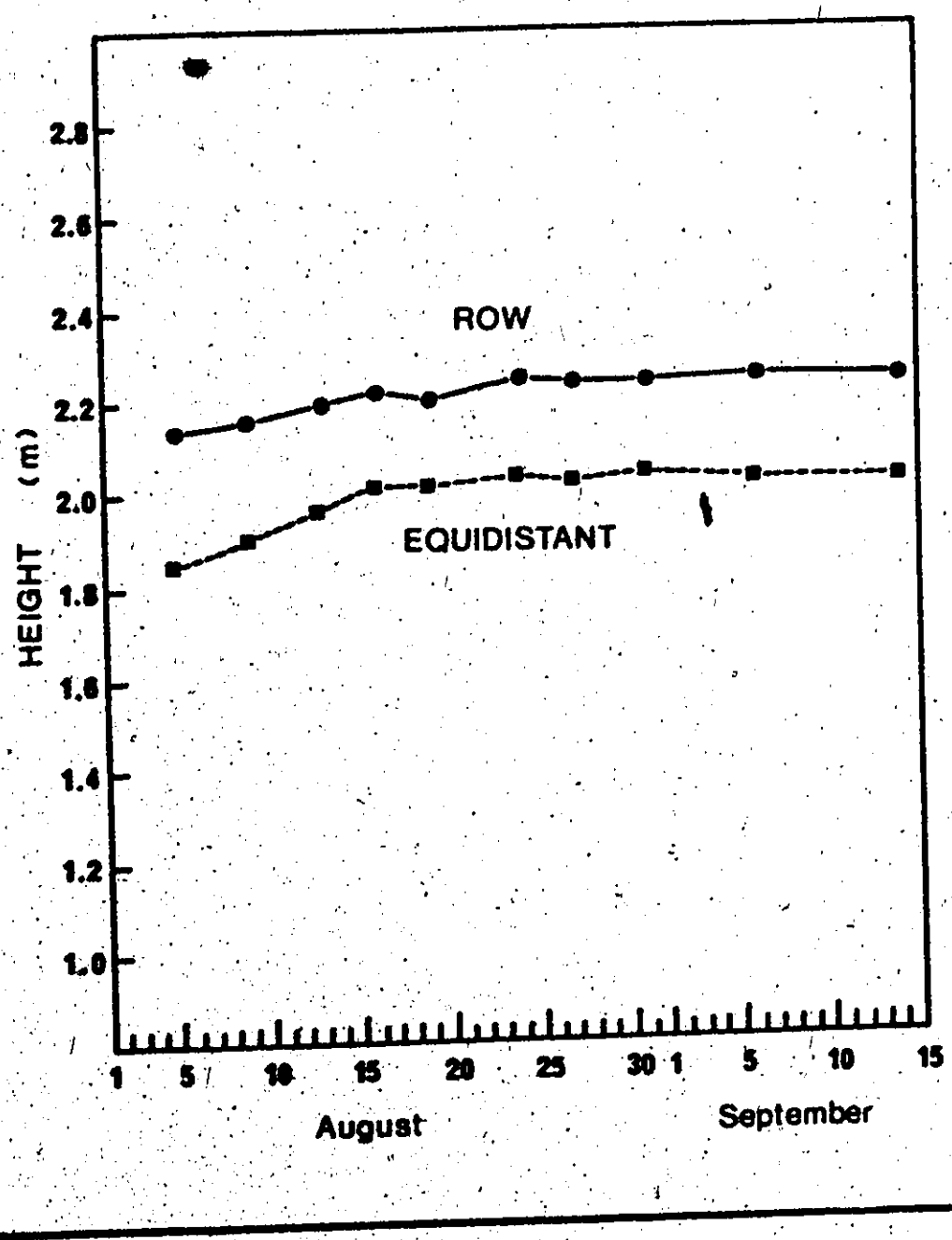

results will be found in Appendix III.

(b) Leaf orientation and inclination

The position of leaves in space is completely determined by their azimuth and the inclination of the plane through each leaf element (de Wit, 1965). Previous investigations in corn (Nichiporovich, 1961; Ross and Nilson, 1967) show no preferred azimuth orientation. In the present study, measurements of orientation were made in each plot to verify this observation. The methods and results are presented in Appendix III.

If the leaves of a canopy have no preferred orientation with regard to azimuth, then their positions are completely characterised by the cumulative frequency distribution of inclination of the leaves. Field measurements of leaf inclination were made to determine leaf distribution functions. Appendix III contains details of the investigation and the results obtained.

3. Observations and procedure

Measurements of global, net solar and net radiation were made above and at four levels within the two plots. Due to the high cost of precision radiometers and problems associated with the maintenance of a complex tramway system, fluxes were not measured concurrently in one plot nor were they measured simultaneously in both plots. Differences in ambient conditions between the periods of measurements were minimised by using only cloudless days for observations.

The transect length and speed of traverse were governed by crop

characteristics and the response time of the sensors. Ideally, the sensors should have an instantaneous response in order that its 'memory' (effect of previous incident flux density) is minimised. In practice, this is not possible due to the slower response time of the sensors. To compensate for this effect, the sensors were traversed more slowly and external ambient conditions assumed constant for the period of traverse.

Based on the response times of the sensors, a traverse speed of 1.5 m per minute was used. To sample the crop representatively a three metre transect length was used. One transect of the tramway required 2 minutes. To ensure a good sample, five traverses were made over a ten minute period. These 10 minute runs were repeated at half-hourly intervals throughout the day to obtain information on the temporal variation of the fluxes. Each signal was scanned every 10 seconds, the logger's maximum scanning rate, which permitted 60 samples in each 10 minute run.

Maintaining instruments in peak operating condition in the canopy environment, and thus minimising errors, is difficult. Consequently, a consistent procedure was adopted to check instruments at the start of each day. Each morning the sensors were uncovered and the shields dried and cleaned to remove dew and/or plant debris which may have accumulated. At this time, the domes of the Swissteco instruments, which are subject to transmission changes due to ageing, were replaced if necessary. The aspiration system was checked and the silica gel dessicant replaced. The instruments were then carefully checked for levelness to ensure that the measured fluxes refer to a horizontal

plane. Finally, a visual inspection of connections and tramway components was made. On completion of these procedures the system was started and ran for 10 minutes. During this period any anomalies indicating malfunction could be corrected.

CHAPTER 4

SPATIAL VARIATION OF RADIANT FLUX DENSITIES AND ITS INFLUENCE ON CANOPY RADIATION REGIMES

A. Radiation frequency distributions

In the past, most of the investigations of radiation regimes in crops have used spatial and sometimes temporal averaging when evaluating those regimes. While spatial and temporal averaging is a convenient method of assessing the distribution of radiation within the canopy, particularly in the vertical, such averages give no information concerning the spatial variation of radiation in the horizontal.

To obtain information on the horizontal spatial variation the data were analysed in terms of the frequency distributions of radiant flux densities measured by the sensors at each level.

1. Global and net solar radiation

Figure 4 represents three sample frequency distributions obtained from traverse data in the equidistant plot. All such distributions were of a similar type. The global radiation flux density has a bimodal frequency distribution, particularly at sampling heights below 2 m above the ground. The sensor is either in a sunfleck or in the shadow of leaves. In addition, the proportion of radiation in various flux density classes varies with depth into the crop. Near the top of the canopy the radiometer is exposed to full radiation most of the time. At 1.5 and 1 m there is a division between shade and

FIGURE 4. FREQUENCY DISTRIBUTIONS OF GLOBAL SOLAR RADIATION FLUX DENSITY AND OF PERCENT LEAF COVER IN EQUIDISTANT CORN.

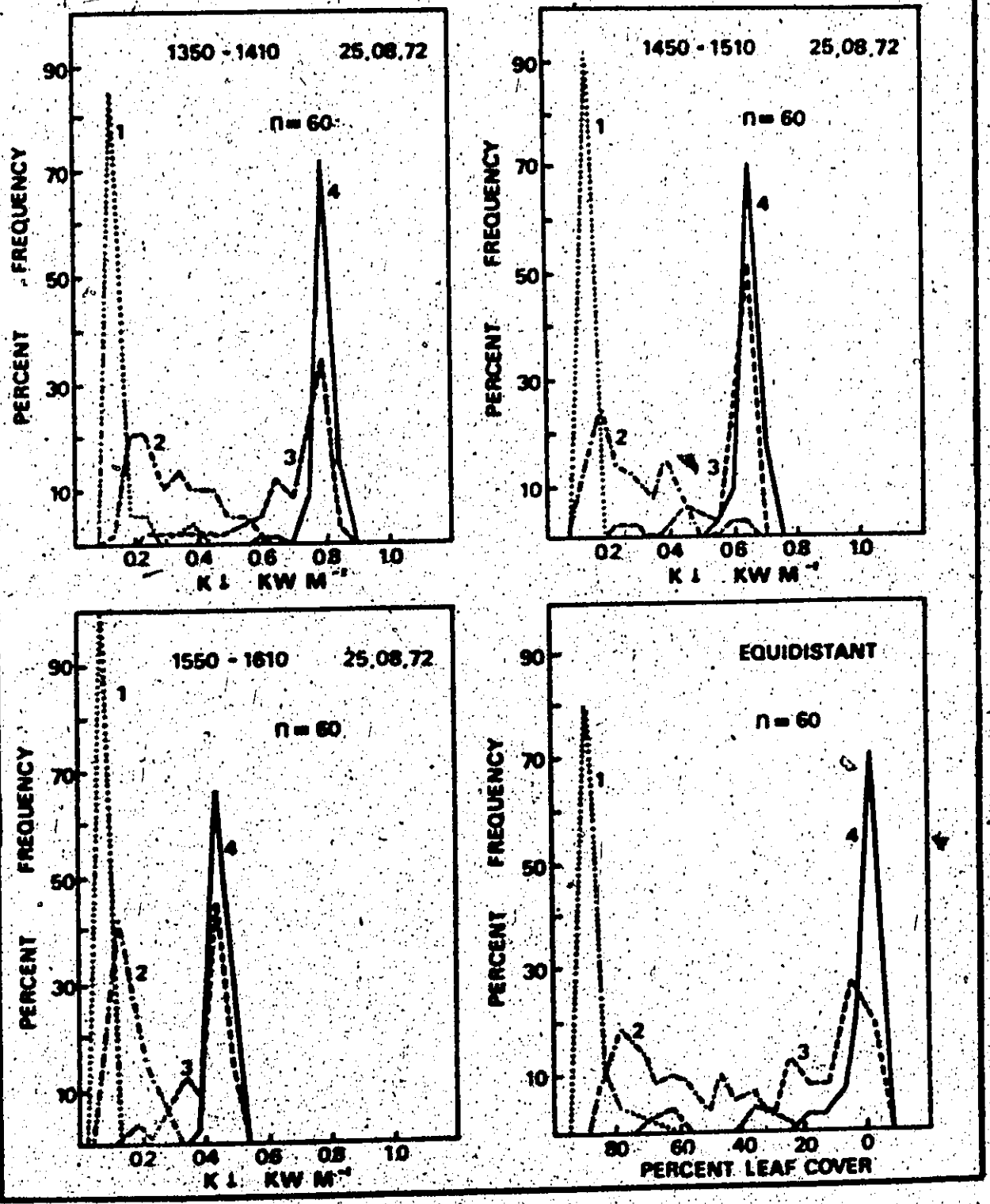

sunfleck. The upper of the two levels has a greater proportion of sunflecks and the lower level, a greater proportion of shade areas. At the lowest measurement height, 0.5 m, the sensor is nearly always in the shade.

The bi-modal frequency distributions also exhibit a diurnal variation. The shade flux density varies only slightly throughout the day with a value around 0.1 to 0.15 kW m^{-2}. The sunfleck flux density exhibits a diurnal trend. This trend is most marked in the upper layers of the crop and is related to solar position.

Under cloudless skies the observed frequency distributions are determined by canopy structure and solar position. To illustrate the role of the canopy in this regard, frequency distributions of percent leaf cover along each transect in the canopy were computed from field data. At each station across the transect the approximate percentage leaf area to open space above the sensor was measured by placing a grid card divided into 100 squares on the sensor mount. The number of squares in shade was expressed as a fraction of the total. This procedure was repeated at each measurement location. Because this procedure depends on solar position the study was undertaken at solar noon and the results were corrected to zero zenith angle using the cosine of the solar zenith angle at noon on the day of the investigation.

The results are presented in Figure 4 for the equidistant plot. The bi-modal nature of the frequency distributions and their similarity in shape to the frequency distributions of global radiation flux density demonstrates the strong inverse relationship between sunfleck location and the amount of leaf cover between the measurement level and

FIGURE 5. FREQUENCY DISTRIBUTIONS OF GLOBAL SOLAR RADIATION FLUX DENSITY AND OF PERCENT LEAF COVER IN ROW CORN.

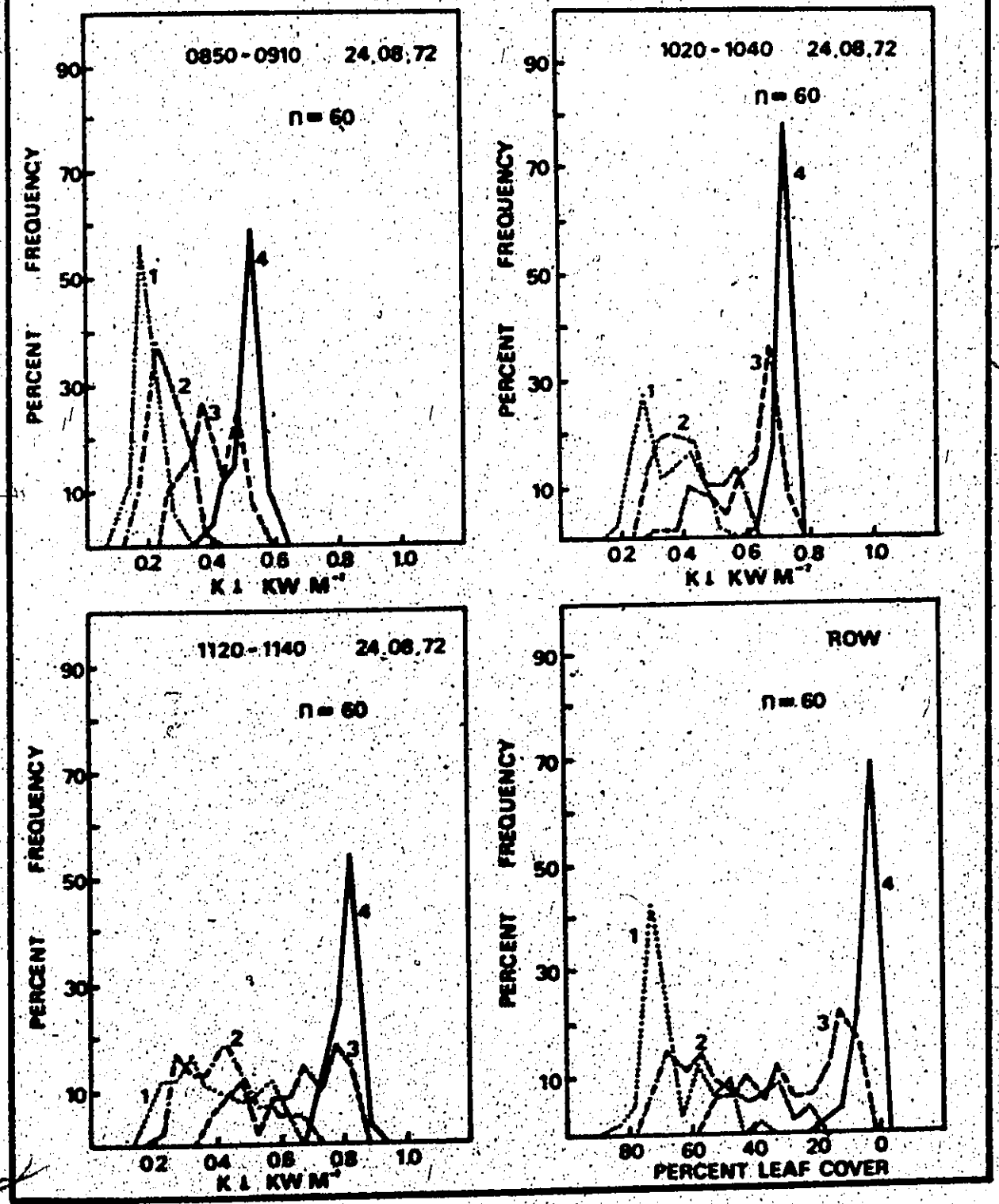

the top of the crop.

The row plot data were analysed in the same manner. Again, bi-modal frequency distributions were obtained (Figure 5). One important difference is that the row plot distributions are not as markedly bi-modal as those obtained for the equidistant plot. This is very evident for distributions near solar noon. The cause of this difference is likely to be found in the more open structure of the row plot, characterised by a lower total leaf area index and more even leaf density distribution throughout the depth of the crop. For these reasons, the probability of sunflecks at the lowest canopy height is higher, particularly at low solar zenith angles.

The distributions are again correlated with percent leaf cover distributions (Figure 5). This supports the conclusion that the frequency distributions of global radiation depend strongly on leaf cover distributions.

Figure 6 and 7 show four sample frequency distributions obtained in the two plots for net solar radiation. In both cases the frequency distributions are similar to those obtained for global radiation. In both plots, however, the bi-modal form all but disappears for distributions obtained near solar noon. This tendency is particularly strong in the row plot. This may be attributed to the more open structure of the row plot as discussed earlier or to the effect of row alignment. At solar noon in the row plot the sun is shining along the rows where there is a much lower leaf density and hence greater penetration of global radiation. This reduces the fraction of the leaves in shade and thus tends to make the distributions more uni-modal.

FIGURE 6. FREQUENCY DISTRIBUTIONS OF NET SOLAR RADIATION FLUX DENSITY IN EQUIDISTANT CORN.

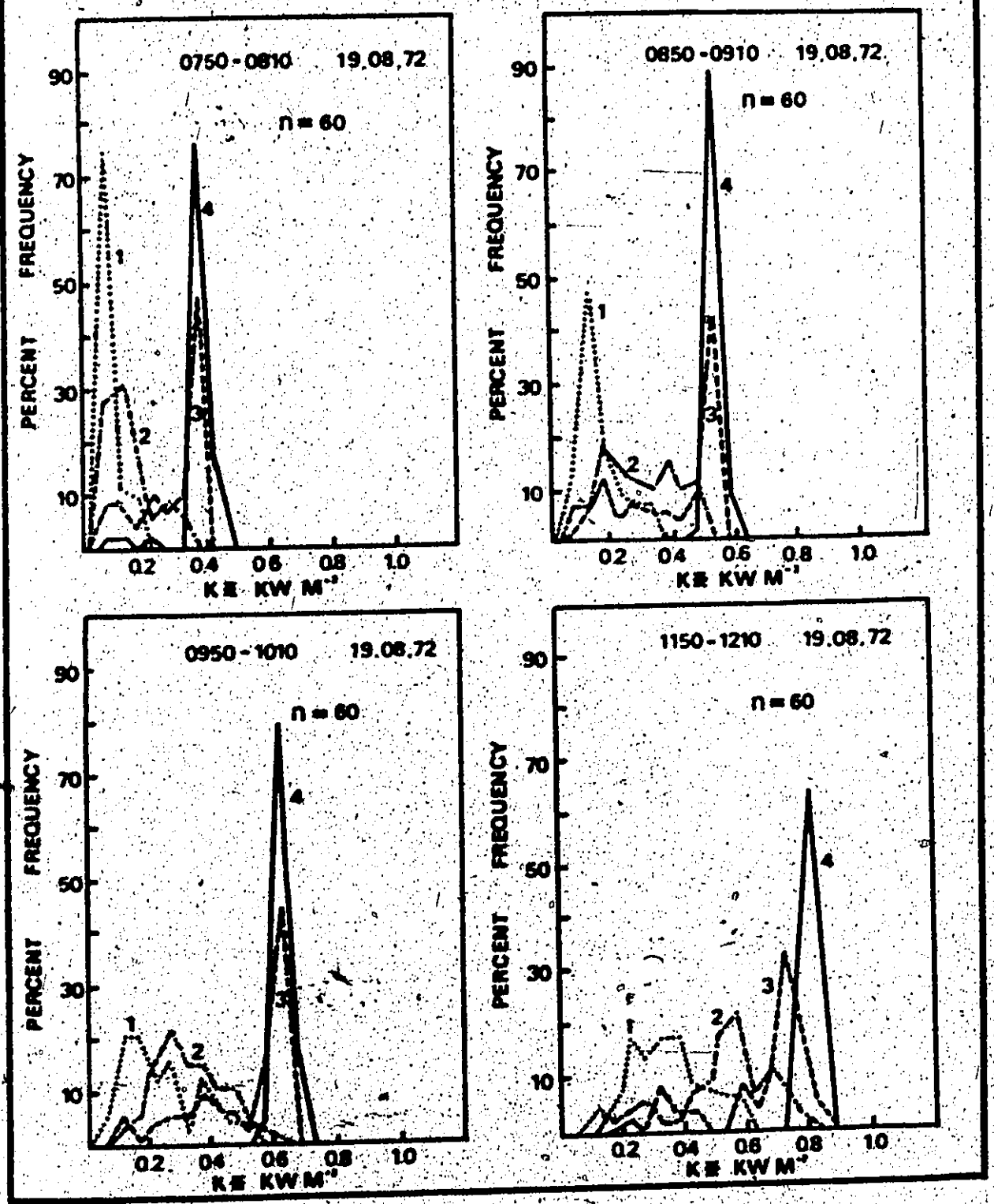

FIGURE 7. FREQUENCY DISTRIBUTIONS OF NET SOLAR RADIATION FLUX DENSITY IN ROW CORN.

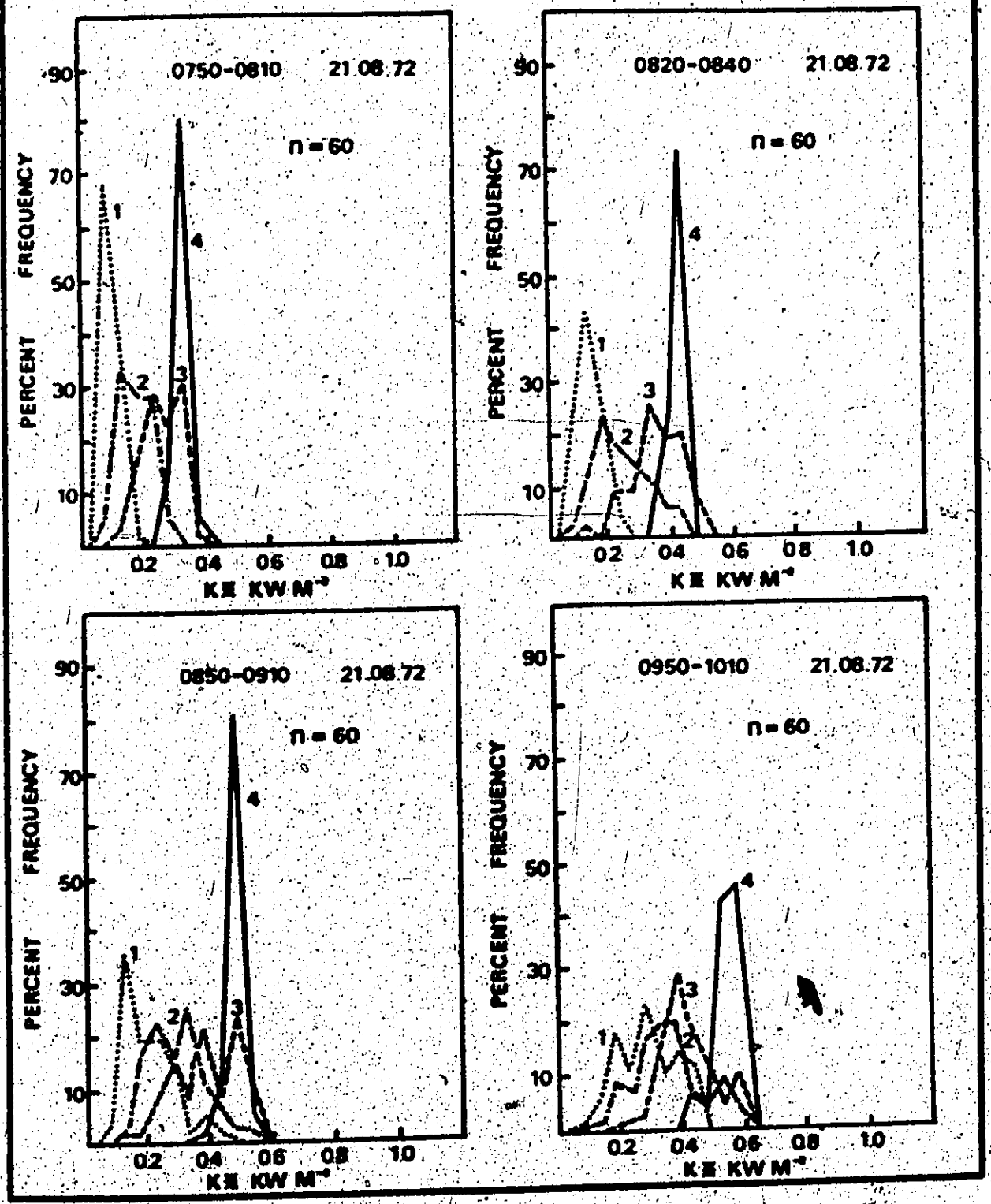

2. Net radiation

Figures 8 and 9 show four sample frequency distributions obtained in both plots. In each case there is a tendency to bi-modal distributions illustrating the dependence of net radiation on global radiation. The row plot is less markedly bi-modal suggesting that net radiation is closely related to net global radiation as would be expected from theory.

The physical basis for this relationship may be considered in terms of canopy structure. If we postulate that global solar radiation frequency distributions are controlled by the frequency distributions of sunflecks and shade area caused by leaf cover variations then the sunfleck areas will be warmer than the shade areas. In effect, local 'hot-spots' are created surrounded by cooler areas (Allen and Lemon, 1972). In the hot-spots the terrestrial radiation flux density is higher than in the surrounding areas. This process, combined with the distribution of net solar radiation leads to a net radiation distribution which is similar to that distribution.

The distribution of net radiation is not as closely linked to percent leaf cover distributions. This may be the result of the alternation of hot and cool areas causing active natural convection within the crop. This would introduce lags in the Q^* distribution. Alternatively, the phenomenon may be a feature of sensor 'memory'. Although both global and net radiation sensors were traversed at the same rate, the response time of the net radiometer is longer than that for the pyranometer (Table 1). Thus the Q^* distributions may be influenced, to some degree, by the instrument's past history as it moved along the

FIGURE 8. FREQUENCY DISTRIBUTIONS OF NET RADIATION FLUX DENSITY IN EQUIDISTANT CORN.

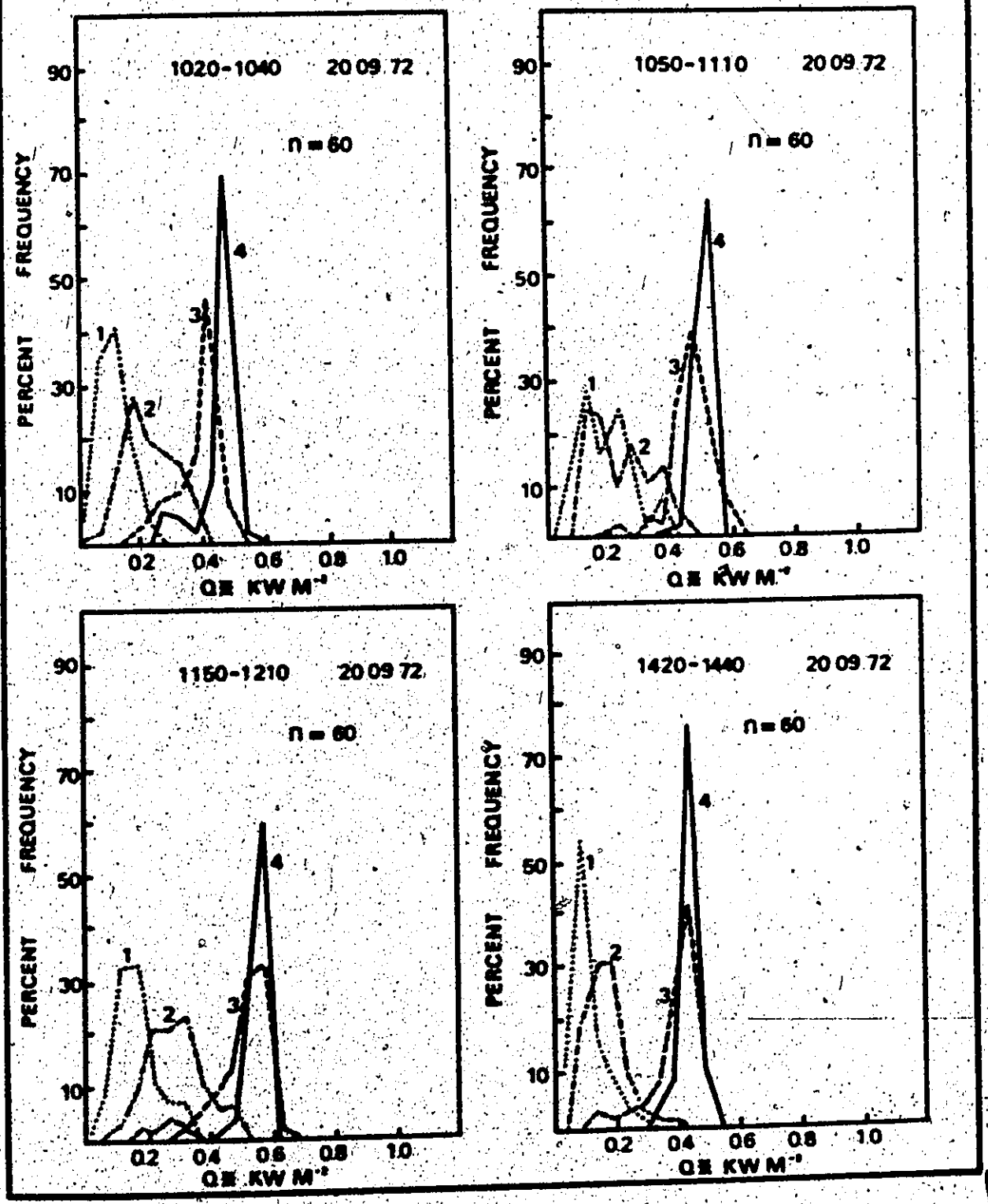

FIGURE 9. FREQUENCY DISTRIBUTIONS OF NET RADIATION FLUX DENSITY IN ROW CORN.

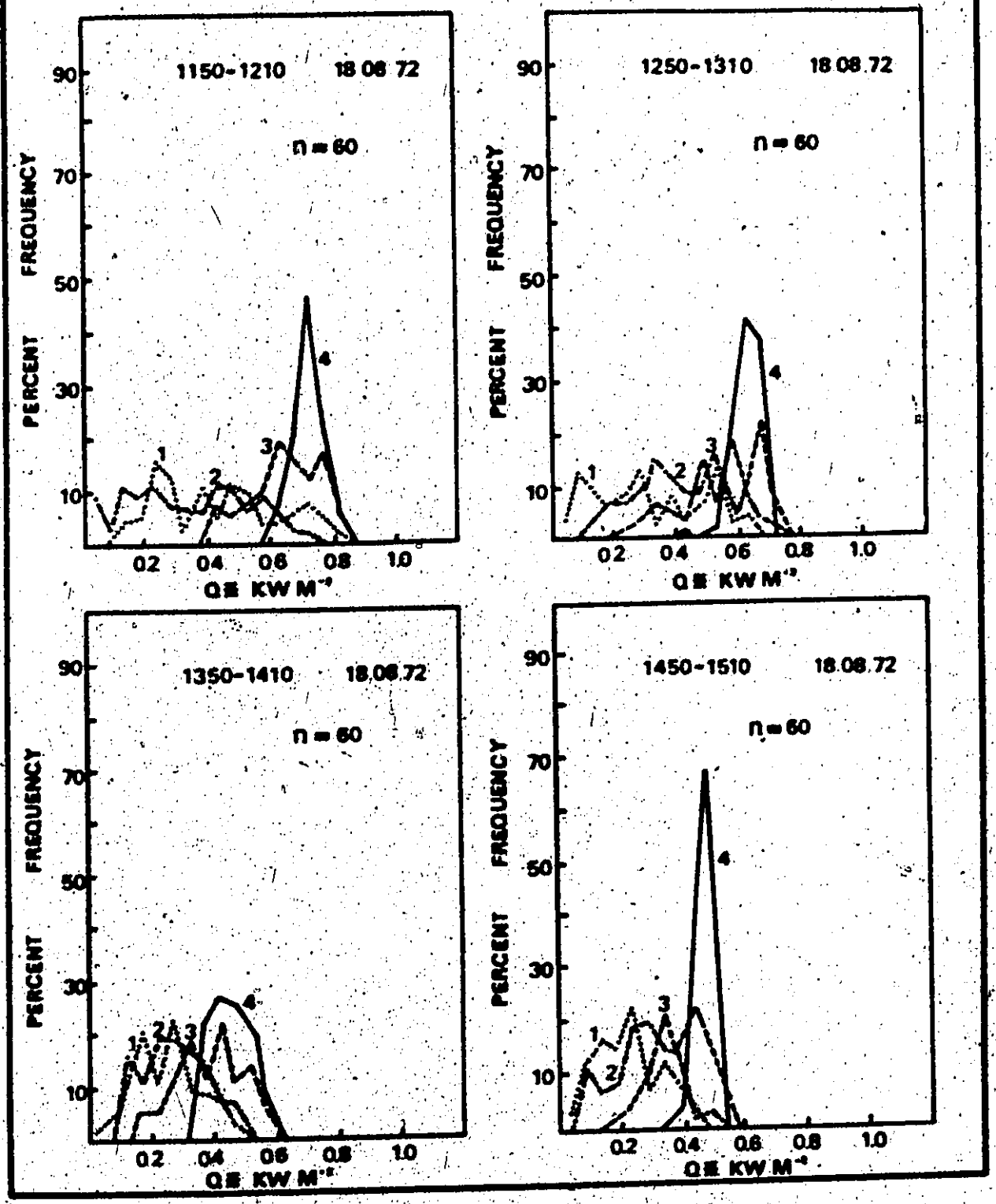

transect as well as the radiation reaching it at any specific point. However, this feature was not evident in the frequency distributions of $K^{\downarrow}$ measured by a similar sensor and the former explanation seems more likely.

In summary, frequency distributions of radiant flux density at four levels in both plots were found to be bi-modal under cloudless skies. The simplest distributions were those for global radiation which were closely correlated with frequency distributions of percent leaf cover. More complex distributions were found for net solar and net radiation. The increased complexity of these distributions has been attributed to the effect of canopy structure on reflected solar radiation and net terrestrial radiation sources and sinks within the crop.

B. Vertical radiation profile characteristics

1. Global and net solar radiation

Mean global radiation flux density profiles in both plots are presented in Figure 10. Only radiation measurements obtained under cloudless skies were used and all profiles are not presented in the diagrams in the interests of clarity. These data were not obtained on the same date so that ambient radiation conditions are slightly different. The results from both plots show similar characteristics. There is little radiation attenuation in the upper quarter of the canopy above the height (1.5 m) where leaves overlap (the transition zone). Large flux divergence occurs in the middle canopy region where leaf density is at a maximum (Figure 11 and Appendix III). The degree of attenuation

FIGURE 10. HALF-HOURLY AVERAGE GLOBAL SOLAR RADIATION PROFILES IN CORN.

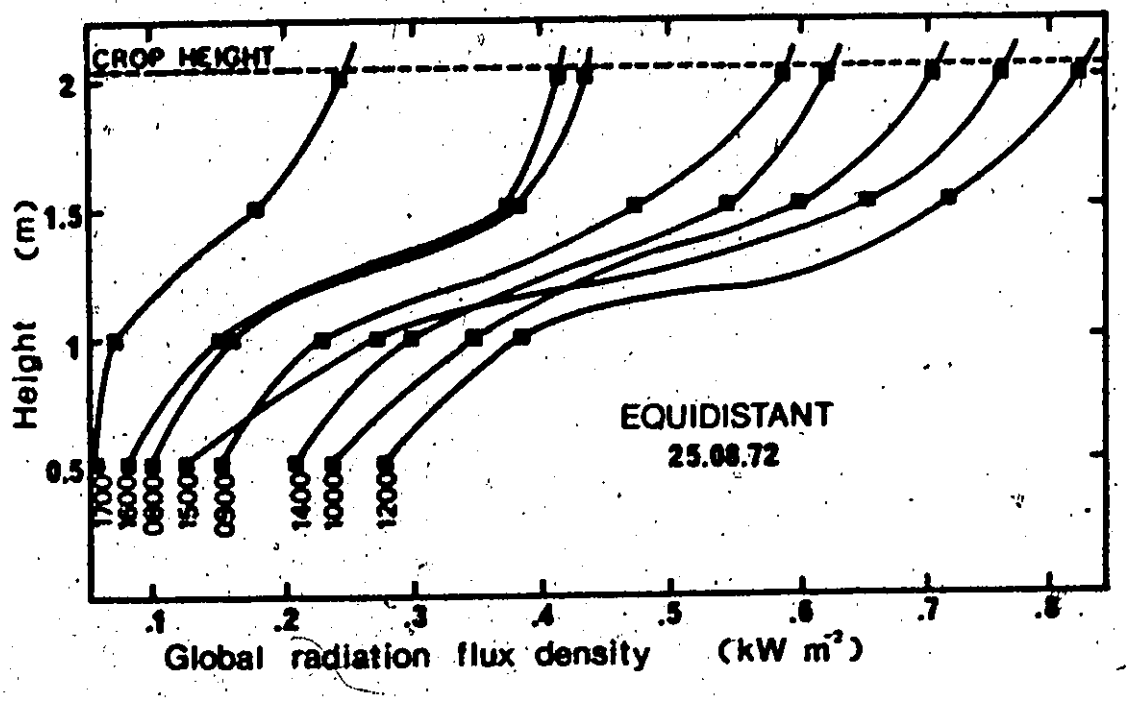

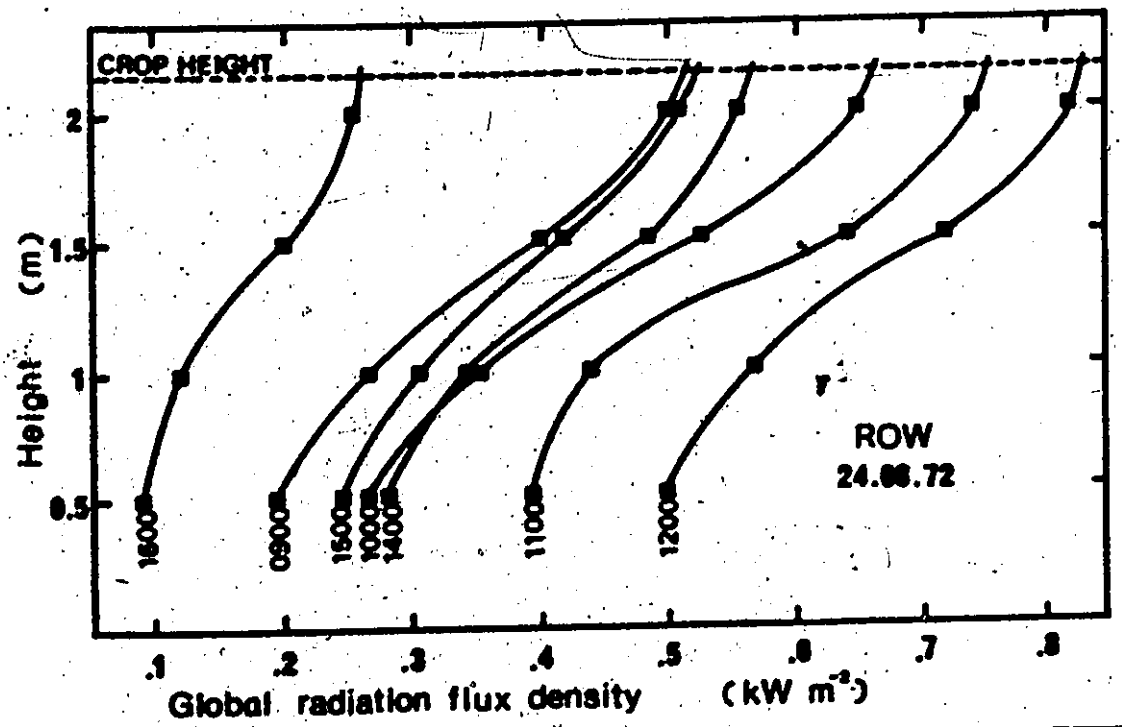

FIGURE 11. LEAF AREA INDEX & LEAF AREA DENSITY PROFILES IN ROW & EQUIDISTANT PLOTS.

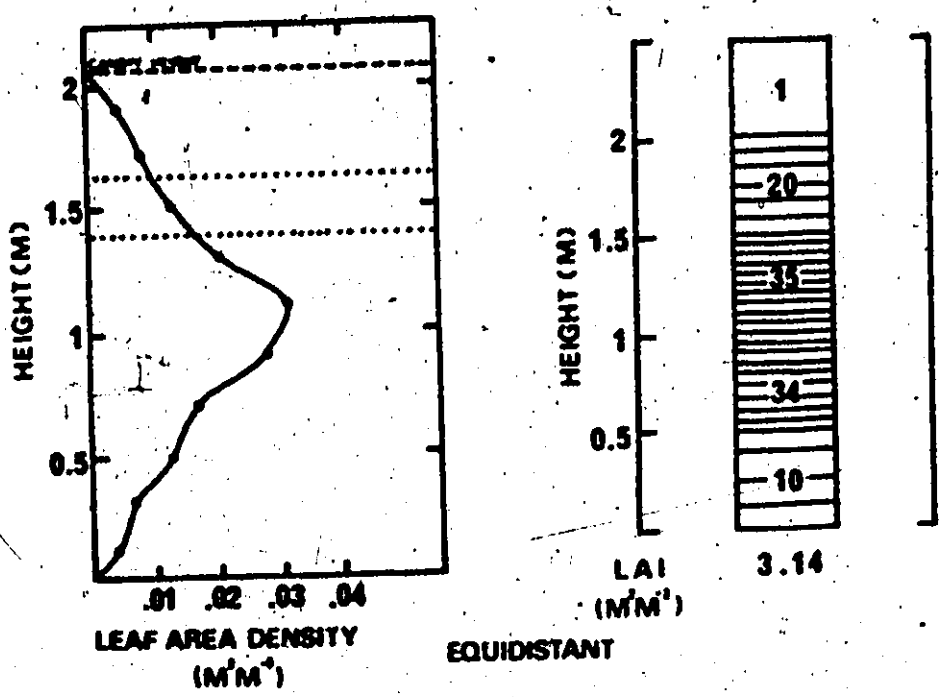

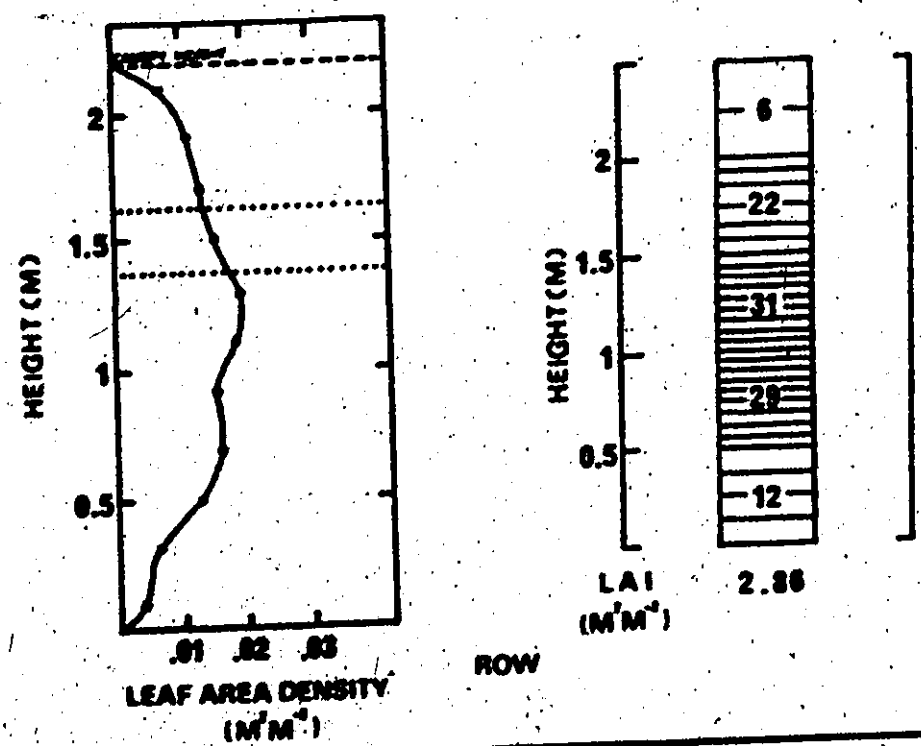

varies throughout the day and is roughly symmetrical about solar noon, showing a dependence on solar position.

The greatest attenuation in the row plot is considerably less than in the equidistant plot probably as a result of the lower foliage density in the middle zone of that plot. No specific characteristic was found in the row plot which might be attributable to influences caused by row alignment.

The vertical divergence of global radiation $\partial K\downarrow/\partial z$ gives a better indication of the vertical distribution of radiation within the crop. Figure 12 presents the divergence calculated by finite differences, $\Delta K\downarrow/\Delta z$, for a constant Δz of 20 cm. The presence of two distinct zones in the canopy is immediately apparent. Below the transition zone the canopy was complete and relatively uniform. In this complete canopy region (CCR) the divergence of global solar radiation is a function of leaf density and other crop parameters. Above the transition zone the canopy is not complete but consists of discontinuous clusters of foliage elements regularly grouped and surrounded by open space. In this incomplete canopy region (ICR), divergence of global radiation is small, particularly at low solar zenith angles. This is due to the absence of intervening attenuating material.

Figure 12 also demonstrates the lower attenuation rate in the row plot. Throughout the depth of the crop the row plot leaf area density is lower and more uniform (Figure 11). This feature influences the shape of the divergence profiles and results in lower attenuation.

Figure 13 shows mean vertical profiles of net solar radiation

FIGURE 12. GLOBAL SOLAR RADIATION FLUX DENSITY DIVERGENCE IN CORN.

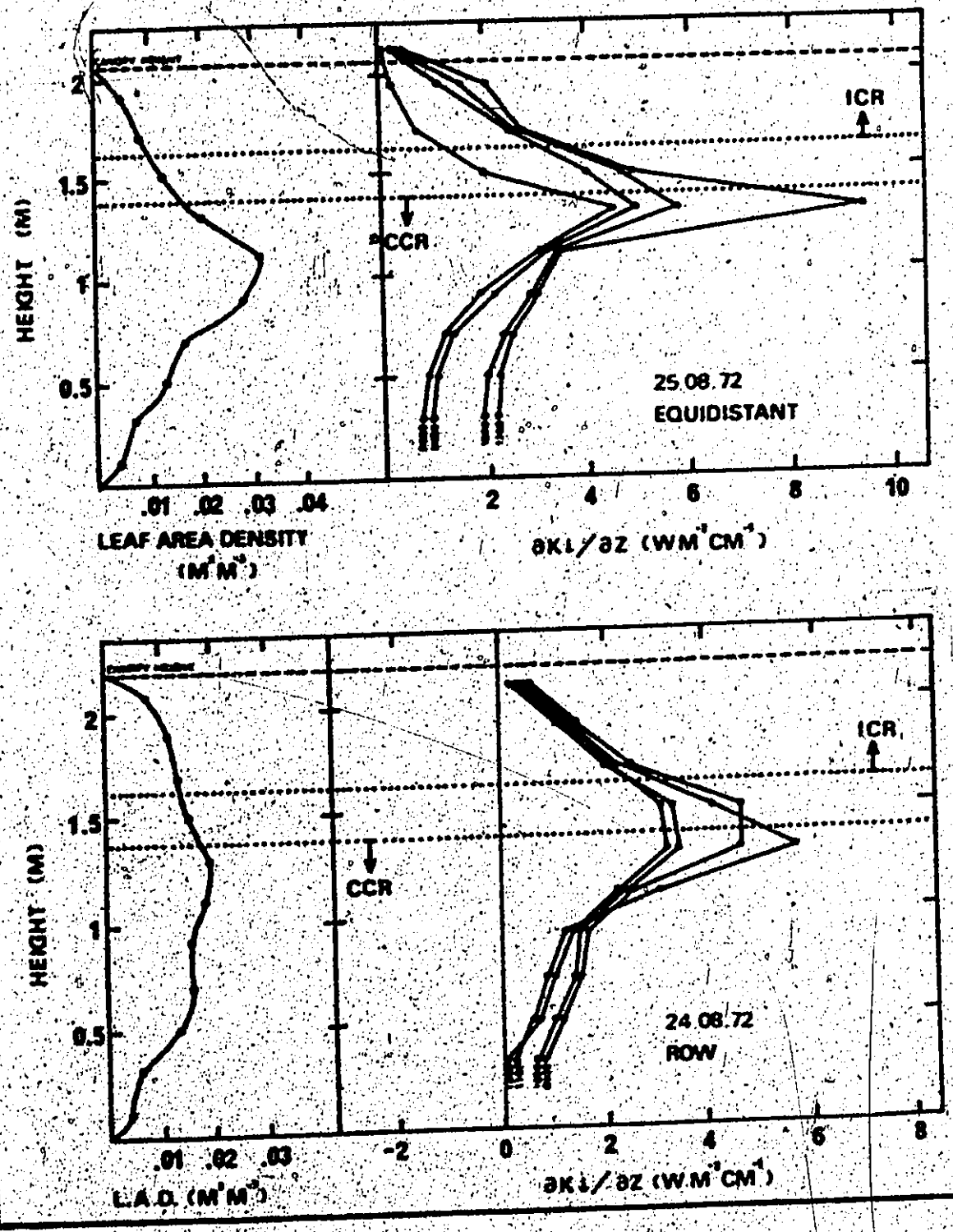

in both plots. In general, the characteristics are very similar to those presented for global radiation. Two important differences can be observed between the profiles obtained in the two plots. First, the lower attenuation rate in the row plot already referred to and attributable to lower foliage density is evident. Second, an increase in the $K^{\downarrow}$ flux density below 1 m in the row plot at solar noon is a feature which may be attributed to row alignment. At solar noon, the relative azimuth angle (the angle between the sun and the row) is zero. In effect the sun is shining along the row where the foliage area density is at a minimum. This permits greater penetration and scattering of the radiation within the canopy and increases the $K\uparrow$[1] flux density.

The vertical divergence, $\partial K^{\downarrow} / \partial z$, is shown in Figure 14. As before two distinct zones are apparent. Comparison of Figures 12 and 14 indicates two major differences. First, the maximum flux density divergence of net solar radiation is 60 percent lower than for global radiation. Second, the zone of maximum divergence occurs at a higher level in the canopy for net solar radiation. Both of these features are due to the reflected solar radiation flux density divergence. If this is not constant throughout the depth of the canopy then the upward flux of reflected radiation from various depths in the crop will alter and the relative shapes of the global and net solar radiation profiles will be different.

---

[1] upward solar radiation reflected by the earth's surface, and diffused by the atmospheric layer between the ground and the point of observation.

FIGURE 13. HALF-HOURLY AVERAGE NET SOLAR RADIATION PROFILES IN CORN.

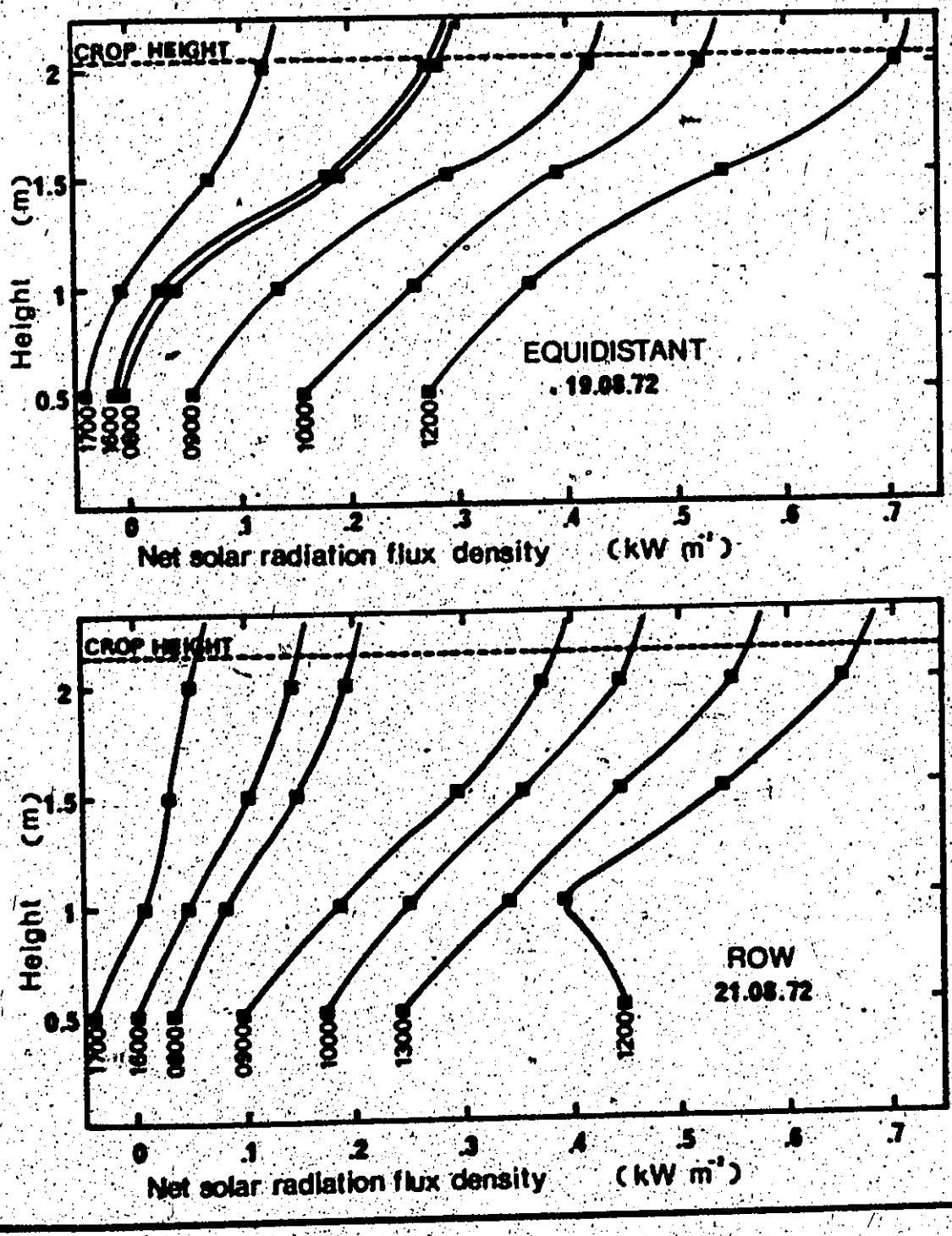

FIGURE 14. NET SOLAR RADIATION FLUX DENSITY DIVERGENCE IN CORN.

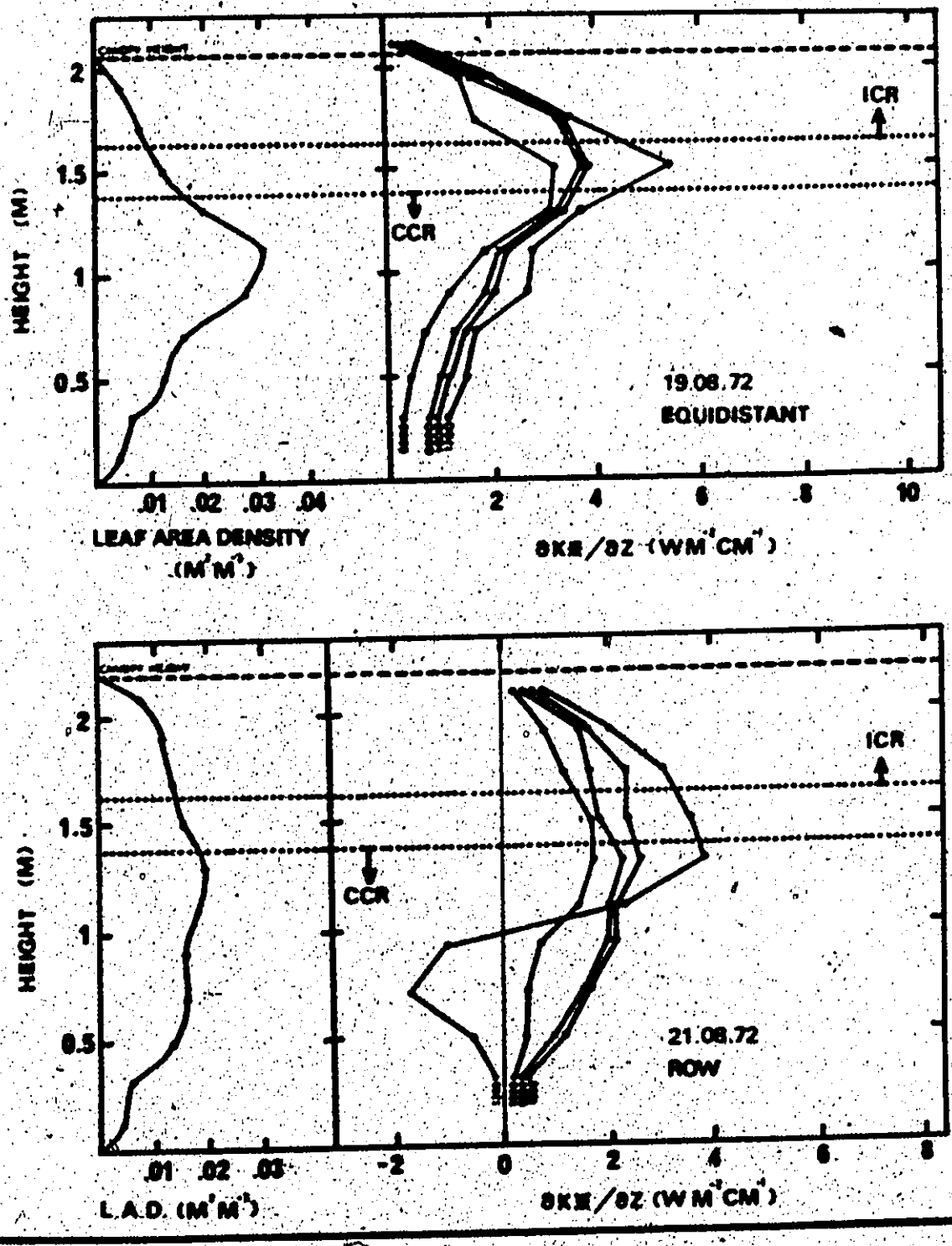

2. Net radiation

Figure 15 presents mean vertical net radiation flux density profiles in both plots. In common with profiles of $K\downarrow$ and $K^{\uparrow}$, they exhibit a diurnal trend and greatest vertical divergence in the middle canopy region. They do not, however, show as high a degree of symmetry about solar noon. In the afternoon, the canopy elements will be at a higher temperature due to the absorption of global radiation. This will tend to increase the upward terrestrial radiation flux and cause assymetry in the net radiation profiles. An anomaly in the row plot, which may be attributed to row alignment, is apparent in the period close to solar noon. The increase in $K^{\uparrow}$ flux density at this time plus the consequent local heating deeper in the canopy could result in an increase in net terrestrial radiation $L^{\uparrow}$ and thus increase the net radiation flux.

The vertical divergence profiles, $\partial Q^{*} / \partial z$, for both plots (Figure 16) reflect this dependence on canopy structure. With the exception of the noon profile in the row plot, all others are similar. The noon profile in the row plot exhibits the increase in flux density (negative $\partial Q^{*} / \partial z$) postulated in the previous paragraph to be a result of local heating of the foliage elements deep within the crop at this time.

C. Specification of a representative profile

The amount of information which can be extracted from mean profiles is limited. Even under cloudless skies the flux density of radiation on a horizontal plane below the top of the canopy varies

FIGURE 15. HALF-HOURLY AVERAGE NET RADIATION PROFILES IN CORN.

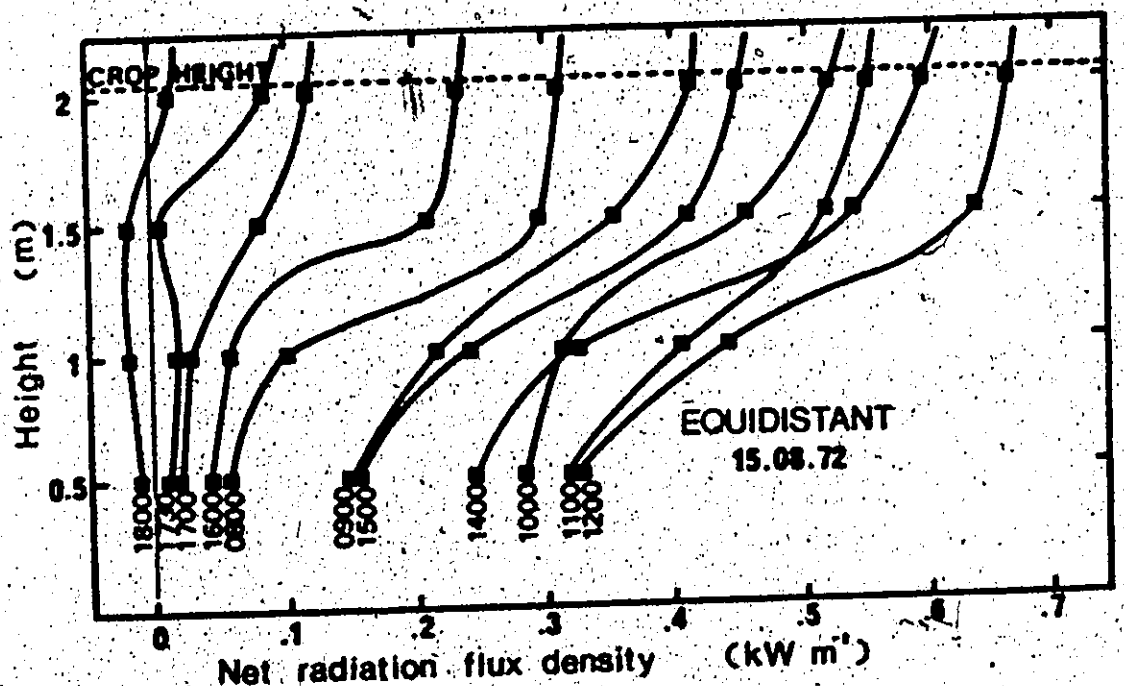

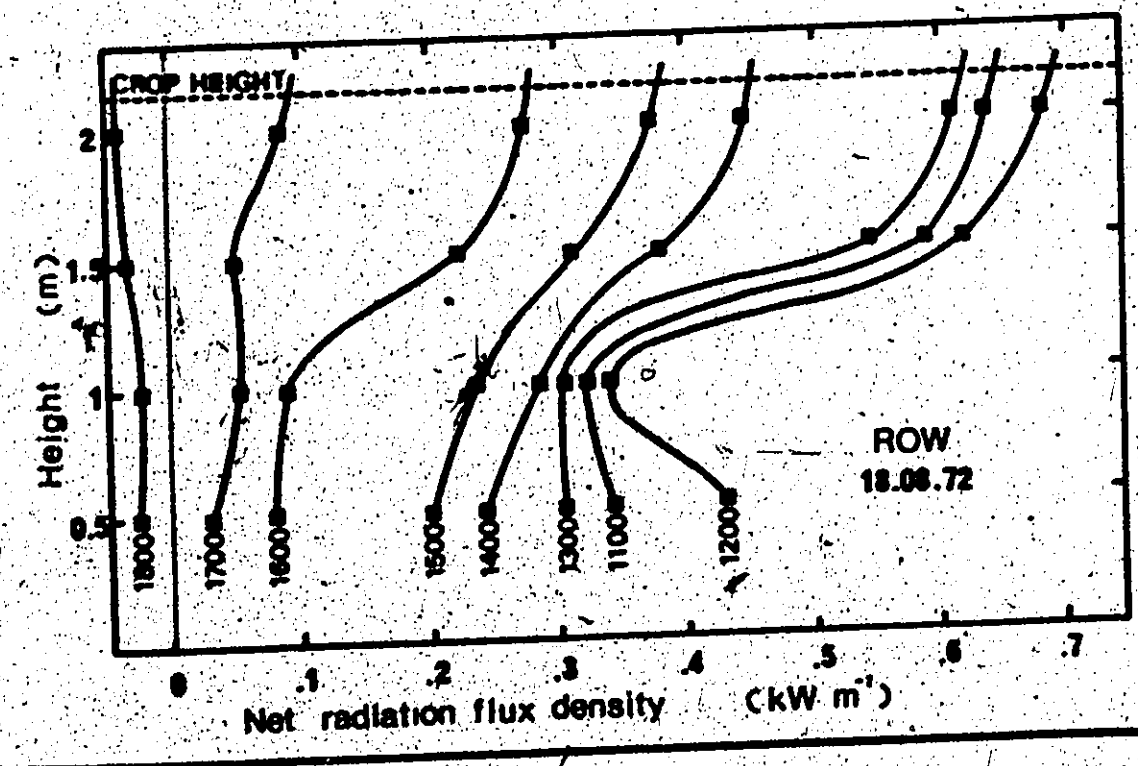

FIGURE 16. NET RADIATION FLUX DENSITY DIVERGENCE IN CORN.

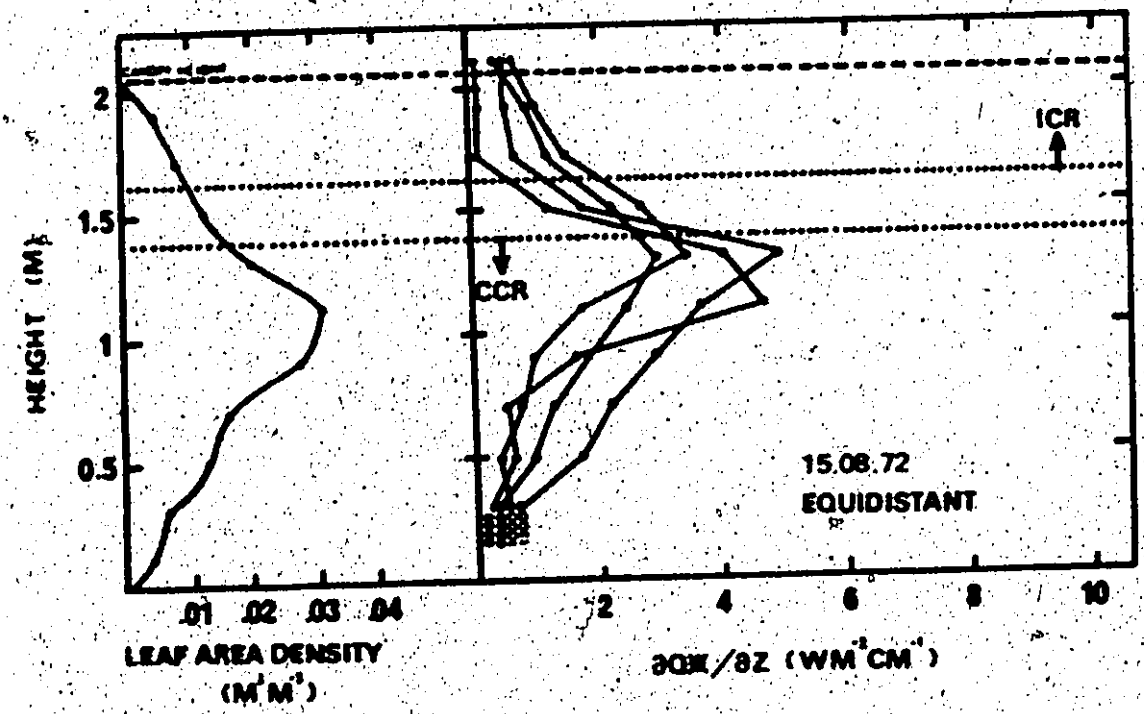

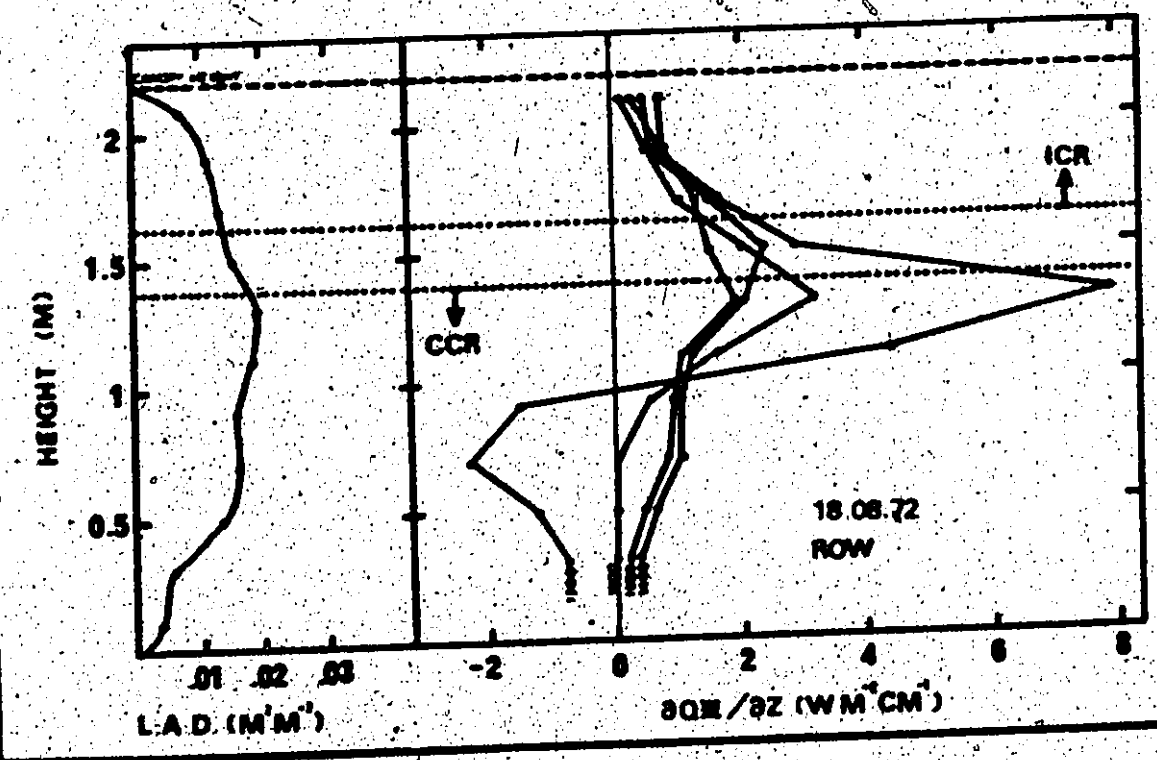

considerably due to the distribution of sun and shade resulting from the heterogeneous nature of the foliage distribution. As a result of the observed frequency distributions of radiation the validity of the mean profile as a representative value for the 'average' flux density at any height in the crop can be questioned.

Theoretical studies by Mototani (1968), Norman, Miller and Tanner (1971) and Miller and Norman (1971) and the experimental evidence presented in this study and by Allen and Lemon (1972) enable some general conclusions concerning the horizontal spatial variability of radiation fluxes within a crop to be made. First, variability is greatest when the ratio of direct to diffuse radiation is highest. Under cloudy skies, when the diffuse component is large, variability is considerably reduced. Second, the distribution of sunflecks and shade area is not random but is determined by the frequency distribution of percent leaf cover. As a result the flux density distribution in the upper region is strongly negatively skewed. This means that the greatest frequency of occurrence is at flux densities representative of sunflecks. In the lower part of the crop, the distribution is positively skewed with the greatest frequency of occurrence at flux densities corresponding to shade areas. In these cases a suitable measure of central tendency, other than the arithmetic mean, may have to be used.

CHAPTER 5

EVALUATION OF THE EXPONENTIAL MODEL AND A PROPOSED MODIFIED EXPONENTIAL MODEL

A. The exponential model, results and evaluation

The extinction coefficient in the Monsi and Saeki (1953) exponential model was computed for half-hourly profiles of $K\downarrow$, $K^{\uparrow}$ *and* $Q^{\uparrow}$ in both plots from the slope of the regression line relating the logarithm of $K\downarrow_z/K\downarrow_h$, $K^{\uparrow}_z/K^{\uparrow}_h$ and $Q^{\uparrow}_z/Q^{\uparrow}_h$ to the downward cumulative leaf area index with the intercept constrained at zero. There was a pronounced diurnal variation in the extinction coefficient, as shown previously in other work (Impens and Lemeur, 1969; Kyle, 1971; McCaughey and Davies, 1974). This is shown in Figure 17 and Table 5 and is due to the changing path length of direct solar radiation in the canopy during the day.

A plot of all the data in the equidistant plot (Figure 18) demonstrates that, in the incomplete canopy region, there are substantial deviations from an ideal exponential model behaviour, particularly in the case of $K\downarrow$ and $Q^{\uparrow}$. Similar results were obtained in the row plot. This deviation implies significant departure from a random distribution of foliage elements in this zone. The pronounced clustering of foliage elements in the incomplete canopy region leads to little attenuation of radiation. The downward cumulative leaf area index over-estimates

FIGURE 17. DIURNAL VARIATION OF THE EXPONENTIAL MODEL EXTINCTION COEFFICIENT.

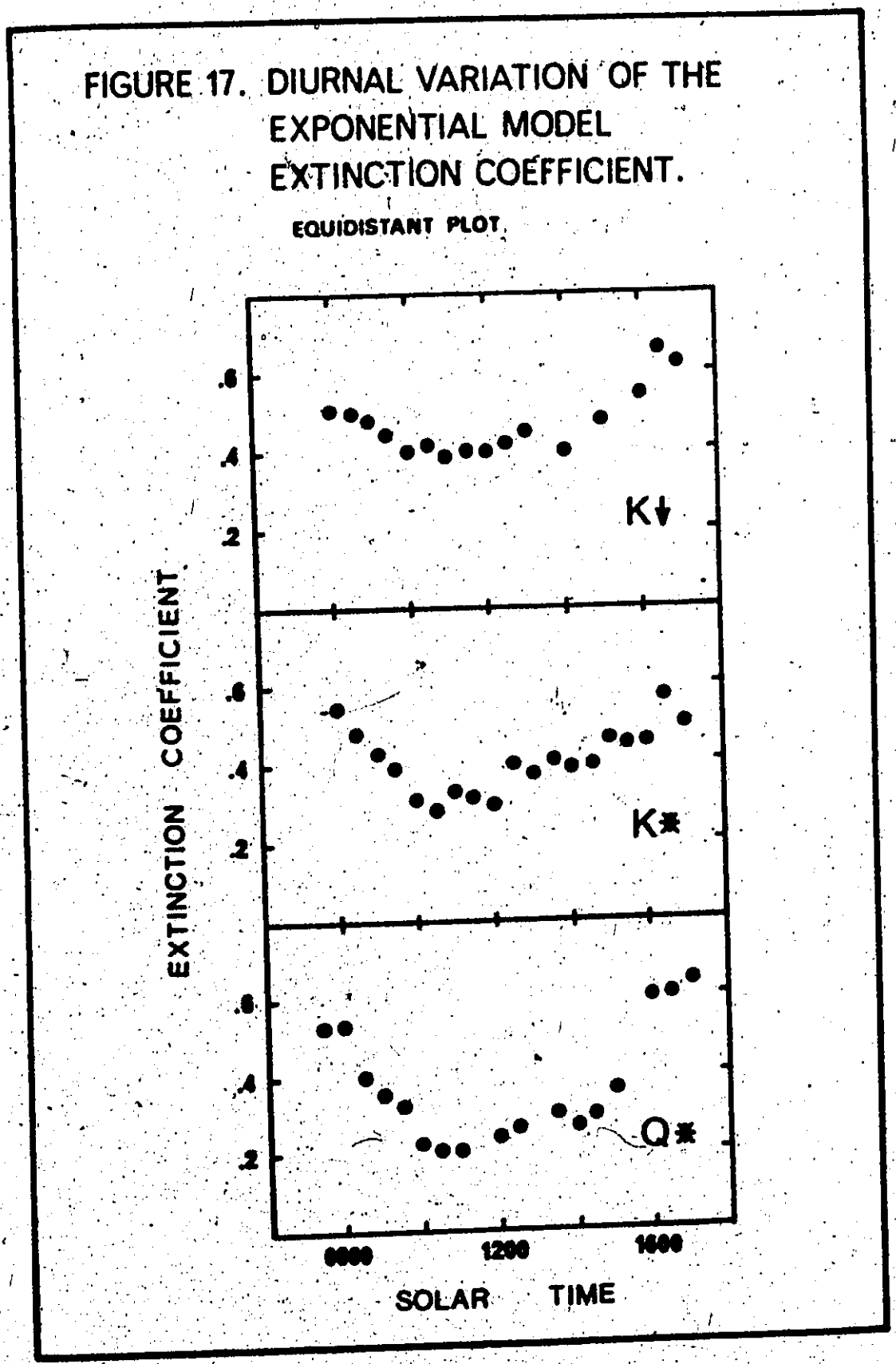

TABLE 4. Diurnal variation in the exponential model extinction coefficient for $K\downarrow$, $K^{\uparrow}$ and $Q^{\uparrow}$ in both plots

ROW				EQUIDISTANT		
$K\downarrow$	$K^{\uparrow}$	$Q^{\uparrow}$	TIME	$K\downarrow$	$K^{\uparrow}$	$Q^{\uparrow}$
--	--	—	0730	--	—	-.532
--	-.451	—	0800	-.515	-.553	-.535
-.416	-.381	—	0830	-.500	-.476	-.400
-.419	-.342	—	0900	-.479	-.430	-.352
-.350	-.332	—	0930	-.453	-.392	-.327
-.357	-.290	—	1000	-.404	-.313	-.234
-.302	-.225	—	1030	-.426	-.290	-.214
-.280	-.298	—	1100	-.390	-.336	-.214
-.311	—	-.354	1130	-.405	-.329	—
-.315	-.305	-.386	1200	-.404	-.305	-.242
—	—	-.445	1230	-.424	-.413	-.267
—	-.239	-.406	1300	-.440	-.379	—
-.322	-.281	-.346	1330	—	-.416	-.304
-.319	—	-.302	1400	-.405	-.394	-.273
-.331	-.282	-.272	1430	—	-.398	-.296
-.300	-.307	-.266	1500	-.468	-.464	-.362
-.353	-.348	-.323	1530	—	-.456	—
-.399	-.356	-.458	1600	-.555	-.459	-.602
-.442	-.423	—	1630	-.665	-.578	-.603
-.463	-.370	—	1700	-.637	-.504	-.640

FIGURE 18. COMPARISON OF EXPERIMENTAL & EXPONENTIAL MODEL FLUXES OF K↓, K*, & Q* (EQUIDISTANT).

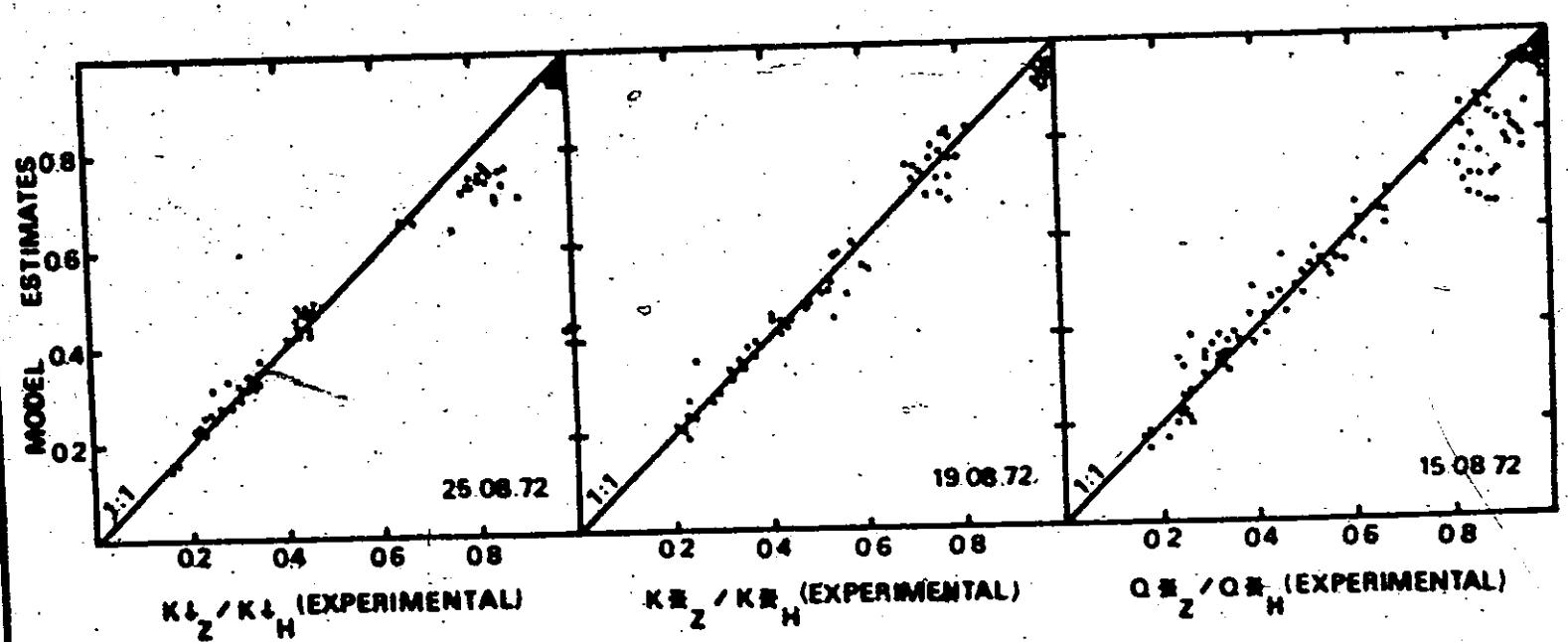

the amount of foliage available for interception in this zone.

From these findings it is clear that the decrease of radiation through the crop cannot be described by the simple exponential model. Both shortcomings reduce the value of the model for estimating short-term (half-hourly) fluxes of $K\downarrow$, $K^{\uparrow}$ and Q^{*} in a crop.

B. A modified exponential model

1. Theory and development

A modified exponential model was developed to account for these disadvantages of the exponential model. To correct for under-estimation in the incomplete canopy region an effective foliage area index f' is defined:

$$f' = \lambda f , \qquad (9)$$

where λ is a function of the degree of clustering of the foliage elements (Hototani, 1968). In the incomplete canopy region $\lambda < 1$ and $f' < f$. Below the transition zone where there is no clustering of the foliage elements $\lambda = 1$ and $f' = f$.

The diurnal variation is accommodated using the solar zenith angle, since it determines the solar beam path length through the vegetation. Diffuse radiation is independent of path length. Hence, $-k f'$ is corrected by sec ζ Δ where Δ is the fraction of direct solar radiation in the global radiation flux.

This modification still assumes that the leaves of a crop are horizontal and randomly distributed in space. Following Acock, Thornley and Warren Wilson (1970) non-randomness can be ignored in mature corn

canopies. The leaves, however, are not horizontal (Appendix III) and the use of the solar zenith angle assumes that this is the case.

A relative zenith angle ξ is defined as:

$$\xi = (\zeta - \beta') \qquad (10)$$

in which β' is a normalised leaf angle equal to $(\beta - \zeta')$ where ζ' is the minimum zenith angle attained on a given day. ξ is therefore the angle between the solar beam (angle of penetration) and the mean leaf angle of the foliage elements β, re-oriented from the horizontal plane to a plane normal to the maximum angle of incidence of the solar beam β'. This latter angle depends on latitude and time of year.

The final form of the modified exponential model is:

$$H_z / H_h = \exp(-\kappa f' \sec \xi \Delta), \qquad (11)$$

where κ is an extinction coefficient.

2. Evaluation

The modified exponential model was evaluated using field data for both plots. Cloudless sky measurements were used. Mean leaf angles for each plot were obtained from measurements of leaf inclination taken during the investigation (Appendix III). The mean leaf angle in both plots was similar, 57° in the equidistant and 56° in the row plot. Both of these values are close to the theoretical value for a spherical leaf distribution, 56.1°.

The model was tested for mean profiles of $K\downarrow$ at half-hourly intervals. The values of κ computed from equation 11 are shown in Table 6. There was no significant difference at the 95% confidence level (Student's t-test) between half-hourly values. Hence the variation in the extinction coefficient has been successfully reduced. Using the mean extinction coefficient the systematic deviations from the 1:1 line in Figure 17 disappear (Figure 19). Similar results are obtained in the row plot. These results show that this modified form of the exponential model can provide a good estimate of the mean $K\downarrow$ profile on a half-hourly basis if an extinction coefficient can be assigned.

The values of the extinction coefficient obtained for $K^{\star}$ and $Q^{\star}$ were significantly different at the 95% level. The poorer performance of the model for $K^{\star}$ and $Q^{\star}$ is attributable to the absence of parameters controlling reflected solar radiation and net terrestrial radiation. In the case of $K\downarrow$ the reduction in flux density with depth is an attenuation, but for $K^{\star}$ and $Q^{\star}$ it is not.

From the results presented it is shown that the modified exponential model as formulated provides a useful method of eliminating the major deficiencies of the basic model. However, only if the same or similar values for the extinction coefficient are found for other corn crops is the model a useful predictive tool. In addition, the near constancy of the extinction coefficient must be demonstrated for other crops in other locations. The second point raised by these results concerns which profile is to be modelled. Data were presented earlier

TABLE 5. Variation in the extinction coefficient for global radiation in row and equidistant corn plots under cloudless skies

ROW		EQUIDISTANT	
TIME	K	TIME	K
0830	0.414	0800	0.484
0900	0.435	0830	0.497
0930	0.378	0900	0.499
1000	0.396	0930	0.490
1030	0.341	1000	0.449
1100	0.320	1030	0.481
1130	0.357	1100	0.447
1200	0.361	1130	0.467
1330	0.365	1200	0.465
1400	0.355	1230	0.488
1430	0.359	1300	0.505
1500	0.315	1400	0.453
1530	0.353	1500	0.492
1600	0.378	1600	0.526
1630	0.390	1700	0.517
1700	0.379		
1730	0.349		
Mean	0.367	Mean	0.484
Standard deviation	±0.031	Standard deviation	±0.031

FIGURE 19. COMPARISON OF EXPERIMENTAL & MODIFIED EXPONENTIAL MODEL FLUXES OF K↓, K*, & Q* (EQUIDISTANT).

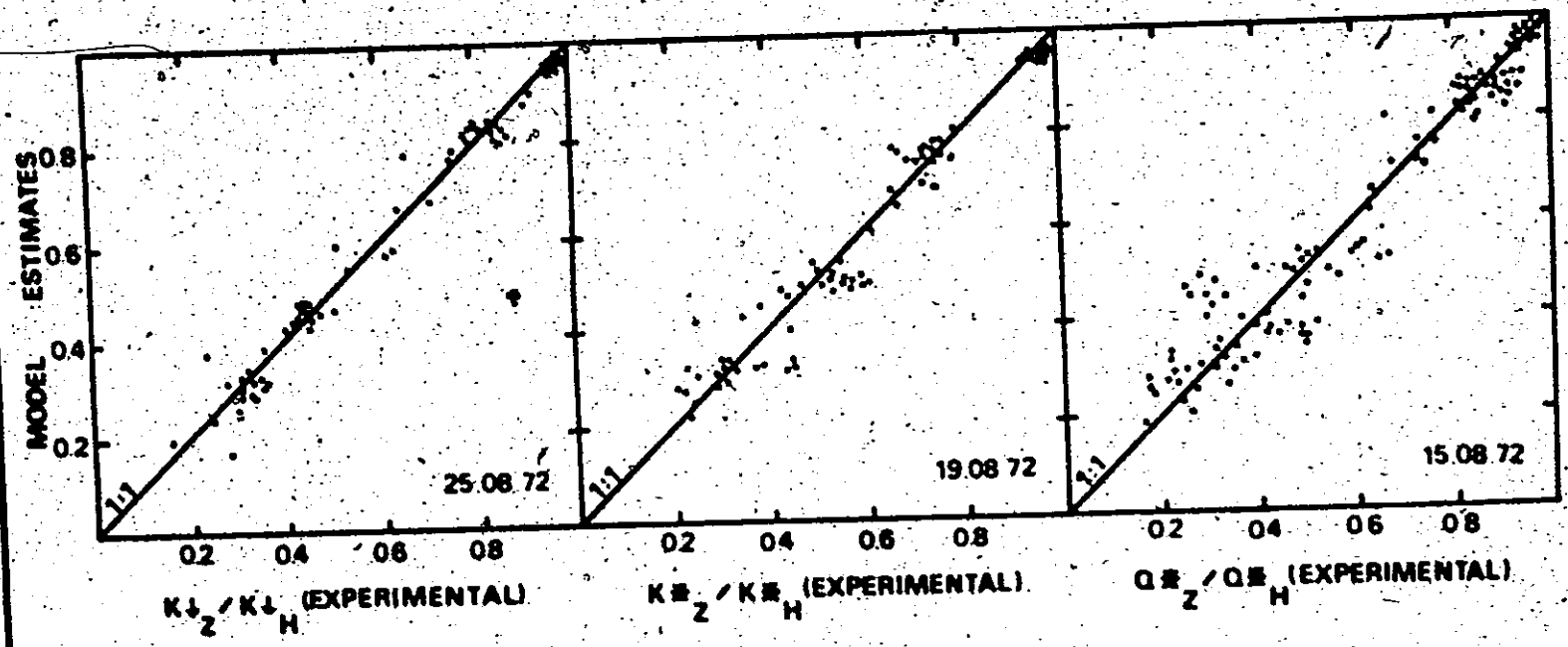

to illustrate the great variability in radiation flux densities in a crop and some comments were made on the representativeness of the mean. It is of questionable value to model the mean profile in a crop using the modified exponential model if that mean profile is not representative of the radiation regime. The model can, however, be easily adapted to estimate any other profile, since the only change will be in the value of K.

CHAPTER 6

MODELLING THE RADIATION REGIME IN A CROP CANOPY

A theoretical model of the radiation regime in a crop canopy has the advantage that the model flux densities are independent of the data used for evaluation. Although the radiation regime within a crop is complex certain simplifying assumptions may be made to obtain an acceptable estimate of the canopy radiation distribution. A simple model should minimise the number of input parameters. Disadvantages arise from over-simplification (Niilisk, Nilson and Ross, 1970). However, existing models are complex and many of the necessary parameters are either unmeasurable or very difficult to obtain (Duncan, Loomis, Williams and Hanau, 1967; Cowan, 1968; Kuroiwa, 1968; Anderson and Denmead, 1969). A reasonably accurate, though simple model based on theoretical considerations is desirable. This is the purpose of the model now presented.

A. A simple layer model for global and net solar radiation (SOLCOMP)

1. Theory and development

The model provides estimates of global solar and net solar radiation in a canopy by a layer method analogous to models of radiation attenuation in the atmosphere (Nunez, Davies and Robinson, 1971). Plant parameters contributing to the attenuation are considered an integral part of the process in each layer. Individual leaf properties rather than canopy properties are used for absorptance, reflectance and

transmittance. Absorption spectra for a corn plant and a corn plant community do not vary widely, the community absorption tending to be higher (Lemon, 1967). Canopy reflection coefficients tend to be lower than individual leaf reflectances (Monteith, 1959). The resultant sum of reflection and absorption coefficients is nearly constant for both individual corn leaves and the crop community.

The following plant properties are used: 1. effective crop leaf area index, f'; 2. leaf reflectance, α; 3. leaf absorptance, a; and 4. ground reflectance, α_g. The plant community is represented by n horizontal layers with constant effective leaf area index f'_1, f'_2, f'_3, ... f'_n over the complete depth of the canopy. The number of layers is determined by the total leaf area index, F, and canopy density S (Idso, 1968). The parameter S, introduced by Monsi and Saeki (1953), supposes that the area of leaves in each layer is S times the area of the soil ($0 < S < 1$). When $S=1$ the leaves are arranged in closed layers of $f=1$ and no radiation penetrates to the second layer of leaves. At the other extreme, when $S=0$ the leaves are considered to be infinitely small and distributed at random in the canopy space. Idso and de Wit (1970) consider $S = 0.1$ a suitable value for corn. An effective rather than a true leaf area index is used to accommodate the effect of clustering of foliage elements in the incomplete canopy region. Further consideration of this point will be given later. These horizontal layers represent the 'quantity' of attenuating material contained in each layer.

The leaves in each layer are assumed to be randomly distributed

and inclined at some mean leaf angle to the horizontal. Further, they are assumed to grow equally in all directions around individual stems and to act as Lambertian surfaces reflecting radiation non-directionally. Transmitted direct radiation is assumed to be transformed into diffuse radiation.

If I_i is the direct solar radiation ($I \cos \zeta$) and D_i is the diffuse sky radiation above the crop, then the interaction of these radiation streams as they meet a foliage layer f'_i may be considered as follows (Figure 20). The change in direct beam radiation ΔI_i has two components:

a. downward reflection of intercepted direct radiation,

$$f'_i \, (\alpha / 2) \, I_i \; ; \tag{12}$$

b. leaf absorption and upward reflection of intercepted direct radiation,

$$(- f'_i \, (\alpha / 2 + \alpha) \, I_i \, . \tag{13}$$

The total change in direct radiation is then

$$\Delta I_i = \{ f'_i \, (\alpha / 2) \, I_i - f'_i \, [(\alpha / 2 + \alpha)] \, I_i \} \sec \xi \, . \tag{14}$$

where $\sec \xi$ is a correction for foliage mass, analogous to air mass, dependent on a relative zenith angle ξ. A relative zenith angle is defined since the leaves are not horizontal but are inclined at a

FIGURE 20. SIMPLE LAYER MODEL: INTERACTION OF DIRECT AND DIFFUSE RADIATION WITH CROP CANOPY.

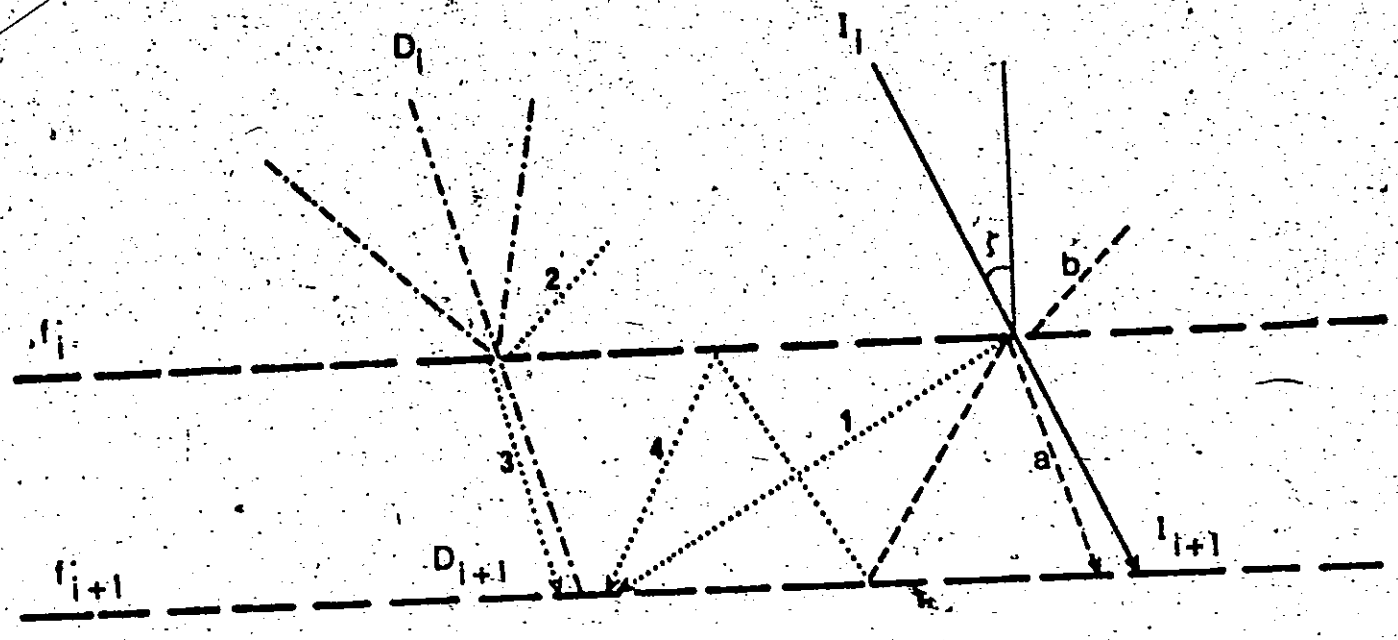

mean leaf angle β.

$$\xi = (\zeta - \beta') \quad . \tag{15}$$

In Equation 15 β' is a normalised leaf angle equal to (β - ζ') where ζ' is the minimum solar zenith angle attained on any given day. ξ is therefore the angle between the solar beam (angle of penetration) and the mean leaf angle of the foliage elements β, re-oriented from the horizontal plane to the plane normal to the maximum angle of incidence of the solar beam β'. Hence, the direct radiation incident on the layer f_{i+1} is

$$I_{i+1} = I_i + \Delta I_i \quad . \tag{16}$$

The change in diffuse radiation ΔD_i has four components:

1. intercepted direct radiation transmitted as diffuse radiation,

$$1 - (\alpha + a) \; | \Delta I_i | \; ; \tag{17}$$

2. diffuse radiation absorbed by the leaves and diffuse radiation reflected upwards,

$$- f'_i \; (\alpha / 2 + a) \; D_i \; ; \tag{18}$$

3. intercepted diffuse radiation reflected downwards,

$$f'_i \; (\alpha / 2) \; D_i \; ; \tag{19}$$

4. unintercepted direct radiation scattered within the layer,

$$\alpha f'_{i+1} \quad \alpha f'_{i} \quad I_{i+1} \cdot \tag{20}$$

The total change in diffuse radiation is given by the algebraic sum of the components as before.

$$\Delta D_i = [1 - (\alpha + a) \ |\Delta I_i|] - [f'_i (\alpha / 2 + a) D_i] + [f'_i (\alpha / 2) D_i] + [\alpha f'_{i+1} \quad \alpha f'_i \quad I_{i+1}], \tag{21}$$

and the incident diffuse radiation at the layer f'_{i+1} is

$$D_{i+1} = D_i + \Delta D_i \cdot \tag{22}$$

By incrementing I_i and D_i through each layer the global radiation profile is obtained. Flux values are calculated as the radiation passes through each layer corresponding to a known effective leaf area index.

Net solar radiation at each level is calculated by the following procedure (Figure 21). The reflected radiation from the lowest level, which incorporates the reflection from the ground, is given by

$$R_{n+1} = \alpha_g (I_{n+1} + D_{n+1}) \cdot \tag{23}$$

The reflected radiation from subsequent layers moving upward through the canopy is obtained from

FIGURE 21. SIMPLE LAYER MODEL: REFLECTED RADIATION COMPONENTS.

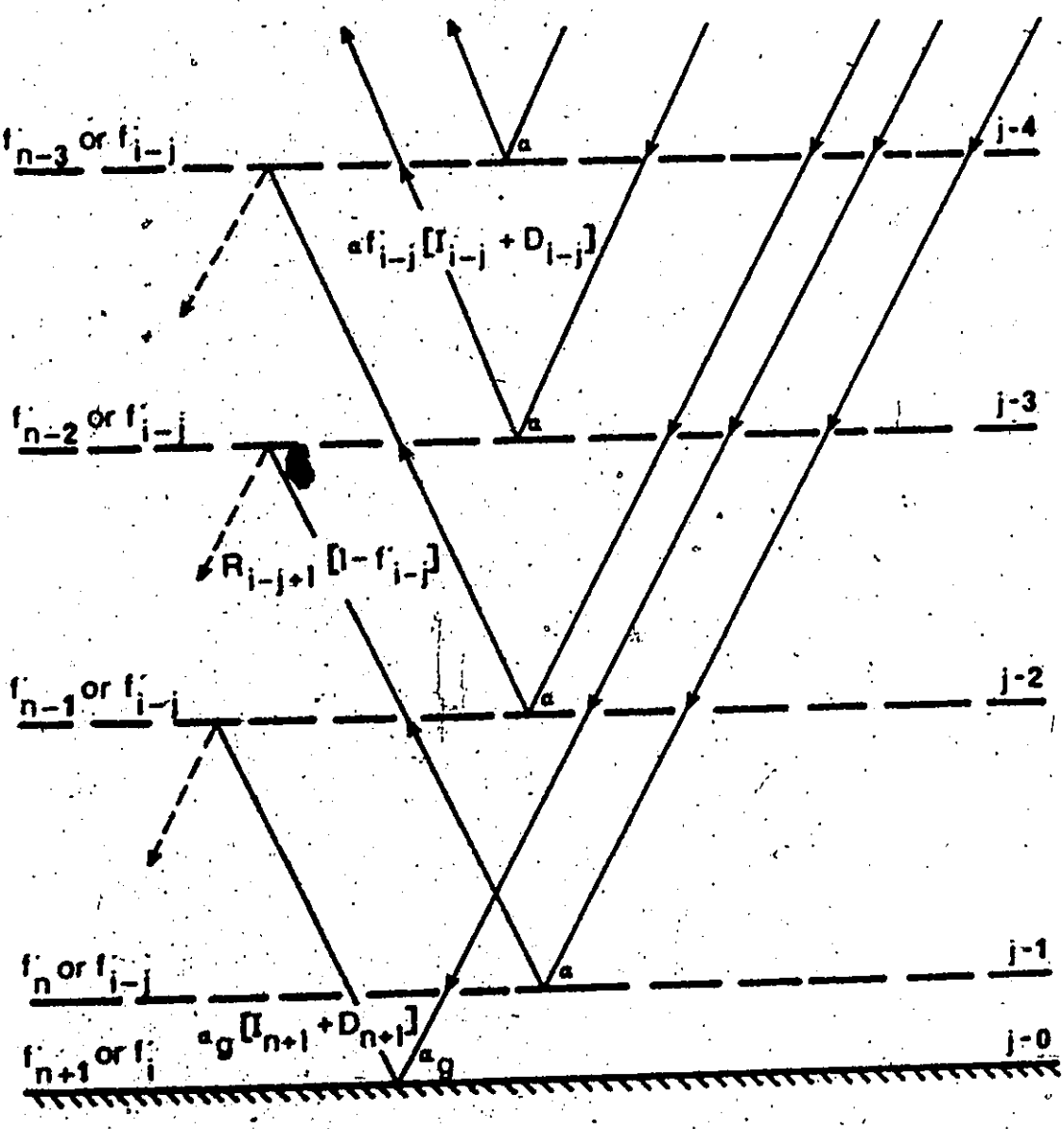

$$R_{i-j} = \alpha f'_{i-j} (I_{i-j} + D_{i-j}) + (1 - f'_{i-j}) R_{i-j+1} . \quad (24)$$

For the layer immediately above the ground $R_{i-j+1} = R_{n+1}$. The reflected radiation is subtracted from the global radiation at each level to obtain the net solar radiation profile. The crop reflection coefficient α_c is obtained from

$$\alpha_c = (K\downarrow - K^*) / K\downarrow , \quad (25)$$

where $K\downarrow$ and K^* are the global and net solar radiation calculated at the top of the crop.

The result of this series of calculations is a sequence of calculated global and net solar radiation fluxes corresponding to n horizontal layers with constant effective leaf area index f'_1, f'_2, $f'_3 \cdots f'_n$. To find the corresponding heights of these layers an effective downward cumulative leaf area index curve is constructed from the true leaf area profile. In the complete canopy region, where it is assumed that the leaves fill the canopy space, the effective leaf area index is equal to the true leaf area index. In the incomplete canopy region a 'clustering' factor is defined as the decimal fraction of horizontal area containing foliage to the total area of any horizontal plane. This 'clustering' factor g is dependent on solar zenith angle up to a maximum value of 1 to accommodate the changing proportion as the solar angle changes.

$$f' = g \sec \zeta f) . \qquad (26)$$

An example of the procedure is presented in Table 7. Once the f' values have been calculated for the incomplete canopy region the downward cumulative effective leaf area index profile is easily determined and from it the heights corresponding to f'_1, f'_2, $f'_3 \cdots f'_n$ calculated. The programs for the calculations of global and net solar radiation and for effective leaf area index are found in Appendix V. They are written in Fortran IV for a CDC 6400.

2. Evaluation

The simple layer model (SOLCOMP) was evaluated using data collected on clear days only. The model profile was compared with mean values of flux density at each level obtained from transect data.

Figure 22 shows the correlation between model and experimental values for $K\downarrow$ in both plots. The high correlation coefficients obtained in each case attest to the high predictive ability of SOLCOMP for global solar radiation. SOLCOMP over-estimates the flux density obtained from the mean profile in the upper crop and under-estimates in the lower canopy region. This observation again raises the question of the suitability of the mean profile as a representative value. Despite this reservation, the model produced a standard error of the estimate of 0.909 or 9.1% and 0.900 or 9% in the equidistant and row plots respectively. Both these figures are just within the limit of experimental error.

TABLE 6. Sample calculations of downward effective cumulative leaf area index (f'_o).

Time	sec ζ	Layer	θ	θ'	f	f'	f'_o
0800	2.01	1	0.25	0.50	0.089	0.045	0.045
19		2	0.50	1.00	0.578	0.578	0.623
08		3	1.00	1.00	1.120	1.120	1.743
72		4	1.00	1.00	1.063	1.063	2.806
		5	1.00	1.00	0.290	0.290	3.096
1100	1.20	1	0.25	0.30	0.089	0.027	0.027
19		2	0.50	0.60	0.578	0.347	0.374
08		3	1.00	1.00	1.120	1.120	1.494
72		4	1.00	1.00	1.063	1.063	2.557
		5	1.00	1.00	0.290	0.290	2.847

FIGURE 22. COMPARISON OF EXPERIMENTAL & LAYER MODEL FLUXES OF GLOBAL SOLAR RADIATION IN CORN.

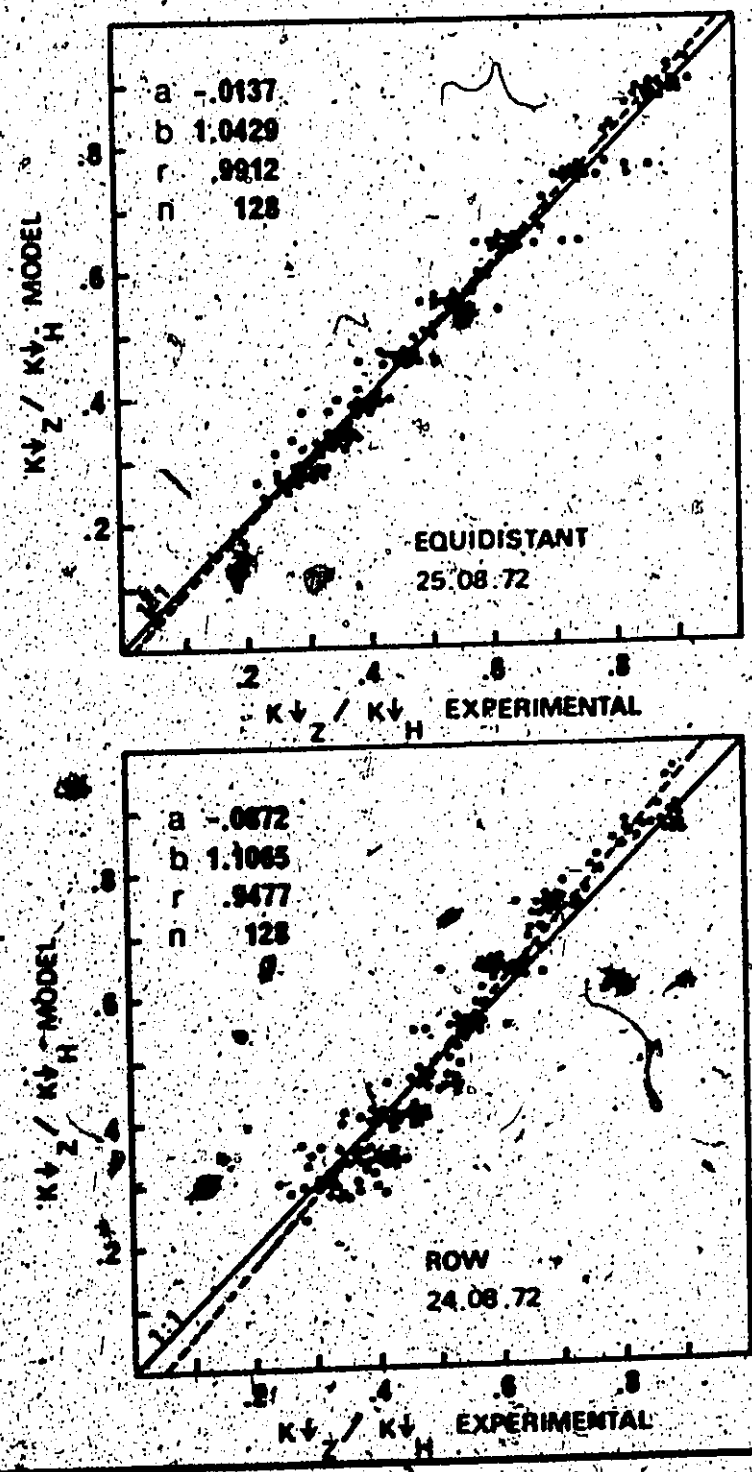

The correlation between model and experimental values of $K^{\downarrow}$ is presented in Figure 23. The increased simplification involved in the calculation of reflected radiation results in a poorer performance for net solar radiation. This is most noticeable in the lower canopy region. An important finding concerns the slopes of regression lines, 1.239 and 1.167 respectively, perhaps indicating the same problem concerning the standard of comparison.

B. A simple layer model for net radiation (NETCOMP)

1. Theory and development

The net radiation regime within a crop is more complex than the global and net solar radiation regimes because of the additional terrestrial radiation components. Since the emission temperature of the crop elements contributes to radiation in this wavelength range, variations in emission temperature will induce changes in the net terrestrial radiation flux within the crop. In practice, divergence of net terrestrial radiation within a crop canopy is often small, except in infrequent cases which are the direct result of row influences. Thus, it is probable that a simple layer model could be used to calculate net radiation in a crop.

The additional parameters required for NETCOMP are downward atmospheric radiation above the crop, $L\downarrow$[1], leaf emissivity for longwave radiation ε, and the temperature at canopy closure T_c. The model assumes that

---

[1] downward longwave atmospheric radiation (wavelengths greater than 3.0 μm), mainly emitted by the atmosphere.

FIGURE 23. COMPARISON OF EXPERIMENTAL & LAYER MODEL FLUXES OF NET SOLAR RADIATION IN CORN.

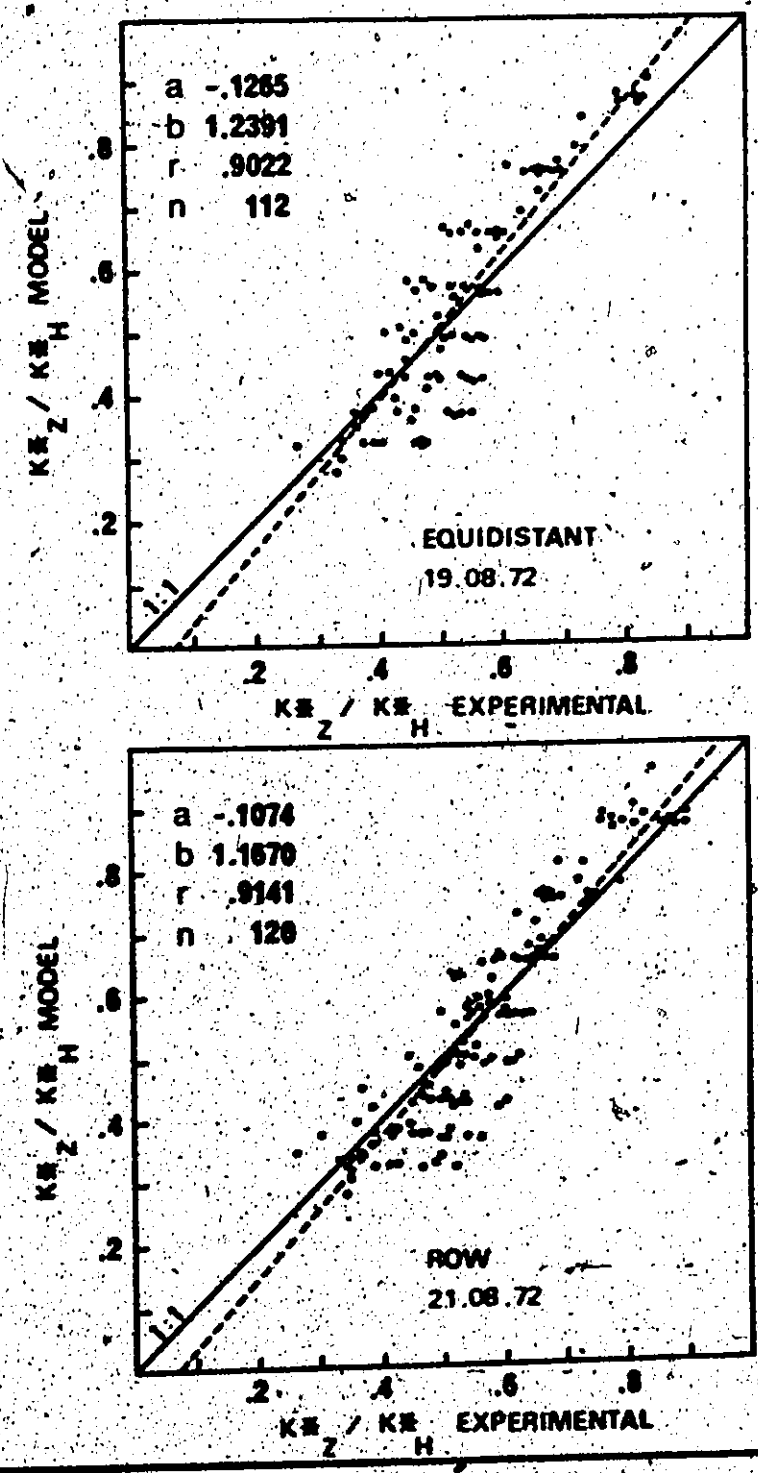

the net radiation profile can be obtained from the net solar radiation profile (SOLCOMP) by addition of the net terrestrial radiation profile. A further section is inserted in SOLCOMP to calculate net terrestrial radiation. The canopy is represented as a 'slab' emitting terrestrial radiation and reflecting downward atmospheric radiation. The temperature of emission is assumed to be the temperature measured at canopy closure and the emissivity is that obtained for individual leaves (Idso, Jackson, Ehrler and Mitchell, 1969). Since emitted terrestrial radiation is relatively insensitive to temperature of emission, the error involved in using canopy closure temperature as opposed to some unknown integral temperature of foliage elements and within canopy air space is small. Net terrestrial radiation at the top of the canopy is the

$$L^{\downarrow} = L\downarrow - (1 - \varepsilon) L\downarrow + \varepsilon \sigma T_{\sigma}^{4}) , \qquad (27)$$

where σ is Stefan Boltzmann's constant = 5.6697×10^{-8} Wm^{-2} K^{-4}. Since $\partial L^{\downarrow} / \partial z$ is assumed equal to zero, $L^{\downarrow}$ is constant throughout the canopy depth. Net radiation at each layer is then obtained from

$$Q^{\downarrow} = K^{\downarrow} + L^{\downarrow} , \qquad (28)$$

and the heights corresponding to each layer obtained as before (Appendix V).

2. Evaluation

The simple layer model for net radiation (NETCOMP) was

evaluated in the same manner as SOLCOMP (Figure 24). Immediately evident is the almost total under-estimation of the model in all cases but most noticeably in the lower half of the row plot canopy. Consider the simpler case of the equidistant plot first. Further inspection of Figure 24 reveals that in this plot there is a systematic under-estimation throughout the depth of the canopy. This feature suggests that the assumption of zero divergence of $L^{\downarrow}$ in the canopy is correct in this case, but that $L^{\downarrow}$ is of the wrong flux magnitude. Errors in $L^{\downarrow}$ may be caused by incorrect values for $L\downarrow$, ε, or T_o (equation 27). If we initially assume that ε and T_o are correct, then the error lies in $L\downarrow$. The instrument used to measure $L\downarrow$ (Eppley, pyrgeometer) is widely suspected to be in error due to absorption of solar radiation (Davies, Latimer, personal communication). If this was the case, then, assuming upward terrestrial radiation, $L\uparrow$[1], is correct, $L\downarrow$ is over-estimated. Correction of such an over-estimation in $L\downarrow$, with $L\uparrow$ unchanged, results in even lower flux densities than obtained and is therefore unlikely to be the source of the under-estimation.

Upward terrestrial radiation is determined by ε and T_o. The former parameter is unlikely to be in error. However, T_o is used to represent the emission temperature of the crop mass. If this temperature was too low by 5 - 15 K this would almost completely account for the observed under-calculation. At present, it is difficult to conduct a

---

[1] upward terrestrial surface and longwave atmospheric radiation.

FIGURE 24. COMPARISON OF EXPERIMENTAL & LAYER MODEL FLUXES OF NET RADIATION IN CORN.

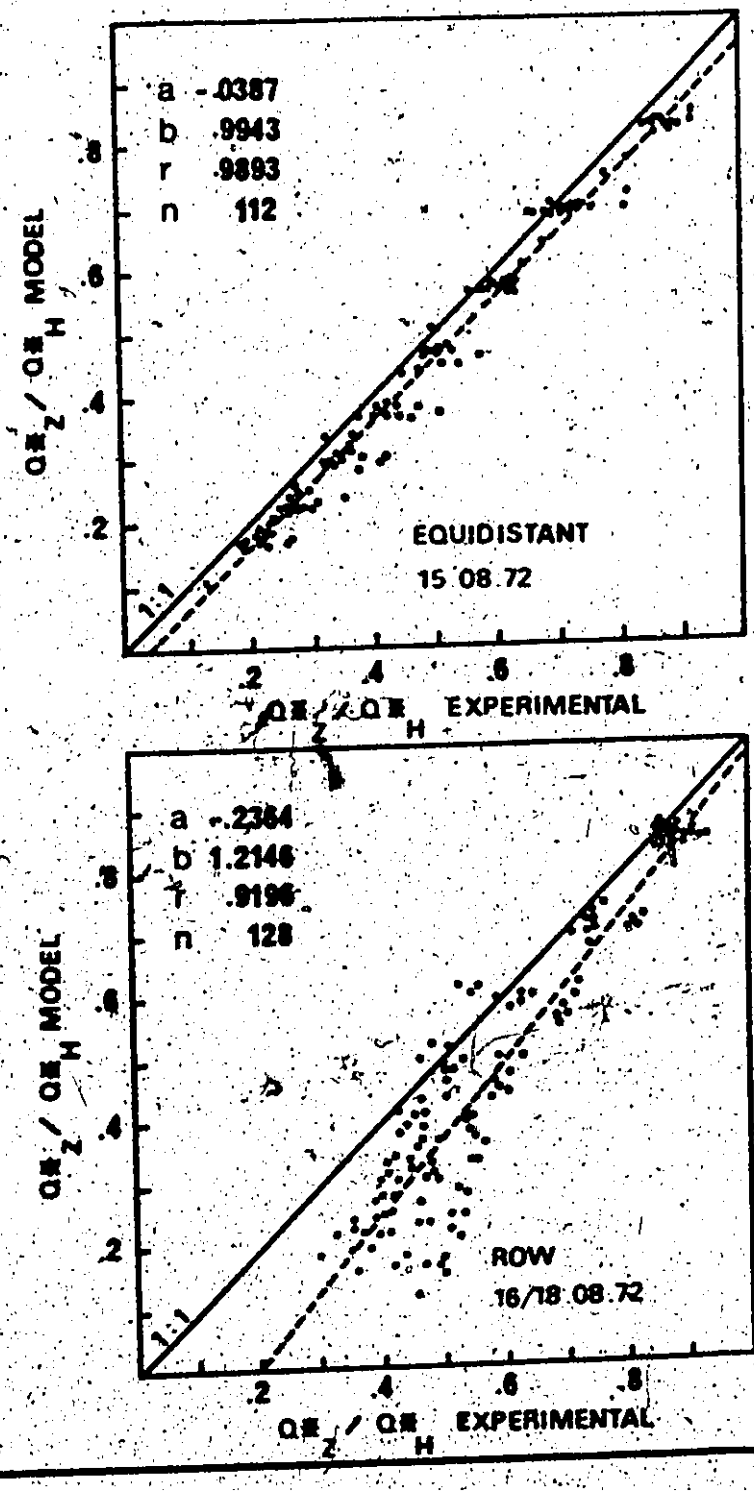

rigorous analysis due to a dearth of available temperature data associated with this investigation. It seems likely that further investigation could resolve this problem by providing a better estimate of canopy emission temperature.

When the row crop is considered, the upper half of the calculated profile is similar to that in the equidistant plot. In the lower half much more serious under-calculation is encountered, the lowest values being obtained between 1030 and 1330 solar time. Evidently, this phenomenon is related to the more open structure of the row crop and to a row effect (Figure 15). In such a situation it is unlikely that the assumption of zero L^4 divergence is valid and thus the model performs poorly.

The foregoing analysis is crude due to the lack of information, but suggests that a simple layer model such as NETCOMP is capable of reasonable simulation of the canopy net radiation regime. Further information, particularly of canopy emission temperature and the row effect is required to enable NETCOMP to be developed further.

CHAPTER 7

SUMMARY AND CONCLUSIONS

In the first part of this chapter the results of the investigation are summarised and conclusions relating specifically to the objectives outlined in Chapter 1 are presented. Later, the broader implications and contributions of this research to the knowledge of radiation regimes within a crop are considered.

Objectives 1 and 2. The data collected in this investigation using a transecting system are of high quality and illustrate the suitability of an aerial tramway system, properly sited and carefully maintained, for study and measurement of radiation flux densities within an agricultural crop such as corn. Results from transect data show very considerable horizontal spatial variation within the canopy. This variation is not consistent at various heights within the crop but is dependent on canopy structure. In the upper part of the crop the frequency distributions of flux density are negatively skewed and in the lower part, positively skewed. This is consistent with the finding of Allen and Lemon (1972). Both these distributions are related to the distribution of sunflecks and shade-areas governed by the frequency distribution of foliage elements and open space.

The frequency distributions of $K\downarrow$ are the simplest and most highly correlated with leaf frequency distributions. When $K^{\uparrow}$ and $Q^{\uparrow}$ fluxes are

considered, the combination of one or more fluxes results in a less clear frequency distribution and a poorer correlation with canopy structure. The influence of crop arrangement on the frequency distributions and hence on the vertical profiles is confined to the resultant differences in leaf frequency distributions across a transect and to the peculiar feature caused by row arrangement which permits greater penetration of $K\downarrow$ at a relative azimuth angle of zero.

Objective 3. The most common solution to the problem of a representative profile is the use of the mean flux density. Based on the nature of the frequency distributions, the validity of the assumption may have to be challenged.

Objective 4. A modified exponential model was developed as an empirical solution to the problem of estimating radiation fluxes. The repeatability, by other workers, of extinction coefficients obtained for this model will be the main criterion for assessing its usefulness. In addition, a resolution of the problem of a representative profile is necessary. It is of doubtful usefulness to amass extinction coefficients (either from a simple exponential model or any modification of it) if the profile thereby calculated is not representative of the flux density in the crop.

SOLCOMP, a simple layer model for global and net global radiation, was developed from theoretical considerations. Its performance against experimental data suggests that it is very suitable as a single, yet accurate, model of the radiation regime in a crop for many

micrometeorological and agronomic purposes. A further development, NETCOMP, suitable for calculating net radiation showed potential but could not be fully tested due to lack of information.

The fundamental importance of the characterisation of canopy radiation regimes has been stressed in the introductory chapter of this investigation. Spatial variability of flux densities caused by the heterogeneous nature of the distribution of foliage elements is a central problem. The implications and contribution of this research to this problem are threefold.

First, the description of measured frequency distributions permits quantitative investigation of the variability of flux densities and the nature of the sampling problem. This has already been used in the investigation of the reliability of a mean profile and might be further used to determine the optimum length of a linear integrating sensor for measurement of radiation fluxes in a given crop. Second, the possibility of modifying the exponential model to obtain a good simulation of the canopy radiation regime is shown to be valid. The technique, however, is only suitable after one has determined a representative profile since the extinction coefficients are determined empirically. Third, SOLCOMP and NETCOMP illustrate the important point that it is possible to model the radiation regime in a crop with a simple, theoretically-based construct using a small number of easily measured input parameters. This last conclusion presents the major contribution of this investigation.

APPENDICES

APPENDIX I

LIST OF SYMBOLS

Roman alphabet

a	leaf absorptance
A	unit area of foliage
A_h	area of shadow cast by leaves on a horizontal plane
f	leaf or foliage area index (Watson, 1947)
f'	effective leaf or foliage area index
f_o	downward cumulative leaf or foliage area index
f'_o	effective downward cumulative leaf or foliage area index
F	total leaf or foliage area index
g	true 'clustering' factor
g'	effective 'clustering' factor
h	crop height
H	horizontal irradiance
H_f	radiant flux density on a horizontal plane at f
H_o	radiant flux density on a horizontal plane above canopy
k	exponential model extinction coefficient
K	modified exponential model extinction coefficient (McCaughey, 1972)
$K\downarrow$	global solar radiation
$K\uparrow$	reflected solar radiation

$K^{\downarrow}$	net solar radiation
$L\downarrow$	downward atmospheric radiation
$L\uparrow$	upward terrestrial radiation
$L^{\downarrow}$	net terrestrial radiation
n	canopy layer
P	angle of penetration of radiation into canopy
$Q\downarrow$	downward total radiation
$Q\uparrow$	upward total radiation
$Q^{\downarrow}$	net radiation or radiation balance
R	reflected radiation
S	canopy density (Idso, 1968)
T	temperature
T_c	temperature at canopy closure
z	depth or height in canopy

Greek alphabet

α	leaf reflectance
α_c	calculated crop reflection coefficient
α_g	ground reflection coefficient
β	mean leaf angle of foliage elements
β'	normalised leaf angle of foliage elements
Δ	fraction of direction radiation in global radiation flux
ϵ	leaf emissivity for terrestrial radiation
ζ	solar zenith angle
ζ'	solar zenith angle at local solar noon

K	modified exponential model extinction coefficient
λ	'clustering' function (Mototani, 1968)
Λ	leaf inclination angle
ξ	relative zenith angle
σ	Stefan Boltzmann constant
ϕ	solar azimuth angle

Subscripts and superscripts

c	cumulative, calculated, canopy closure
g	ground
h	height of canopy, top of canopy
i,j,n	canopy layer flags
o	above canopy
z	height or depth in canopy

APPENDIX II

A TRAMWAY SYSTEM FOR RADIATION MEASUREMENT WITHIN PLANT CANOPIES

Introduction

When measurements of radiation fluxes are made within a plant canopy the positioning of sensors within the foliage is a major problem. This is a direct result of the spatial variation of radiation regimes caused by heterogeneity in the foliage elements. The radiation regime within a plant stand is closely related to its structure since the gaps in the canopy determine how much radiation can penetrate into the foliage. Thus, spatial averaging is desirable.

Two alternative methods are generally considered. Large numbers of small instruments can be located at various positions in the canopy (Impens, Lemeur and Moermans, 1970) or some form of linear sensor capable of integrating radiation in the horizontal can be used (Szeicz, Monteith and dos Santos, 1964). The length of such a sensor will be determined by the nature of the crop and the row spacing. A further alternative, not often considered, is to construct an aerial tramway so that instruments can be moved among the foliage elements. This type of system is particularly amenable in the case of crops such as corn where the foliage elements are widely spaced and linear sensors may not be of great value. Due to the high cost of radiometric instruments,

which precludes replication, a tramway provides a feasible alternative. In addition, measurements of radiation from a moving tramway can yield valuable information on the frequency distribution of the radiation flux across the transect. This is obscured by the integrating property of a linear sensor. Standard radiation instruments have been used in this case but, the system, with minor modifications, is suited to measure other meteorological variables.

Design and construction

Towers. To support the ends of the tramway, towers of the type normally used for television antennae are used. Each section of triangular steel tower is about 1 foot on a side and 10 feet long.[1] one section was sufficient for use in a field corn canopy for which the tramway was designed but vertical extension for higher canopies is easily achieved.

The base of the tower is embedded in concrete ensuring that the section is vertical. Each tower is guyed with three steel guy cables. Anchors for the guy cables are placed at a distance from the tower such that the guy cable angle is approximately 60° from the horizontal. A variety of anchoring systems may be used. In this case steel stakes were found to be satisfactory.

Tramway. A prerequisite for a good tramway system for radiation flux measurement is that it is stable and level. To fasten the tramways to the towers clamp kits available from TV suppliers are attached to the

---

[1] British units are used for dimensions of materials to avoid confusion caused by conversion of standard materials to metric units.

FIGURE 1 - AERIAL TRAMWAY SYSTEM.

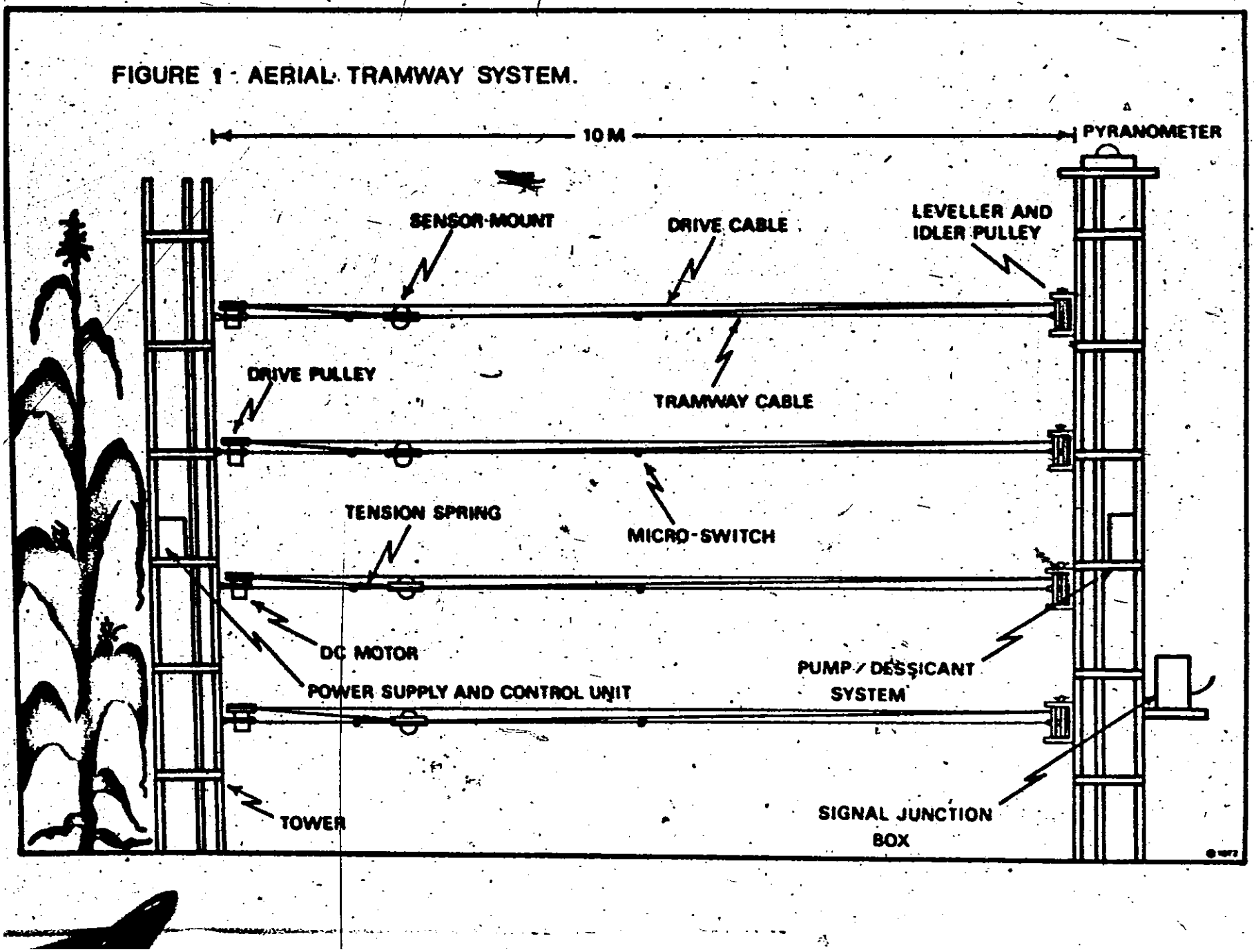

desired heights. These consist of a galvanised steel plate, U-bolts and saddle brackets. At one end of the tramway cables (1/16", 7 x 7 standard stainless steel aircraft wire) are connected to the backplate by means of turnbuckles (backed off initially) (Fig. 2). After the tramway cables are fastened to one tower and the sensor-mount and other ancillary equipment attached, they are led over to the other tower and connected to the leveller assembly (Fig. 3). When pulled taut the cables are secured and cable tension adjusted with the turnbuckles. Cable tension adjustment is achieved by concurrent adjustment of the leveller assembly and the guy cable turnbuckles. In this way cable sag is minimised and levelness is attained by checking the level bubble on the sensor-mount when it is positioned in the middle of the tramway.

A small sensor-mount was built to hold the radiometers. It is constructed from 1/4" Plexiglas and has several attachments to support various types of sensors (Fig. 4). Modifications of attachments to suit specific instruments or purposes can be made easily.

Operation.

Traverse drive system. An endless drive cable and a D.C. motor are used to move the sensor along the tramway. This method seems to be reliable and involves fewer complications than a single motor and pulley system. A 35 V, gear-reduced, D.C. motor (American model 3255P) and drive pulley is attached, in a vertical position, to the backplate at the opposite end of the tramway from the leveller assembly (Fig. 2). The drive cable is fastened to the sensor-mount, through a tension spring, round the drive pulley, across the tramway, round the idler pulley at the opposite end and back to the mount.

FIGURE 2. MOTOR & DRIVE PULLEY ARRANGEMENT.

FIGURE 3 LEVELLER ASSEMBLY & IDLER PULLEY SYSTEM.

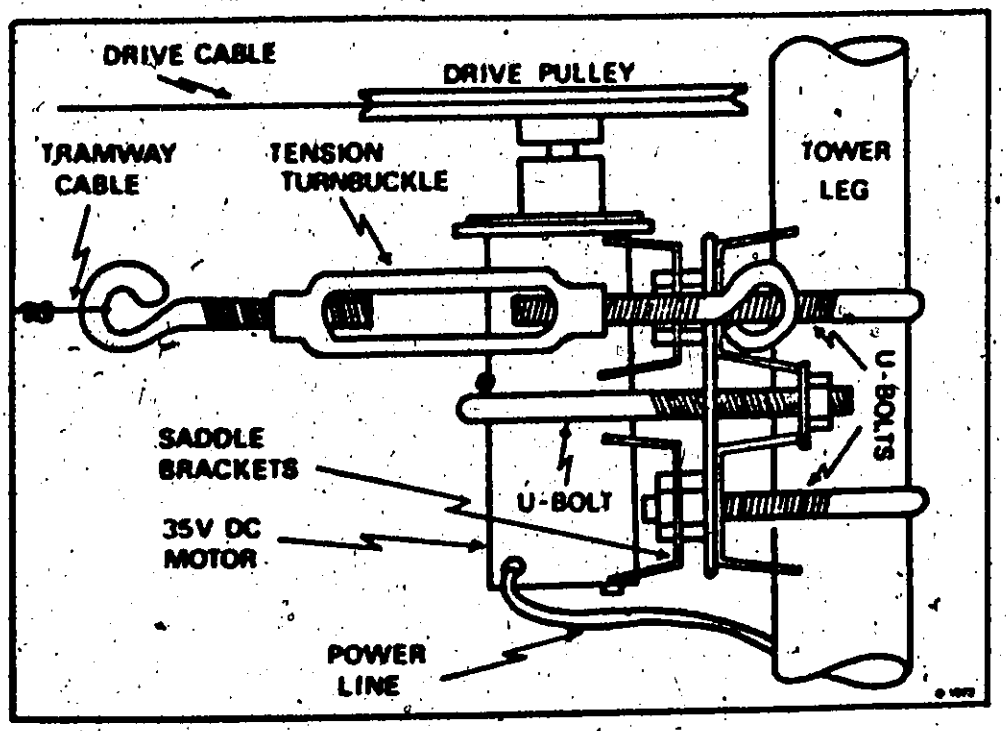

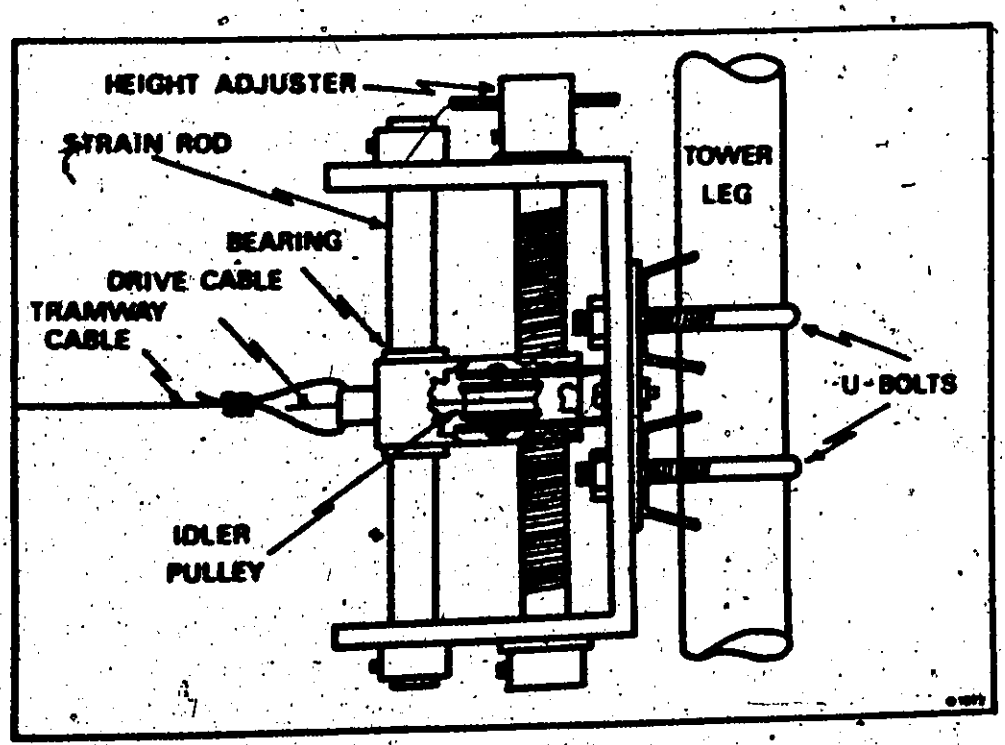

FIGURE 4 TRAMWAY SENSOR-MOUNT

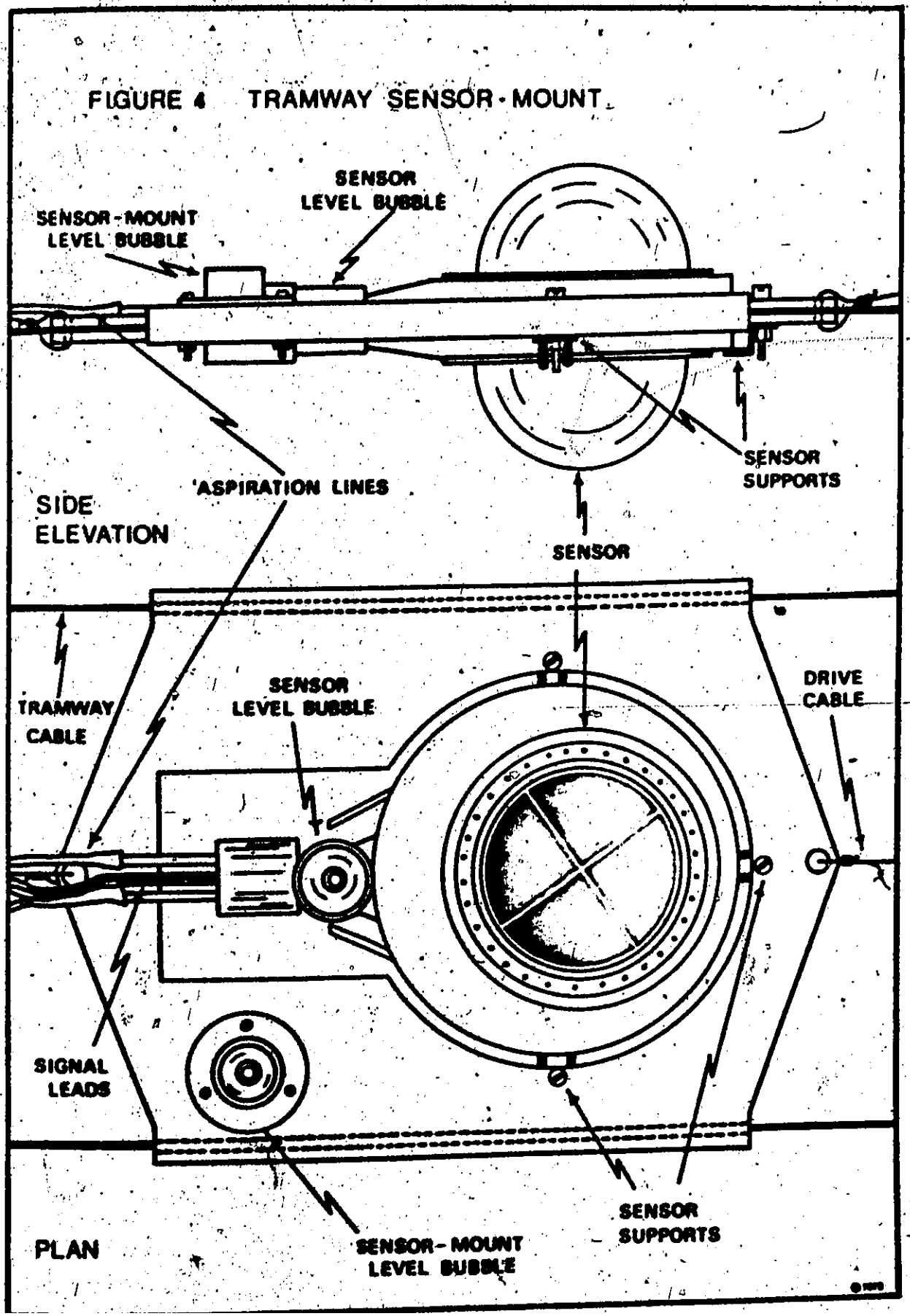

The transect length is delimited by microswitches (Cherry Electric E23), positioned at the extremes of the transect. The motor reverses polarity, and hence direction of traverse, when the mount triggers the microswitches. The drive system is powered and controlled by a power supply at the tower. This was designed by the McMaster University electronics shop. The unit powers the motors, controls the microswitch operation by means of relays and allows speed adjustment. Hence it is a relatively simple matter to alter transect length and speed of traverse by appropriate positioning of microswitches and adjustment of speed controls (Bourns trimpot 3010L-1-103 10K) and/or drive pulley dimensions.

Signals are led by two conducter shielded cable, attached to the drive cable, to a junction box at the tower. From there all signals can be relayed to a remote recording station. When shielded net radiometers are used, ventilation is also needed to inflate and purge moisture from the domes. In this case Tygon tubing is also attached to the drive cable and a suitable purging system (dried air or nitrogen) is positioned on the tower adjacent to the signal junction box.

The sensors are levelled by means of the adjusters on the mount and, if necessary, by the runway levellers.

APPENDIX III

CROP ANALYSIS

Leaf area index

For quantitative descriptions of foliage, Watson's (1947) leaf area index (leaf area, one side only, subtended per unit area of land) has become a basic tool. As refinements, the vertical distribution of leaf area index, estimated by stratified clip techniques, is now a commonly used method in canopy analysis.

The leaf area index was determined by using three sample areas each of 1 m^2 in both plots. All the leaves in a vertical volume above each area were collected according to strata corresponding to the heights of the tramways i.e. 0.0 - 0.5, 0.5 - 1.0, 1.0 - 1.5, 1.5 - 2.0 and above 2.0 m above the ground. When leaves protruded from one layer into the next, they were cut and those pieces added to the appropriate stratum. The areas of the leaves were measured by means of an Automatic Area Meter Type AAM-5 (Hayashi-Denko, Tokyo) which had been previously calibrated.

Downward cumulative leaf area index for both plots is presented in Fig. 1. In both cases the samples differed only slightly and the mean vertical distribution of leaf area was used. Since data were available by strata another method of presenting leaf area distribution is to calculate the percentage of total leaf area in each "box". This

FIGURE 1. LEAF AREA INDEX FOR BOTH PLOTS.

EACH PROFILE IS THE MEAN OF THREE SAMPLES.

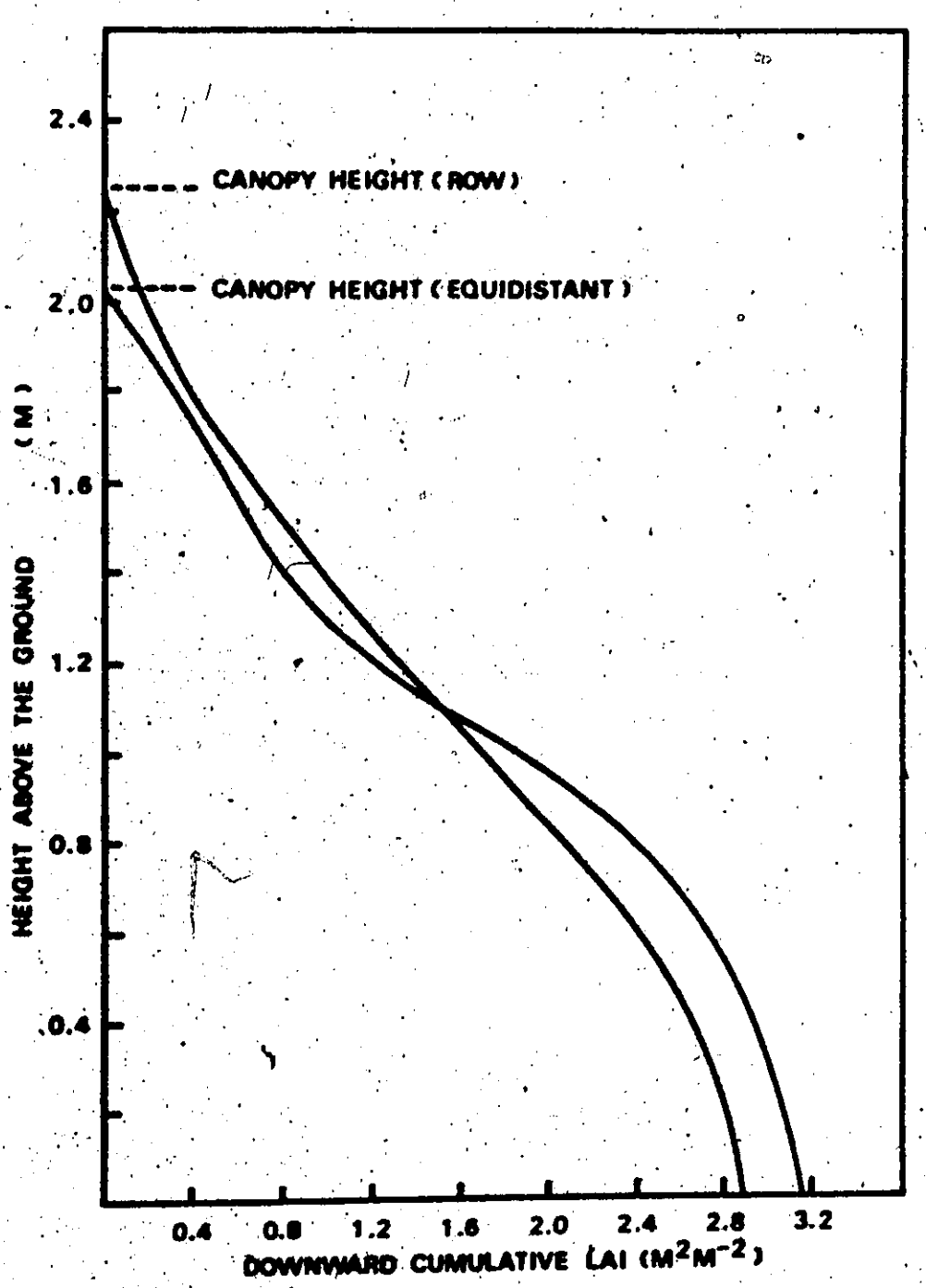

is presented in Fig. 2. From these diagrams it is evident that in both plots the majority of the leaf area occurs in the strata between 0.5 and 2.0 m above the ground. Also evident is the slightly greater concentration of leaf area in the middle strata of the equidistant plot. Although the vertical distribution of leaf area index is an improvement in canopy description evidence has been accumulating (de Wit 1965; Anderson 1966; Duncan, Loomis, Williams & Hanau 1967) that the leaf angle is influential in determining the efficiency of energy utilisation by plant communities. Hence, it is desirable to determine not only the vertical distribution of leaf area and the mean angle of inclination in various layers, but also the distribution of leaf area by angle classes within each stratum (Loomis, Williams, Duncan, Dovrat and Nunez 1968).

With this object in mind further leaf area measurements by stratum were made. Additional measurements of the percentage of the total leaf area in each stratum falling in three angle classes 0° - 30°, 30° - 60°, and 60° - 90° from the horizontal were made. Leaf inclinations were assessed using a leaf inclinometer (Fig. 3). The base of the instrument was laid parallel to the leaf or leaf section and the angle between the horizontal and the leaf surface was measured directly from the position of the pointer on the scale. The data obtained in this way are presented in Table 1 and Table 4. What is most striking is the similarity between the sample plants in the two plots, both in terms of the percentage of total leaf area in each angle class and in the vertical distribution by strata. This suggests that the plants in both plots have essentially the same structure despite differences in

FIGURE 2 LEAF AREA DISTRIBUTION IN BOTH PLOTS.

NUMBER OF LINES IN EACH 0.5M STRATUM 'BOX' IS PROPORTIONAL TO LEAF DENSITY. NUMBERS SHOW PERCENT OF TOTAL LAI IN EACH STRATUM.

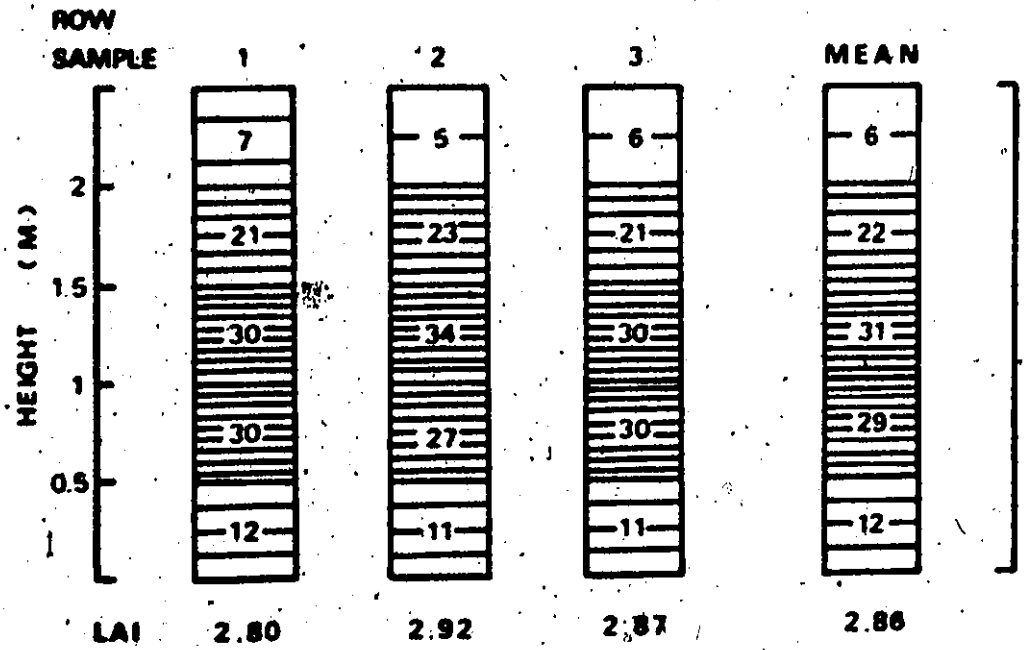

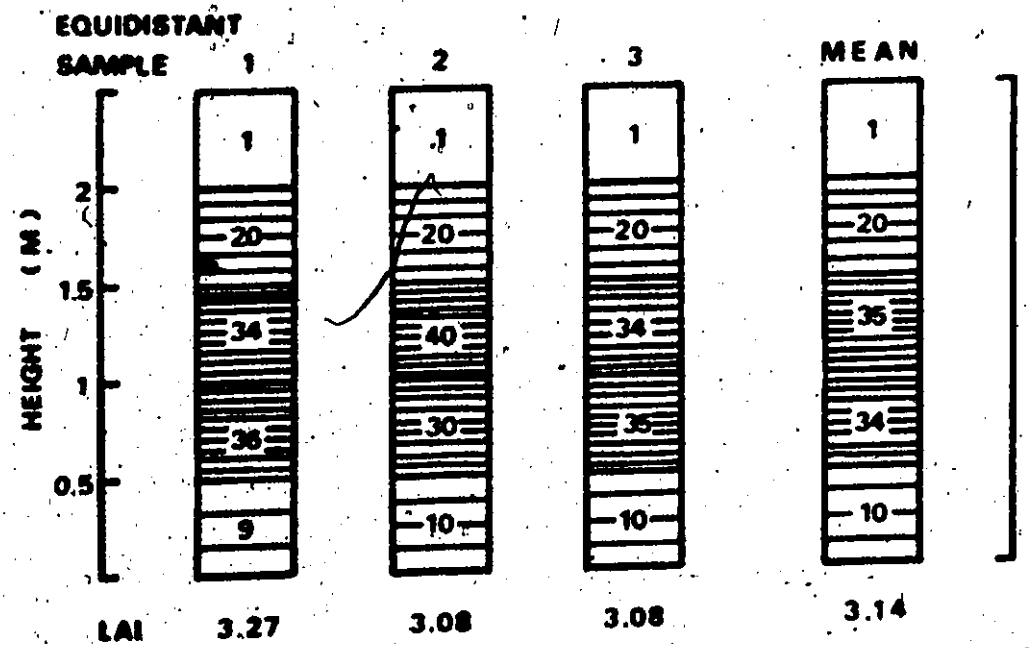

FIGURE 3 LEAF INCLINOMETER, modelled after Nichiporovich, 1961.

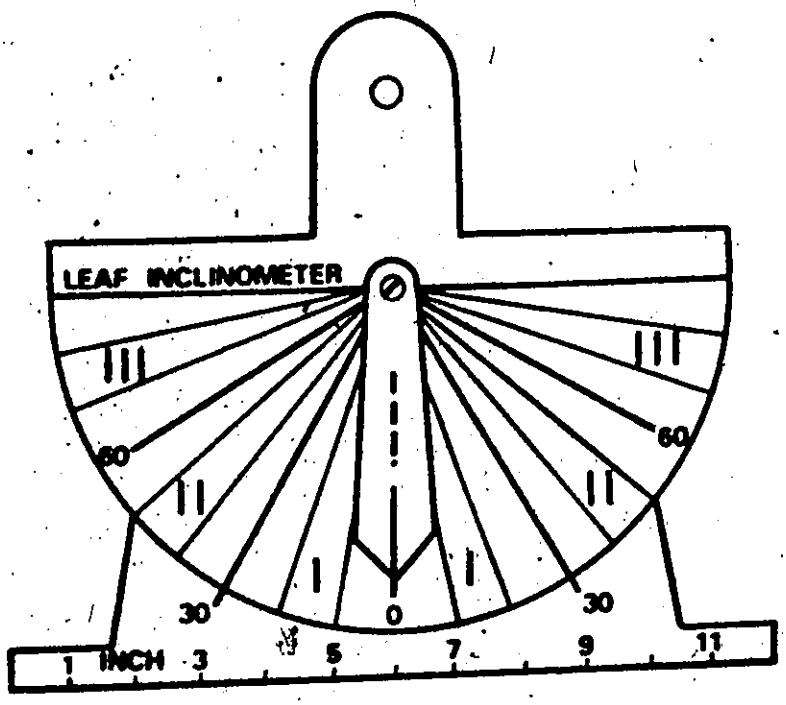

TABLE III (I). Percentage leaf area in each stratum falling in three angle classes

ROW Stratum	% leaf area in angle class 0° -30°	30° -60°	60° -90°	% leaf area in stratum
1	3.10	1.97	0.99	6.06
2	2.12	0.87	9.94	21.93
3	4.25	8.88	17.89	31.02
4	3.28	10.85	14.91	29.04
5	1.05	4.93	5.97	11.95
Total	13.80	36.50	49.70	100.00
EQUIDISTANT				
Stratum	0° -30°	30° -60°	60° -90°	% leaf area in stratum
1	0.68	0.51	0.19	1.38
2	2.38	6.84	10.82	20.04
3	4.83	10.96	19.21	35.00
4	3.27	15.26	15.48	34.01
5	2.74	3.03	3.80	9.57
Total	13.90	36.60	49.50	100.00

planting procedure. Further investigation of the canopy structure using leaf distribution functions was warranted in an attempt to clarify this situation.

Leaf distribution functions

Among other factors, the radiant energy distribution within a canopy depends on the posture of the leaves in space. This posture may be completely determined by the azimuth and the inclination of the plane through the leaf. According to Nichiporovich (1961) and de Wit (1965) the leaves of a canopy have, in general, no preferred azimuth orientation so that their positions are completely characterised by the cumulative frequency distribution of leaf inclination.

The orientation of the leaf blades in eight sectors of 45° each was used to determine the azimuth distribution of the leaves in both plots. The sectors were based on the cardinal points. The direction of the central vein from the stem was measured by a simple device constructed for the purpose. It consisted of a pointer, aligned with the central vein of a leaf during a reading, which traversed a circle divided into sectors as described above (Fig. 4). Initial orientation of the instrument was achieved by means of a small compass located on the north-south axis of the instrument.

In this investigation no preferred azimuth direction was noted in the equidistant plot. However, in the row plot, some azimuth preference was measured presumably due to the constraining effect of the other plants in the row (Fig. 5). The azimuth orientation plan in the former case may be approximated to a circle whereas in the latter case a close approximation

FIGURE 4 LEAF AZIMUTH METER.

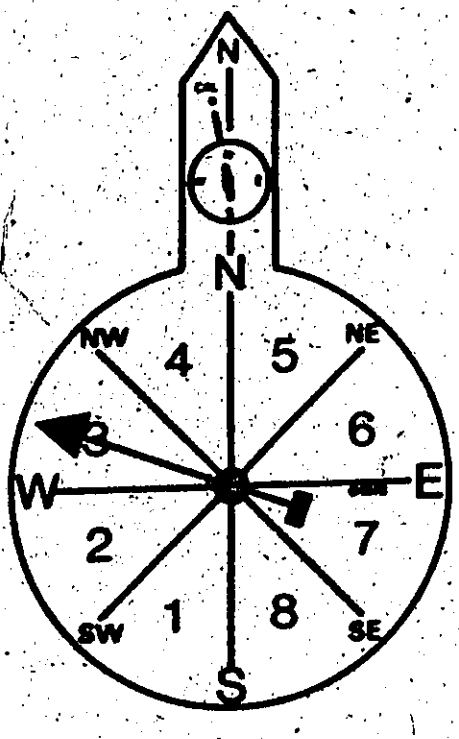

FIGURE 5. CANOPY STRUCTURE FOR CORN PLOTS.
NUMBER OF LINES IN EACH 'BOX' IS EQUAL TO PERCENT OF TOTAL LEAF AREA IN EACH STRATUM FALLING IN EACH ANGLE CLASS

ROW

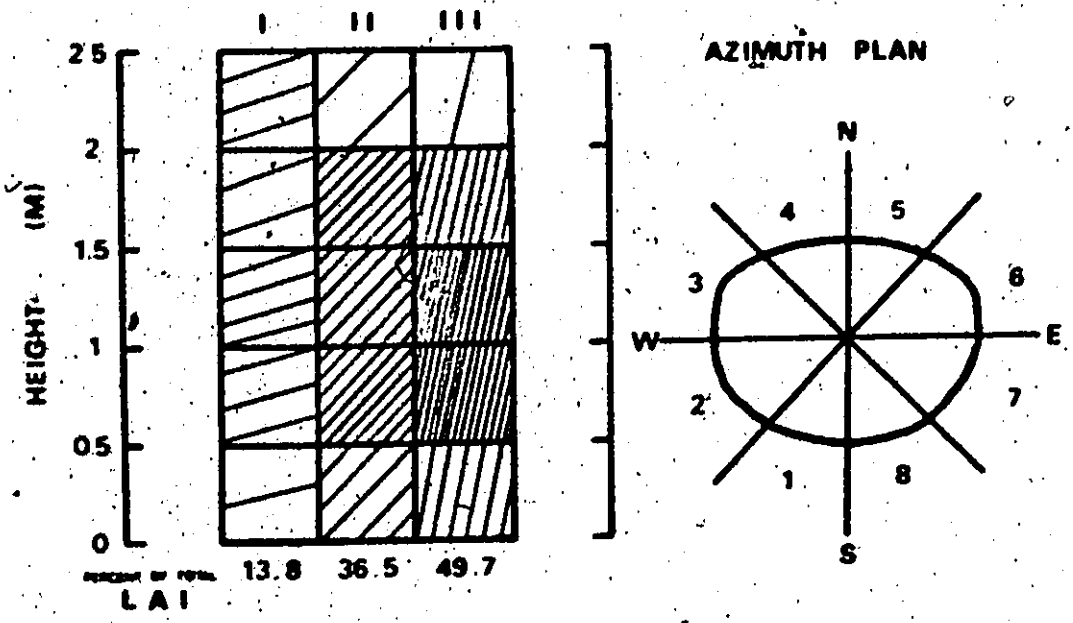

EQUIDISTANT

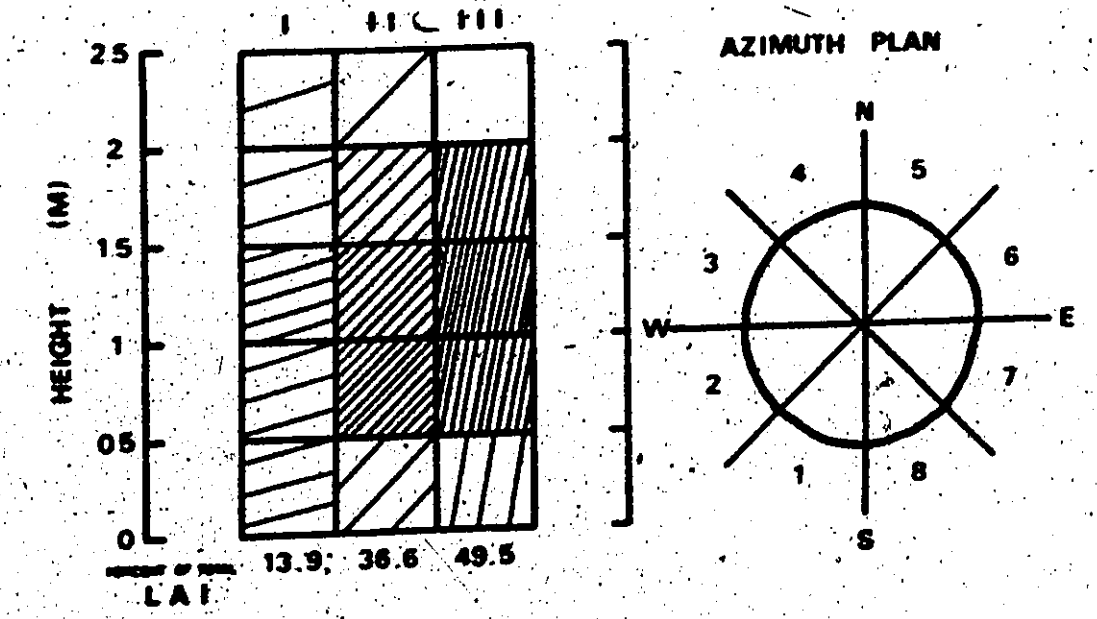

is an ellipse with a ratio of semi-major to semi-minor axes of 14 : 11. To compare the present data with published data it is necessary to re-calculate the data in terms of the percentage of leaves in 90° sections facing the four cardinal points. This is presented in Table 2. Data from Michiporovich (1961) show an intermediate azimuth distribution to the two extremes found in the present investigation.

TABLE III (2). Percentage of leaves in 90° sectors facing the four cardinal points.

	South	West	North	East
Row plot (1972)	22.2	28.0	21.8	28.0
Equidistant plot (1972)	25.0	25.1	25.1	24.8
Michiporovich (1961)	23.0	27.0	24.0	26.0
Ross and Nilson (1967)	26.8	26.0	21.5	23.0

He concluded that there is no azimuth preference in his crop. De Wit (1965) also comes to the conclusion that his experience indicates no azimuth preference. Data from Ross and Nilson (1967) are difficult to compare with the present results because their rows were oriented in a NE by SW direction. Their data do, however, show a preference for orientation across the rows.

In the equidistant plot there is no azimuth preference, but a question can be raised concerning the row plot. Certainly the data indicate a preference for more leaves to be oriented in the

east-west plane (across the rows) than in the north-south plane (along the rows). Whether this tendency is enough to warrant the incorporation of an azimuth preference in determining the canopy posture is a question which will be considered later. However, at this point it is worth mentioning that results obtained by Ross and Nilson (1967) lead to the general conclusion that to a first approximation the spatial organisation of leaves in a square sown stand may be regarded as uniform. In drilled stands, the orientation of leaves is elongated with respect to azimuth in the direction perpendicular to the rows, this elongation increasing with the density of the stand.

In a canopy with no preferred orientation it is sufficient to characterise the positions of leaves by their inclinations alone. A convenient method of representing such distribution functions is by plotting the cumulative frequency of occurrence of the inclinations against the angle of inclination, ranging from 0° for a horizontal leaf to 90° for a vertical leaf (de Wit 1965). Generally, canopies of four different types, depending on their leaf distribution, are recognised (Fig. 6). Planophile canopies have mainly horizontal leaves and erectophile canopies have mainly vertical leaves. Plagiophile canopies are characterised by the greatest frequency of leaves occurring at some oblique inclination. Extremophile canopies have the least frequency of inclination at an oblique angle.

Leaf inclination was measured with a leaf inclinometer as before. Initially leaf inclination was assessed in terms of three groups with angles of inclination to the horizontal within the limits: Class I: 0° - 30° (near horizontal leaves); Class II: 30° - 60° (oblique leaves);

FIGURE 6 THE FOUR MAIN TYPES OF LEAF DISTRIBUTION FUNCTIONS, after de Wit, 1965.

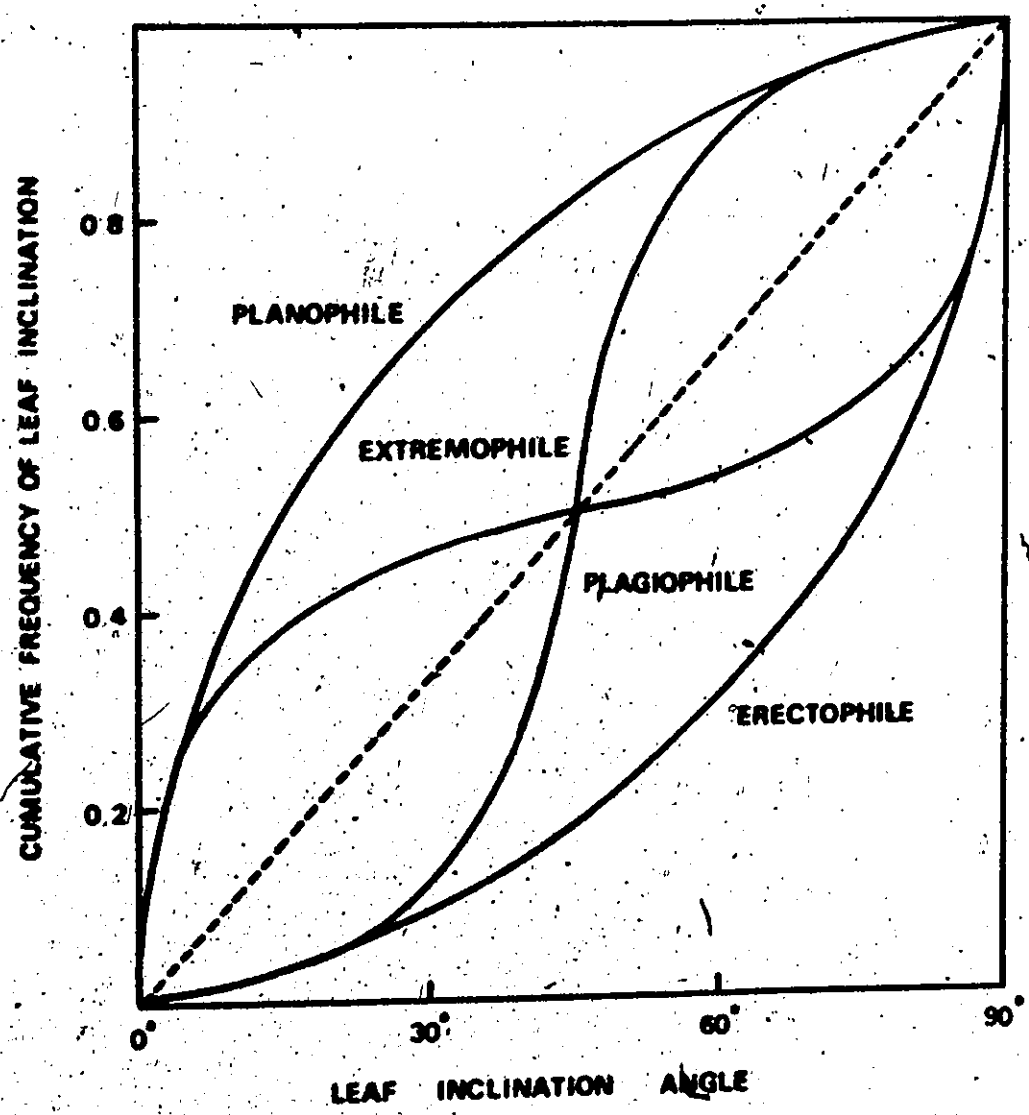

Class III: 60° - 90° (near vertical leaves). Table 3 gives the percentage of total leaf area in each angle class for both plots and for data presented by Nichiporovich (1961). Clearly corn is an erectophile

TABLE III (3). Distribution (%) of leaves in groups based on the angle of inclination to the horizontal plane

Source	Class I	Class II	Class III
Row plot (1972)	13.8	36.5	49.7
Equidistant plot (1972)	13.9	36.6	49.5
Nichiporovich (1961)	16.0	36.7	47.3
Theoretical spherical distribution	13.0	37.0	40.0

canopy, approximately 50% of the leaf area having an angle of inclination greater than 60° to the horizontal. All data shown in Table 3 correspond closely to what Nichiporovich (1961) has described as a favourable spatial orientation of leaves, namely one in which their projection fills the surface of a sphere inscribed between the plane of the soil surface and a plane passing through the tops of the plants (Fig. 7). This spherical distribution is an erectophile distribution of a special type and may be described by supposing that the relative frequency of leaf inclinations is the same as the relative frequencies of the inclinations of the surface of a sphere.

When A is the inclination of a leaf, then in the case of a spherical distribution, the cumulative distribution function of A is $1 - \cos A$

FIGURE 7 THEORETICAL LEAF AREA IN ANGLE CLASSES IF LEAVES ARE PROJECTED ON TO THE SURFACE OF A SPHERE. after Nichiporovich, 1961.

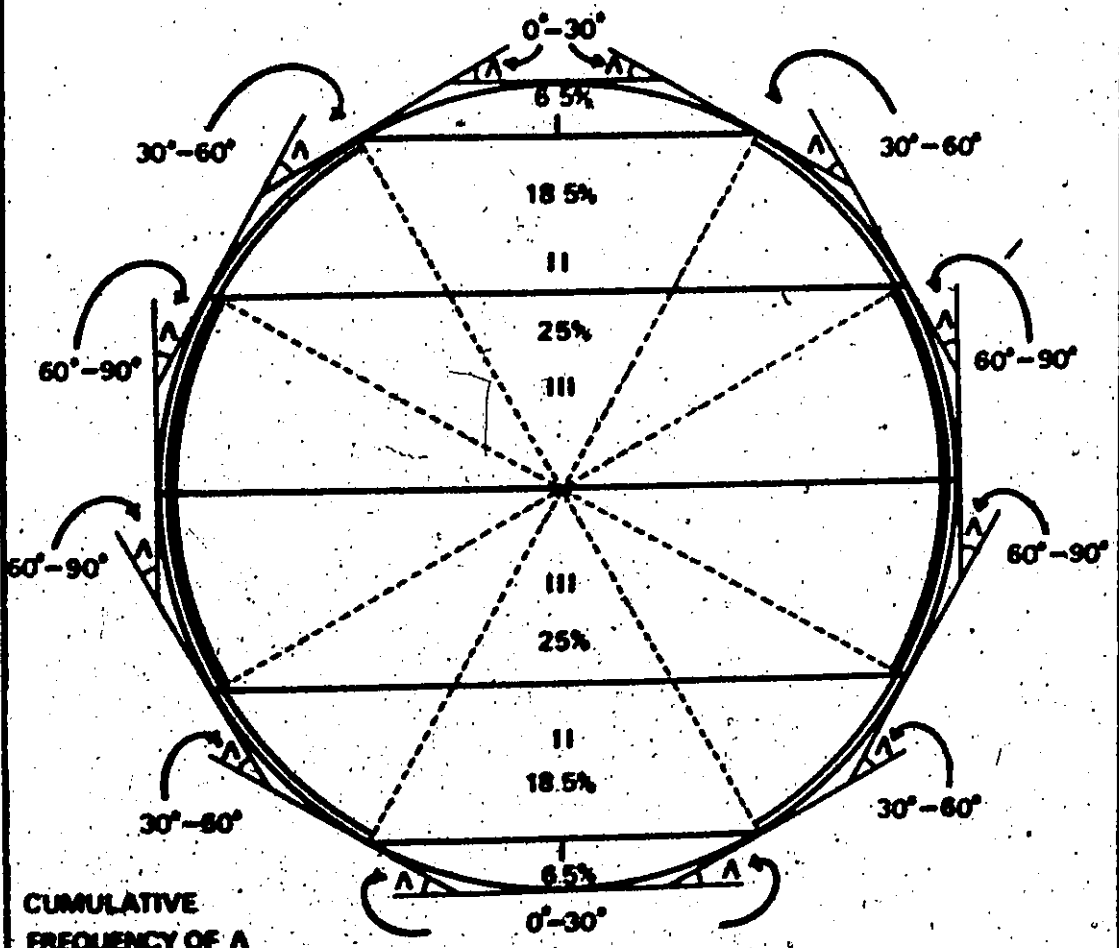

CUMULATIVE FREQUENCY OF A

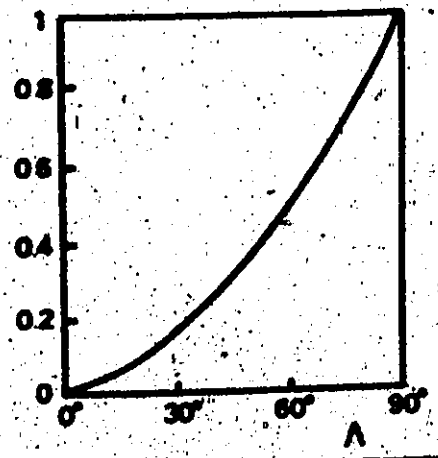

RELATIVE AREAS

Surface of sphere			100 %
Surface of belts			
I	0° – 30° ,	6.5 + 6.5	= 13 %
II	30° – 60° ,	18.5 + 18.5	= 37 %
III	60° – 90° ,	25.0 + 25.0	= 50 %

THEORETICAL LEAF DISTRIBUTION FUNCTION

(de Wit 1965). This theoretical spherical leaf distribution function is shown in the inset of Fig. 7.

To further assess whether the canopies under investigation comply with this theoretical distribution additional measurements of leaf inclination were made at 10° intervals from the horizontal to the vertical. The leaf distribution functions for both plots are presented in Fig. 8 and in Table 4.

The similarity between the theoretical and experimental distributions is remarkable. Regression analyses gave the following correlations between the experimental and theoretical data; row plot $r^2 = 0.995$, equidistant plot $r^2 = 0.998$. Clearly the experimental data fit very closely to the theoretical curve. The standard errors of the estimates were - row plot 2.36%, equidistant plot 1.44%.

Of considerable interest is the closeness of the row plot distribution to the spherical distribution despite earlier indications that there may be some azimuth preference exhibited by the plants in this plot. It might then be expected that the most favourable spatial orientation would be one in which the projections of the leaves entirely fill the surface of an ellipsoid of eccentricity 14 : 11 inscribed between the plane of the soil surface and a plane passing through the tops of the plants. However, when the relative surface areas of the sphere "constructed" for the plants in the equidistant plot and the ellipsoid postulated for the plants in the row plot are compared there is very little difference between them. This suggests that it is not necessary to include the possibility of azimuth orientation in the calculations of leaf posture provided that the azimuth preference is not marked.

FIGURE 8 LEAF DISTRIBUTION FUNCTIONS.

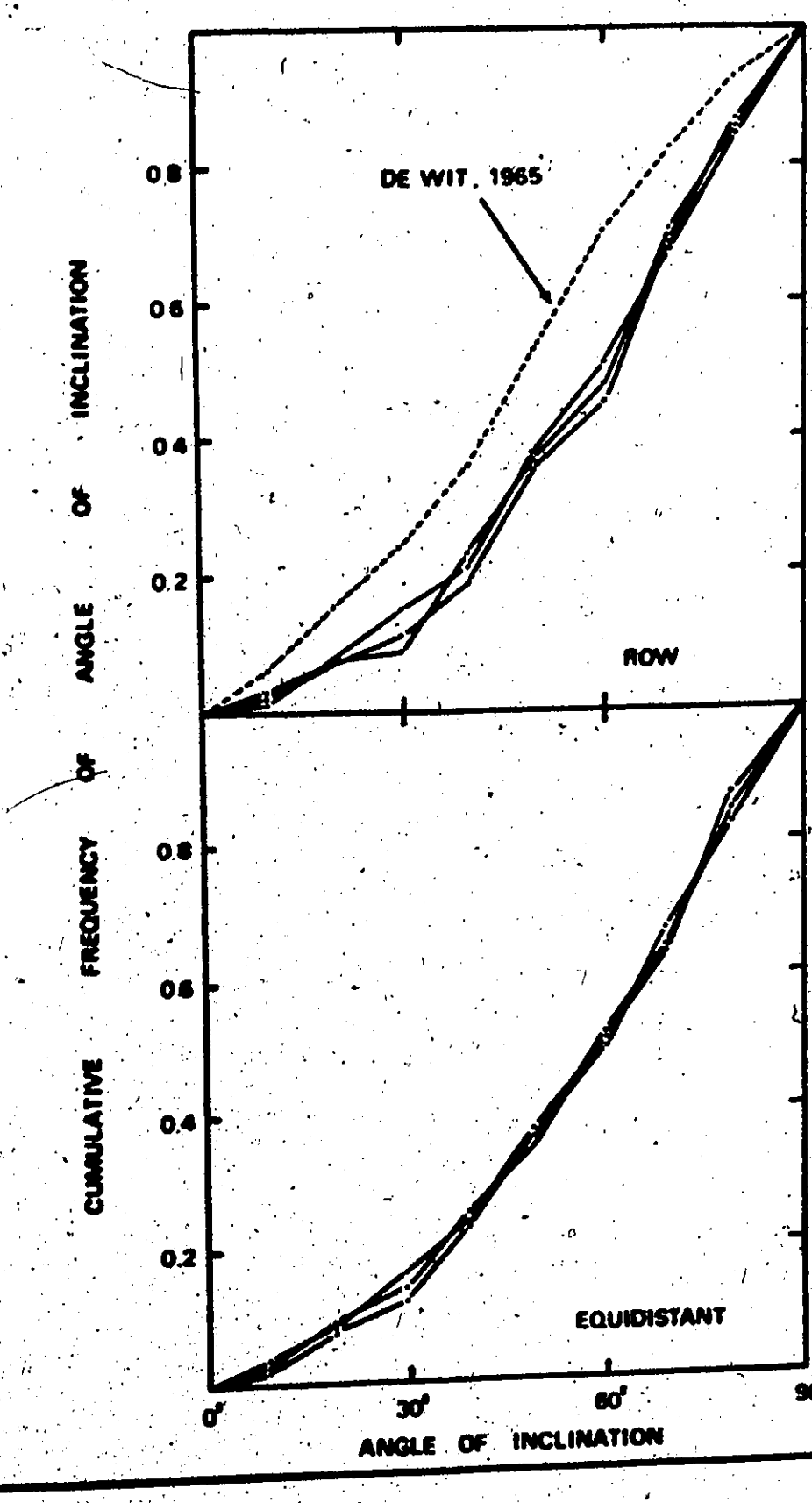

TABLE III (4). Cumulative percentage leaf area in angle classes at 10° intervals for both plots

		ROW			EQUIDISTANT		
ANGLE CLASS	THEORETICAL	1	2	3	1	2	3
0° - 10°	1.519	2.1	3.0	2.5	3.5	2.6	1.4
0° - 20°	6.031	8.4	7.5	7.0	9.0	9.1	8.1
0° - 30°	13.397	15.5	11.0	9.1	16.3	14.4	12.5
0° - 40°	23.396	22.2	20.2	23.1	25.0	26.1	24.1
0° - 50°	35.721	39.0	36.3	37.4	36.8	37.4	38.2
0° - 60°	50.000	50.9	45.6	48.7	49.9	48.9	50.1
0° - 70°	65.798	68.1	69.7	70.9	65.2	67.6	66.4
0° - 80°	82.635	85.5	87.1	86.6	88.0	85.4	83.7
0° - 90°	100.000	100.0	100.0	100.0	100.0	100.0	100.0

APPENDIX IV

SELECTED

RADIATION FLUX DATA

K↓ DATA (W m^{-2})

EQUIDISTANT PLOT DATE 25.08.72

TIME	MEAN					WEIGHTED MEAN				
	height(m)					height(m)				
	above	2.0	1.5	1.0	0.5	above	2.0	1.5	1.0	0.5
0800	429	420	384	171	93	429	418	397	163	90
0830	546	539	429	222	129	546	538	433	195	135
0900	592	586	468	262	144	592	585	475	260	144
0930	618	604	496	271	167	618	606	501	265	153
1000	724	713	594	352	224	724	712	599	341	213
† 1030	536	526	437	236	162	536	524	446	222	151
1100	750	743	633	346	253	750	740	650	331	244
1130	856	848	716	394	277	856	849	748	373	262
† 1200	665	653	546	291	221	665	650	558	282	210
† 1230	618	602	512	275	187	618	600	521	260	174
† 1300	518	515	430	220	150	518	515	439	208	142
1400	788	773	672	352	254	788	775	722	294	239
1500	640	627	548	274	163	640	626	561	257	154
1600	450	444	381	155	92	450	440	400	138	91
1630	339	330	259	87	54	339	331	288	72	53
1700	248	243	166	70	43	248	242	180	64	43

† some cloud present during experimental run.

K↓ DATA (W m^{-2})

ROW PLOT DATE 24.08.72

TIME	MEAN					WEIGHTED MEAN				
		height(m)					height(m)			
	above	2.0	1.5	1.0	0.5	above	2.0	1.5	1.0	0.5
0830	446	437	345	225	150	446	435	362	216	143
0900	541	507	406	257	190	541	506	422	243	188
0930	601	595	488	326	246	601	597	506	301	232
1000	654	649	533	339	269	654	650	558	292	251
1030	714	708	602	414	333	714	706	640	376	312
1100	751	742	642	425	388	751	740	676	392	374
† 1130	529	524	446	281	253	529	525	461	269	238
† 1200	599	584	486	334	277	599	580	495	317	260
† 1330	309	305	247	183	134	309	306	233	172	125
† 1400	569	560	465	319	256	569	558	488	301	248
† 1430	554	549	443	317	238	554	550	461	306	230
† 1500	510	506	417	323	228	510	507	436	308	218
† 1530	407	403	323	228	163	407	405	334	216	160
† 1600	254	251	200	135	95	254	252	209	128	92
† 1630	343	332	252	164	110	343	332	258	157	107
† 1700	86	84	61	41	26	86	84	61	42	25

† some cloud present during experimental run.

$K^{\downarrow}$ DATA ($W\ m^{-2}$)

EQUIDISTANT PLOT DATE 19.08.72

TIME	MEAN					WEIGHTED MEAN				
	height (m)					height (m)				
	above	2.0	1.5	1.0	0.5	above	2.0	1.5	1.0	0.5
0800	376	369	278	128	81	376	370	286	116	80
0830	472	450	343	198	119	472	454	359	179	117
0900	538	529	389	246	160	538	531	398	228	154
0930	595	582	438	300	194	595	581	456	281	188
1000	646	632	497	353	272	648	634	522	340	260
1030	691	675	556	398	304	691	676	581	369	295
† 1100	509	498	376	305	186	509	498	394	286	171
† 1130	436	433	361	259	163	436	430	383	241	158
1200	832	817	646	464	359	832	821	699	447	330
† 1400	335	328	257	171	104	335	330	280	160	97
† 1430	588	579	457	331	170	588	580	351	322	157
† 1500	221	206	158	114	48	221	210	127	102	40
† 1530	383	375	272	153	109	383	375	171	141	101
1600	383	377	290	146	78	383	379	165	137	72
1700	227	225	167	100	51	227	224	118	89	51

† some cloud present during experimental run.

$K^{\downarrow}$ DATA (W m^{-2})

ROW PLOT DATE 21.08.72

TIME	MEAN					WEIGHTED MEAN				
		height(m)					height(m)			
	above	2.0	1.5	1.0	0.5	above	2.0	1.5	1.0	0.5
0800	322	313	257	172	90	322	316	268	166	90
0830	425	414	345	231	154	425	418	359	220	153
0900	483	471	382	283	195	483	475	396	261	188
0930	511	507	435	276	222	511	510	458	260	216
1000	574	538	445	360	274	574	556	462	351	258
1030	601	587	575	385	341	601	592	587	363	336
† 1100	484	446	378	260	245	484	458	389	248	229
† 1300	595	548	452	370	346	595	552	464	351	331
† 1330	587	543	460	349	301	587	553	476	322	288
† 1430	504	457	375	331	244	504	461	391	318	226
† 1500	430	374	306	282	191	430	381	320	276	170
† 1530	351	301	240	212	141	351	322	261	201	128
† 1600	268	240	199	152	105	268	249	213	144	98
† 1630	248	213	176	134	77	248	226	189	124	72
† 1700	177	153	125	110	61	177	160	138	102	60

† some cloud present during experimental run.

Q^* DATA ($W\ m^{-2}$)

EQUIDISTANT PLOT DATE 15.08.72

TIME	MEAN					WEIGHTED MEAN				
		height(m)					height(m)			
	above	2.0	1.5	1.0	0.5	above	2.0	1.5	1.0	0.5
0800	315	309	280	85	81	315	311	288	83	80
0830	368	365	306	177	117	368	365	318	169	115
0900	427	424	359	226	155	427	425	367	216	152
0930	483	477	393	248	200	483	478	404	228	196
1000	536	535	464	324	289	536	534	482	304	277
1030	580	579	498	392	318	580	576	513	376	306
1100	619	612	540	421	336	619	614	556	410	315
1200	673	672	554	450	333	673	670	568	429	319
1230	667	660	589	445	294	667	661	599	426	279
1330	612	604	549	375	244	612	606	566	358	233
1400	566	561	535	343	254	566	562	542	339	246
1430	516	513	473	309	213	516	513	488	300	202
1500	469	460	429	252	158	469	462	438	240	147
1600	328	325	294	96	61	328	326	306	94	60

† some cloud present during experimental run.

Q^* DATA (W m^{-2})

ROW PLOT DATE 16/18.08.72

TIME	MEAN					WEIGHTED MEAN				
		height(m)					height(m)			
	above	2.0	1.5	1.0	0.5	above	2.0	1.5	1.0	0.5
† 0800	216	214	178	116	89	216	215	180	115	87
† 0830	346	341	304	198	157	346	342	308	196	156
† 0930	289	287	243	168	144	289	287	246	164	142
† 1000	265	262	219	156	132	265	264	226	148	127
† 1030	317	309	258	177	152	317	312	262	174	148
†1100	255	252	213	149	125	255	253	220	146	124
1130	685	674	598	343	384	685	677	626	336	369
1200	722	704	631	338	437	722	711	658	320	418
1230	649	613	548	275	384	646	626	566	269	362
1300	673	630	549	309	308	673	642	562	289	287
† 1330	525	489	422	282	272	525	496	447	270	253
†1400	474	457	389	284	248	474	460	406	266	239
† 1430	392	381	327	239	200	392	383	344	216	188
1500	468	455	386	291	242	468	460	403	274	236
1600	373	354	228	93	87	373	358	247	90	82

† some cloud present during experiment run.

NOTE: 0800-1100 is 16. 08. 72; remainder is 18. 08. 72.

APPENDIX V

FORTRAN PROGRAMS

This appendix contains the Fortran programs necessary for the calculation of radiation fluxes within the canopy by the layer model. They were written for use on a CDC 6400 computer but are as general as possible to permit usage in most situations.

PROGRAM EFFLAI

```
C     THIS PROGRAM COMPUTES EFFECTIVE DOWNWARD CUMULATIVE LEAF AREA INDEX
C     FROM THE PRODUCT OF AN EFFECTIVE CLUMPING FACTOR (GPRIM) AND TRUE
C     LEAF AREA INDEX (TLAI).  GPRIM EQUALS A TRUE CLUMPING FACTOR (G)
C     MULTIPLIED BY SECANT OF SOLAR ZENITH ANGLE (SECZ) WHEN G IS LESS
C     THAN UNITY.  WHEN G EQUALS 1 THEN GPRIM EQUALS G.
C
C     LIST OF SYMBOLS
C
C     MM          =  NO. OF DAYS
C     M           =  NO. OF CANOPY MEASUREMENT LEVELS
C     NN          =  NO. OF SAMPLE PROFILES
C     DCELAI      =  DOWNWARD EFFECTIVE CUMULATIVE LAI
C     ELAI        =  EFFECTIVE LAI
```

```
C     G          =  TRUE CLUMPING FACTOR
C     GPRIM      =  EFFECTIVE CLUMPING FACTOR
C     SECZ       =  SECANT OF SOLAR ZENITH ANGLE
C     TLAI       =  TRUE LAI
C     XHT        =  HEIGHT ABOVE GROUND LEVEL (CM)
C     ZA         =  SOLAR ZENITH ANGLE (DEGREES)
      DIMENSION G(5),GPRIM(5),DCELAI(5),ELAI(5),TLAI(5),XHT(5)
      DATA NREAD,NPRINT,NPUNCH/5,6,7/
C
      1 FORMAT(2I2)
      2 FORMAT(5F10.5)
      3 FORMAT(I2)
      4 FORMAT(F5.2)
      5 FORMAT(1H1)
      6 FORMAT(10X,*PROGRAM EFFLAI*,10X,*DOWNWARD CUMULATIVE EFFECTIVE LEA
        XF AREA INDEX*,10X,*DATE*///)
      7 FORMAT(40X,*DOWN. CUM. EFF. LAI*,10X,*HEIGHT*)
      8 FORMAT(48X,F5.3,17X,F6.2)
      9 FORMAT(1HO,//)
C
      READ(NREAD,1)MM,M
      READ(NREAD,2)(G(J),J=1,M)
      NCOUNT=1
C
  900 WRITE(NPRINT,5)
      WRITE(NPRINT,6)
```

```
C
      READ(NREAD,3)MM
      READ(NREAD,2)(XHT(J),J=1,M)
      READ(NREAD,2)(TLAI(J),J=1,M)
      DO 800 KK=1,MM
      READ(NREAD,4)ZA
      PHI=3.1416
      ZA=ZA*PHI/180
      SECZ=1./(COZ(ZA))
      DO 100 J=1,M
      IF(G(J).EQ.1.) GO TO 50
      GPRIM(J)=G(J)*SECZ
      IF(GPRIM(J).GE.1.) GPRIM(J)=1.
      GO TO 100
   50 GPRIM(J)=G(J)
  100 CONTINUE
      DO 200 J=1,M
  200 ELAI(J)=TLAI(J)*GPRIM(J)
      DCELAI(1)=ELAI(1)
      DO 300 J=2,M
  300 DCELAI(J)=DCELAI(J-1)+ELAI(J)
      WRITE(NPRINT,7)
      DO 400 J=1,M
  400 WRITE(NPRINT,8)(DCELAI(J),XHT(J),J=1,M)
      WRITE(NPRINT,9)
  800 CONTINUE
```

```
      NCOUNT=NCOUNT+1
      IF(NCOUNT.LE.MM) GO TO 900
      STOP
      END
```

PROGRAM SOLCOMP

```
C     THIS PROGRAM EVALUATES GLOBAL AND NET GLOBAL RADIATION IN A CROP
C     CANOPY USING A SIMPLE LAYER MODEL (KYLE, 1971 AND MODIFICATIONS)
C
C     LIST OF SYMBOLS
C
C     MM        =  NO. OF DAYS
C     NN        =  NO. OF SAMPLE PROFILES
C     N         =  NO. OF CANOPY MEASUREMENT LEVELS
C     A         =  LEAF REFLECTIVITY
C     ABSOR     =  LEAF ABSORBTIVITY
C     ALPHA     =  MEAN LEAF ANGLE (DEGREES)
C     APRIM     =  NORMALISED LEAF ANGLE (DEGREES)
C     ARU       =  ABSORPTION AND UPWARD REFLECTION (A/2+ABSOR)
C     CA        =  CALCULATED CROP ALBEDO
C     CONV      =  CONVERSION FACTOR (DEGREES TO RADIANS)
C     CROP      =  CROP TYPE OR ARRANGEMENT
C     D         =  DIFFUSE SOLAR RADIATION IN CANOPY
C     DELD      =  DIFFERENCE IN DIFFUSE BETWEEN LAYERS
C     DELI      =  DIFFERENCE IN DIRECT BETWEEN LAYERS
C     DO        =  DIFFUSE SOLAR RADIATION ABOVE CANOPY
C     G         =  GLOBAL SOLAR RADIATION (CALCULATED)
C     GN        =  NET GLOBAL SOLAR RADIATION (CALCULATED)
C     IDEL      =  LAYER INCREMENT
```

```
C     ID1,ID2   =  TIME, DAY
C     ID3,ID4   =  MONTH, YEAR
C     IL        =  LAYER NUMBER
C     RD        =  DOWNWARD REFLECTION (A/2)
C     RR        =  REFLECTED SOLAR RADIATION IN CANOPY
C     RS        =  SOIL REFLECTIVITY
C     SC        =  SCATTERING COEFFICIENT (XL(I)*A + XL(I+1)*A)
C     SZ        =  SECANT OF SOLAR ZENITH ANGLE
C     SZN       =  SECANT OF NORMALISED SOLAR ZENITH ANGLE
C     T         =  LEAF TRANSMISSIVITY (1-(A+ABSOR))
C     XI        =  DIRECT SOLAR RADIATION IN CANOPY
C     XIO       =  DIRECT SOLAR RADIATION ABOVE CANOPY
C     XL        =  LEAF AREA INDEX PER LAYER (TOTAL LAI/CANOPY DENSITY)
C     XLDEL     =  LAI INCREMENT
C     XLT       =  TOTAL CROP LAI
C     XS        =  VERT. COMPONENT OF DIRECT SOLAR IN CANOPY
C     ZA        =  SOLAR ZENITH ANGLE (DEGREES)
C     ZN        =  NORMALISED SOLAR ZENITH ANGLE (RADIANS)
C     ZNA       =  NORMALISED SOLAR ZENITH ANGLE (DEGREES)
C     ZPRIM     =  SOLAR ZENITH ANGLE AT NOON (DEGREES)
C     ZR        =  SOLAR ZENITH ANGLE (RADIANS)

      DIMENSION ABU(50),D(50),DELD(50),DELI(50),G(50),GN(50),
      XIL(50),RD(50),RR(50),SC(50),T(50),XI(50),XL(50),XS(50)
      DATA MREAD,MPRINT,MPUNCH/5,6,7/
```

```
C
      1 FORMAT(2I2)
      2 FORMAT(I2)
      3 FORMAT(A4,2I2,I4,A7,A7,2F5.2)
      4 FORMAT(6F10.3)
      5 FORMAT(11F5.3)
      6 FORMAT(3F10.3)
      7 FORMAT(8F10.0)
C
      READ(NREAD,1)MM,M
      NCOUNT=1
  900 READ(NREAD,2)NN
C
      DO 800 KK=1,NN
      READ(NREAD,3)ID1,ID2,ID3,ID4,CROPA,CROPB, ALPHA, ZPRIM
      READ(NREAD,4)XIO,DO,ZA,A,ABSOR,RS
      READ(NREAD,5)(XL(J),J=1,M)
      XL(M+1)=1.
      CONV=3.1416/180.
      APRIM=ALPHA-ZPRIM
      ZHA=ZA-APRIM
      ZR=ZHA*CONV
      ZB=ZA*CONV
      SZ=(1./(COS(ZR)))
      SZR=(1./(COS(ZR)))
```

```
C
C     COMPUTE DIRECT AND DIFFUSE RADIATION ABOVE CROP
C
      XI(1)=XIO
      D(1)=DO
C
      DO 100 J=1,N
      T(J)=1.-(A+ABSOR)
      ARU(J)=A/2+ABSOR
      RD(J)=A/2
      SC(J)=(XL(J+1)*A)*(XL(J)*A)
C
C     COMPUTE DIRECT RADIATION AT EACH LEVEL
C
      DELI(J)=(XI(J)*XL(J)*RD(J))-(XI(J)*XL(J)*ARU(J))*SZN
      XI(J+1)=XI(J)+DELI(J)
C
C     COMPUTE DIFFUSE RADIATION AT EACH LEVEL
C
      DELI(J)=ABS(DELI(J))
      DELD(J)=(DELI(J)*T(J))-(D(J)*XL(J)*ARU(J))
     X+(D(J)*XL(J)*RD(J))+(XI(J+1)*SC(J))
  100 D(J+1)=D(J)+DELD(J)
C
C     COMPUTE REFLECTED RADIATION AT EACH LEVEL
```

```
C
      L=N+1
      RR(N+1)=((XI(N+1)+D(N+1))*RS)
      DO 200 J=1,N
  200 RR(I-J)=((XI(I-J)+D(I-J))*XL(I-J)*A)+(RR(I-J+1)*(1.-XL(I-J)))
C
C     COMPUTE GLOBAL RADIATION AT EACH LEVEL
C
      DO 300 J=1,N
      XS(J)=XI(J)/SZ
      G(J)=XS(J)+D(J)
C
C     COMPUTE NET GLOBAL RADIATION AT EACH LEVEL
C
      GN(J)=G(J)-RR(J)
  300 CONTINUE
C
      XLT=(XL(1)*(N-1))+XL(N)
      CA=(1.-(GN(1)/G(1)))
      IDEL = -1
      DO 400 J=1,N
      IDEL=IDEL+1
  400 IL(J)=IDEL
      XLDEL=0.-XL(1)
      DO 500 J=1,N
```

```
      XLDEL=XLDEL+XL(1)
  500 XL(J)=XLDEL
C
   50 FORMAT(1H1,5X,*DIVERGENCE OF GLOBAL AND NET GLOBAL RADIATION IN A
     X              CANOPY              SOLCOMP MODEL*//)
   51 FORMAT(1HO,10X,*CROP  *,A7,A7,15X,*FOLIAGE INCLINATION ASSUMPTION
     X     INCLINED AT MEAN LEAF ANGLE)
   52 FORMAT(1HO,10X,*DATE  *,I2,*/*,I2,*/*,I4,*          MEAN LEAF ANG
     XLE = *,F5.2,*          NORMALISED LEAF ANGLE = *,F5.2)
   53 FORMAT(1HO,10X,*TIME  *,I4,                SOLAR ZENITH ANGLE = *
     X,F5.2*          RELATIVE ZENITH ANGLE = *,F5.2//)
   54 FORMAT(1HO,*                                        LAYER    LAI
     X  DIRECT     DIFFUSE     GLOBAL     NET GLOBAL*//)
   55 FORMAT(1HO,37X,I2,7X,F3.1,5X,F7.2,5X,F6.2,6X,F6.2,7X,F6.2)
   56 FORMAT(1HO,///)
   57 FORMAT(1HO,*                          TOTAL LAI = *,F6.2,*
     XCROP ALBEDO = *,F4.2)
C
      WRITE(NPRINT,50)
      WRITE(NPRINT,51)CROPA,CROPB
      WRITE(NPRINT,52)ID2,ID3,ID4,ALPHA,ZPRIM
      WRITE(NPRINT,53)ID1, ZA,ZMA
      WRITE(NPRINT,54)
      DO 600 J=1,N
  600 WRITE(NPRINT,55)IL(J),XL(J),XS(J),D(J),G(J),GN(J)
      WRITE(NPRINT,56)
```

```
      WRITE(NRPINT,57)XLT,CA
C
C     PUNCHED OUTPUT OF GLOBAL RADIATION
C
      WRITE(NPUNCH,3)ID1,ID2,ID3,ID4,CROPA,CROPB,ALPHA,ZPRIM
      WRITE(NPUNCH,6)ZA,G(1),G(1)
      WRITE(NPUNCH,7)(G(J),J=2,9)
C
C     PUNCHED OUTPUT OF NET GLOBAL RADIATION
C
      WRITE(NPUNCH,3)ID1,ID2,ID3,ID4,CROPB,CROPB,ALPHA,ZPRIM
      WRITE(NPUNCH,6)ZA,GN(1),GN(1)
      WRITE(NPUNCH,7)(GN(J),J=2,9)
C
  800 CONTINUE
      NCOUNT=NCOUNT+1
      IF(NCOUNT.LE.NO) GO TO 900
      STOP
      END
```

```
                        PROGRAM NETCOMP

C     THIS PROGRAM EVALUATES NET RADIATION IN A CROP CANOPY USING
C     A SIMPLE LAYER MODEL (KYLE,1971 AND MODIFICATIONS)
C
C     LIST OF SYMBOLS
C
C     MM        =  NO. OF DAYS
C     NN        =  NO. OF SAMPLE PROFILES
C     M         =  NO. OF CANOPY MEASUREMENT LEVELS
C     A         =  LEAF REFLECTIVITY
C     ABSOR     =  LEAF ABSORBTIVITY
C     ALPHA     =  MEAN LEAF ANGLE (DEGREES)
C     APRIM     =  NORMALISED LEAF ANGLE (DEGREES)
C     ARU       =  ABSORPTION AND UPWARD REFLECTION (A/2+ABSOR)
C     CONV      =  CONVERSION FACTOR (DEGREES TO RADIANS)
C     CROP      =  CROP TYPE OF ARRANGEMENT
C     D         =  DIFFUSE SOLAR RADIATION IN CANOPY
C     DELD      =  DIFFERENCE IN DIFFUSE BETWEEN LAYERS
C     DELI      =  DIFFERENCE IN DIRECT BETWEEN LAYERS
C     DO        =  DIFFUSE SOLAR RADIATION ABOVE CANOPY
C     E         =  INFRARED EMISSIVITY FOR LEAVES
C     G         =  GLOBAL SOLAR RADIATION (CALCULATED)
C     GN        =  NET GLOBAL SOLAR RADIATION (CALCULATED)
C     IDEL      =  LAYER INCREMENT
```

```
C     ID1,ID2    =  TIME, DAY
C     ID3,ID4    =  MONTH, YEAR
C     IL         =  LAYER NUMBER
C     QN         =  NET RADIATION (CALCULATED)
C     RD         =  DOWNWARD REFLECTION (A/2)
C     RR         =  REFLECTED SOLAR RADIATION IN CANOPY
C     RS         =  SOIL REFLECTIVITY
C     SC         =  SCATTERING COEFFICIENT (XL(I)*A + XL(I+1)*A)
C     SIGMA      =  STEFAN-BOLTZMANN CONSTANT
C     SZ         =  SECANT OF SOLAR ZENITH ANGLE
C     SZN        =  SECANT OF NORMALISED SOLAR ZENITH ANGLE
C     T          =  LEAF TRANSMISSIVITY (1-(A+ABSOR))
C     XI         =  DIRECT SOLAR RADIATION IN CANOPY
C     XIO        =  DIRECT SOLAR RADIATION ABOVE CANOPY
C     XL         =  LEAF AREA INDEX PER LAYER (TOTAL LAI/CANOPY DENSITY)
C     XLDEL      =  LEAF AREA INCREMENT
C     XLT        =  TOTAL CROP LAI
C     XLA        =  DOWNWARD ATMOSPHERIC ABOVE CANOPY
C     XLI        =  DOWNWARD ATMOSPHERIC RADIATION
X     XLO        =  UPWARD TERRESTRIAL RADIATION
C     XLN        =  NET TERRESTRIAL RADIATION
C     XS         =  VERT. COMPONENT OF DIRECT SOLAR IN CANOPY
C     XT         =  TEMPERATURE AT CANOPY CLOSURE (KELVIN)
C     ZA         =  SOLAR ZENITH ANGLE (DEGREES)
```

```
C     ZN          =   NORMALISED SOLAR ZENITH ANGLE (RADIANS)
C     ZNA         =   NORMALISED SOLAR ZENITH ANGLE (DEGREES)
C     ZPRIM       =   SOLAR ZENITH ANGLE AT NOON (DEGREES)
C     ZR          =   SOLAR ZENITH ANGLE (RADIANS)

      DIMENSION ARU(50),D(50),DELD(50),DELI(50),E(50),G(50),GN(50),
     XIL(50),QN(50),RD(50),RR(50),SC(50),T(50),XI(50),XL(50),
     XXLI(50),XLN(50),XLO(50),XS(50),XT(50)
      DATA NREAD,NPRINT,NPUNCH/5,6,7/
C
      1 FORMAT(2I2)
      2 FORMAT(I2)
      3 FORMAT(A4,2I2,I4,A7,A7,2F5.2)
      4 FORMAT(8F10.3/F10.3)
      5 FORMAT(11F5.3)
      6 FORMAT(3F10.3)
      7 FORMAT(8F10.0)
C
      READ(NREAD,1)MM,N
      NCOUNT=1
  900 READ(NREAD,2)MM
C
      DO 800 KK=1,MM
      READ(NREAD,3)ID1,ID2,ID3,ID4,CROPA,CROPB,ALPHA,ZPRIM
      READ(NREAD,4)XIO,DO,ZA,A,ABSOR,RS,XLA,XTC,EML
      READ(NREAD,5)(XL(J),J=1,N)
```

```
      XL(N+1)=1.
      CONV=3.1416/180
      APRIM=ALPHA-ZPRIM
      ZNA=ZA-APRIM
      ZN=ZNA*CONV
      ZR=ZA*CONV
      SZ=(1./(COS(ZR)))
      SZN=(1./(COS(ZN)))
C
C     COMPUTE DIRECT AND DIFFUSE RADIATION ABOVE CROP
C
      XI(1)=XIO
      D(1)=DO
C
      DO 100 J=1,N
      T(J)=1.-(A+ABSOR)
      ARU(J)=A/2+ABSOR
      RD(J)=A/2
      SC(J)=(XL(J+1)*A)*(XL(J)*A)
      E(J)=EML
      XI(J)=XIC
C
C     COMPUTE DIRECT RADIATION AT EACH LEVEL
C
      DELI(J)=(XI(J)*XL(J)*RD(J))-(XI(J)*XL(J)*ARU(J))*SZN
      XI(J+1)=XI(J)+DELI(J)
```

```
C
C     COMPUTE DIFFUSE RADIATION AT EACH LEVEL
C
      DELI(J)=ABS(DELI(J))
      DELD(J)=(DELI(J)*T(J))-(D(J)*XL(J)*ARU(J))
     X+(D(J)*XL(J)*RD(J))+(XI(J+1)*SC(J))
  100 D(J+1)=D(J)+DELD(J)
C
C     COMPUTE REFLECTED RADIATION AT EACH LEVEL
C
      I=N+1
      RR(N+1)=((XI(N+1)+D(N+1))*RS)
      DO 200 J=1,N
  200 RR(I-J)=((XI(I-J)+D(I-J))*XL(I-J)*A)+(RR(I-J+1)*(1.-XL(I-J)))
C
C     COMPUTE GLOBAL RADIATION AT EACH LEVEL
C
      DO 300 J=1,N
      XS(J)=XI(J)/SZ
      G(J)=XS(J)+D(J)
C
C     COMPUTE NET GLOBAL RADIATION AT EACH LEVEL
C
      GN(J)=G(J)-RR(J)
  300 CONTINUE
```

```
C
C       COMPUTE NET TERRESTRIAL RADIATION AT EACH LEVEL
C
        SIGMA=5.6697/(10.**8.)
        DO 400 J=1,N
        XLI(J)=XLA
        XLO(J)=(1.-E(J))*XLI(J)+E(J)*SIGMA*(XT(J)**4.)
        XLN(J)=XLI(J)-XLO(J)
C
C       COMPUTE NET RADIATION AT EACH LEVEL
C
        QN(J)=GN(J)+XLN(J)
  400   CONTINUE
C
        XLT=(XK(1)*(N-1))+XL(N)
        IDEL=-1
        DO 500 J=1,N
        IDEL=IDEL+1
  500   IL(J)=IDEL
        ILDEL=0.-XL(1)
        DO 600 J=1,N
        XLDEL=XLDEL+XL(1)
  600   XL(J)=XLDEL
C
   50   FORMAT(1H1,5X,*DIVERGENCE OF NET RADIATION IN A                CA
       XNOPY                  NETCOMP MODEL*//)
```

```
 51 FORMAT(1HO,10X,*CROP  *,A7,A7,15X,*FOLIAGE INCLINATION ASSUMPTION
   X     INCLINED AT MEAN LEAF ANGLE)
 52 FORMAT(1HO,10X,*DATE  *,I2,*/*,I4,*                    MEAN LEAF ANG
   XLE = *,F5.2,*          NORMALISED LEAF ANGLE = *,F5.2)
 53 FORMAT(1HO,10X,*TIME  *,I4,                  SOLAR ZENITH ANGLE = *
   X,F5.2,*          RELATIVE ZENITH ANGLE = *,F5.2////)
 54 FORMAT(1HO,*                                        LAYER      LAI
   X   GLOBAL  NET GLOBAL  NET TERR.  NET*//)
 55 FORMAT(1HO,37X,I2,7X,F3.1,5X,F7.2,5X,F6.2,6X,F7.2,F6.2)
 56 FORMAT(1HO,///)
 57 FORMAT(1HO,*                              TOTAL LAI  =  *,F6.2)
C
      WRITE(NPRINT,50)
      WRITE(NPRINT,51)CROPA,CROPB
      WRITE(NPRINT,53)ID1,ZA,ZHA
      WRITE(NPRINT,54)
      DO 700 J=1,N
  700 WRITE(NPRINT,55)IL(J),XL(J),G(J),GN(J),XLN(J),QN(J)
      WRITE(NPRINT,56)
      WRITE(NPRINT,57)XLT
C
C     PUNCHED OUTPUT OF NET RADIATION
C
      WRITE(NPUNCH,3)ID1,ID2,ID3,ID4,CROPA,CROPB,ALPHA,ZPRIM
      WRITE(NPUNCH,6)ZA,QN(1),QN(1)
```

```
      WRITE(NPUNCH,7)(QN(J),J=2,9)
C
  800 CONTINUE
      NCOUNT=NCOUNT+1
      IF(NCOUNT.LE.MM) GO TO 900
      STOP
      END
```

REFERENCES

Acock, B., Thornley, J.H.M. and Warren Wilson, J. (1970). Spatial variation of light in the canopy. in *Prediction and Measurement of Photosynthetic Productivity*, P.U.D.O.C., Wageningen, 91-102.

Allen, L.H. and Lemon, E.R. (1972). Net radiation frequency distribution in a corn crop. *Boundary Layer Meteorol.*, 3, 246-254.

Allen, W.A. and Richardson, A.J. (1968). Interaction of light with a plant canopy. *J. Opt. Soc. Amer.*, 58, 1023-1028.

Allen, W.A., Gayle, T.V. and Richardson, A.J. (1970). Plant canopy irradiance specified by the Duntley equations. *J. Opt. Soc. Amer.*, 60, 372-376.

Anderson, M.C. (1966). Stand structure and light penetration II. A theoretical analysis. *J. Appl. Ecol.*, 3, 41-54.

Anderson, M.C. (1969). A comparison of two theories of scattering of radiation in crops. *Agr. Meteorol.*, 6, 399-405.

Anderson, M.C. (1970). Radiation climate, crop architecture and photosynthesis. in *Prediction and Measurement of Photosynthetic Productivity*, P.U.D.O.C., Wageningen, 71-78.

Anderson, M.C. (1971). Radiation and crop structure. in *Plant Photosynthetic Production Manual of Methods*, W. Junk, NV, The Hague, 412-466.

Anderson, M.C. and Denmead, O.T. (1969). Shortwave radiation on inclined surfaces in model plant communities. *Agron. J.*, 61, 867-872.

Brown, K.W. and Covey, W. (1965). The energy budget and micrometeorological transfer processes within a cornfield. *Agr. Meteorol.*, 3, 73-96.

Chartier, P. (1966). Etude du microclimat lumineux dans la végétation. *Ann. Agron.*, 17, 571-602.

Cowan, I.R. (1968). The interception and absorption of radiation in plant stands. *J. Appl. Ecol.*, 5, 367-379.

Davies, J.A. and Buttimor, P.H. (1969). Reflection coefficients, heating coefficients and net radiation at Simcoe, Southern Ontario. *Agr. Meteorol.*, 6, 373-386.

Davies, J.A., Robinson, P.J. and Nunez, M. (1970). *Radiation measurement over Lake Ontario and the Determination of Emissivity.* 1st Rep., Contr. HO 81276, Gov. Canada, Dept. Environment, Canada Centre for Inland Waters, Burlington, 85p.

Duncan, W.G., Loomis, R.S., Williams, W.A. and Hanau, R. (1967). A model for simulating photosynthetis in plant communities. *Hilgardia*, 38, 181-205.

Funk, J.P. (1959). Improved polyethylene shielded net radiometer. *J. Sci. Instr.*, 36, 267-270.

Idso, S.B. (1968). *A Holocoenotic Analysis of Environment-Plant Relationships.* Tech. Bull. 264, Agr. Exp. Sta., U. of Minnesota, St. Paul, 147p.

Idso, S.B. and de Wit, C.T. (1970). Light relations in plant canopies. *Appl. Opt.*, 9, 177-184.

Idso, S.B., Jackson, R.D., Ehrler, W.L. and Mitchell, S.T. (1969). A method for determination of infrared emittance of leaves. *Ecology*, 50, 899-902.

Impens, I.I. and Lemeur, R. (1969). Extinction of net radiation in different crop canopies. *Arch. Meteor. Geophys. Bioklim. Ser. B.*, 17, 403-412.

Impens, I.I., Lemeur, R. and Moermans, R. (1970). Spatial and temporal variation of net radiation in crop canopies. *Agr. Meteor.* 7, 335-337.

Isobe, S. (1969). Theory of the light distribution and photosynthesis in canopies of randomly dispersed foliage area. *Bull. Nat. Inst. Agr. Sci. (Japan), Ser. A*, 1-25.

Kasanaga, H. and Monsi, M. (1954). On the light transmission of leaves and its meaning for the production of matter in plant communities. *Jap. J. Bot.*, 14, 304-324.

Kuroiwa, S. (1965). A new calculation method for total photosynthesis of a plant community under illumination consisting of direct and defined light. *Proc. Copenhagen Symposium, UNESCO, Paris*, ed. F.E. Eckhardt.

Kuroiwa, S. (1968). Theoretical analysis of light factor and photosynthesis in plant communities 3. Total photosynthesis of a foliage under parallel light in comparison with that under isotropic light conditions. *J. Agr. Meteor. (Japan)*, 24, 51-66.

Kyle, W.J. (1971). *Daytime Radiation Regimes within a Corn Canopy.* Pub. Climatol. 2, McMaster Univ., Hamilton, 140p.

Latimer, J.R. (1972). *Radiation Measurement.* I.F.G.Y.L. Tech. Man. Ser. 2, Ottawa, 53p.

Lemon, E.R. (1967). Aerodynamic studies of CO_2 exchange between the atmosphere and the plant. in *Harvesting the Sun,* ed. A. San Pietro, F.A. Greer and T.J. Army, Acad. Press, New York, 263-290.

Leonard, R.E. and Eschner, A.R. (1968). *A Treetop Tramway System for Meteorological Studies.* Res. Paper NE-92, U.S. Forest Service, Northeast Forest Exp. Sta., 10p.

Loomis, R.S., Williams, W.A., Duncan, W.G., Dovrat, A. and Nunez, F. (1968). Quantitative descriptions of foliage display and light absorption in field communities of corn plants. *Crop Sci.,* 8, 352-356.

McCaughey, J.H. (1972). *Energy exchange within a corn canopy.* Ph.D. Thesis, McMaster Univ., Hamilton.

McCaughey, J.H. and Davies, J.A. (1974). Diurnal variation in net radiation depletion within a corn crop. *Boundary-Layer Meteorol.,* 5, 505-511.

Miller, E.E. and Norman, J.M. (1971a). A sunfleck theory for plant canopies, I. Lengths of sunlit segments along a transect. *Agron. J.,* 63, 737-738.

Miller, E.E. and Norman, J.M. (1971b). A sunfleck theory for plant canopies, II. Intensity distributions along sunfleck segments. *Agron. J., 63,* 739-743.

Monsi, M. and Saeki, T. (1953). Uber den Lichtfaktor in den Pflanzengesellschaften und seine Bedeutung fur die Stoffproduktion. *Jap. J. Bot.,* 14, 22-52.

Monteith, J.L., (1959). The reflection of shortwave radiation by vegetation. *Quart. J. Roy. Meteorol. Soc.,* 85, 386-392.

Monteith, J.L. (1965). Light distribution and photosynthesis in field crops. *Ann. Bot. (N.S.)* 29, 17-37.

Monteith, J.L. (1973). *Principles of Environmental Physics.* Edward Arnold, London, 241p.

Monteith, J.L. and Szeicz, G. (1961). The radiation balance of bare soil and vegetation. *Quart. J. Roy. Meteor. Soc.,* 87, 159-170.

Mototani, I. (1968). Horizontal distribution of light intensity in plant communities. in *Photosynthesis and Utilisation of Solar Energy*, Ann. Rep. Jap. Comm. IBP/PP, Tokyo, 25-28.

Nichiporovich, A.A. (1961). Properties of plant crops as an optical system. *Soviet Plant Physiol.*, 8, 428-435.

Nilisk, H., Nilson, T. and Ross, J. (1970). Radiation in plant canopies and its measurement. in *Prediction and Measurement of Photosynthetic Productivity*, P.U.D.O.C., Wageningen, 165-177.

Norman, J.M. (1971). *Sunfleck size and Light intensity distributions in plant canopies.* Ph.D. Thesis, Univ. Wisconsin, Madison.

Norman, J.M., Miller, E.E. and Tanner, C.B. (1971). Light intensity and sunfleck size distributions in several plant canopies. *Agron. J.*, 63, 743-748.

Nunez, M., Davies, J.A. and Robinson, P.J. (1971). *Solar radiation and albedo at a Lake Ontario tower site.* 3rd Rep., Contr. NO 81276, Gov. Canada, Dept. Environment, Canada Centre for Inland Waters, Burlington, 82p.

Panofsky, H.A. and Brier, G.W. (1965). *Some applications of statistics to meteorology.* Penn. State Univ., University Park.

Proctor, J.T.A., Kyle, W.J. and Davies, J.A. (1972). The radiation balance of an apple tree. *Can. J. Bot.*, 50, 1731-1740.

Robinson, N. (1965). *Solar Radiation.* Elsevier, London, 347p.

Ross, J. and Nilson, T. (1963). K teorii radiatsionnogo rezhima rastitel'nogo pokrova. *Issled. Fiz. Atmos. Akad. Nauk. Eston. S.S.R.*, 4, 42-64.

Ross, J. and Nilson, T. (1965). Propeskanye pryamoi radiatsii solntsa se'skokoryaistvennymi posevami. *Issled. Fiz. Atmos. Akad. Nauk. Eston. S.S.R.*, 6, 25-64.

Ross, R. and Nilson, T. (1967). The spatial orientation of leaves in crop stands and its determination. in *Photosynthesis of Productive Systems*, ed. A.A. Nichiporovich, I.P.S.T., Jerusalem, 86-89.

Sellers, W.D. (1965). *Physical Climatology.* Univ. Chicago Press, Chicago, 272p.

Stanhill, G., Hofstede, G.J. and Kalma, J.D. (1966). Radiation balance of natural and agricultural vegetation. *Quart. J. Roy. Meteorol. Soc.*, 92, 128-140.

Szeicz, G. (1974). Solar radiation in crop canopies. *J. Appl. Ecol.*, 11.

Szeicz, G., Monteith, J.L. and dos Santos, J.M., J.M. (1964). Tube solarimeter to measure radiation among plants. *J. Appl. Ecol.*, 1, 169-174.

Tanner, C.B. (1963). *Basic Instrumentation and Measurements for Plant Environment and Micrometeorology*, Soils Bull. 6, Univ. Wisconsin, Madison.

Uchijima, Z. (1962). Studies on the microclimate within plant communities, I. On the turbulent transfer coefficient within a plant layer, *J. Agr. Meteor., (Japan)*, 18, 1-9.

Watson, D.J. (1947). Comparative physiological studies on the growth of field crops. I. Variation in net assimilation rate and leaf area between species and varieties, and within and between years. *Ann. Bot. (N.S.)*, 11, 41-76.

Weinmann, J.A. and Guetter, P.J. (1972). Penetration of solar irradiances through the atmosphere and plant canopies. *J. Appl. Meteor.*, 11, 136-140.

Wilson, J. Warren, (1960). Inclined point quadrats, *New Phytol.*, 59, 1-8.

de Wit, C.T. (1965). *Photosynthesis of leaf canopies*. Agr. Res. Rep. 633, P.U.D.O.C., Wageningen, 57 p.

World Meteorological Organisation (1969). *Guide to Meteorological Instruments and Observing Practices*. Ch. 9, 3rd ed., W.M.O., Geneva.